

FREE RADICAL OH

A Molecule of Astrophysical and Aeronomie Interest

CASE FILE
COPY



NATIONAL AERONAUTICS AND SPACE ADMINISTRATION

FREE RADICAL OH

A Molecule of Astrophysical and Aeronomical Interest

By

Hari Mohan and Shardanand

NASA Wallops Flight Center



Scientific and Technical Information Office

NATIONAL AERONAUTICS AND SPACE ADMINISTRATION
Washington, D.C.

1975

For sale by the National Technical Information Service
Springfield, Virginia 22151
Price \$7.00

FOREWORD

Quantitative spectroscopy is a fundamental ingredient of remote sensing and space sensor development. For this reason the space agency has a definite need for precise spectroscopic knowledge about molecules and atoms. Gaseous spectroscopy is especially important since many planets including our own must normally be viewed through their atmosphere. One important constituent of planetary atmospheric studies is the hydroxyl radical. This monograph presents a review of available OH spectroscopic information supplemented by a brief account of relevant theoretical concepts. This compilation will certainly serve as a foundation and fundamental starting point for hydroxyl radical studies. The work presented herein represents one component of Wallops Flight Center's overall planetary aeronomy program under the direction of Dr. Shadandan.

Robert L. Krieger
Director
NASA Wallops Flight Center

ACKNOWLEDGMENTS

It is our pleasure to acknowledge with thanks the continuous encouragement of Robert F. Fellows in support of this work. Thanks are also to Joseph T. McGoogan and Frank E. Hoge for critical reading of the manuscript. We also extend our thanks to Ann Taylor and Helen Shirk for typing the manuscript of this book.

Hari Mohan
and
Shardanand

C O N T E N T S

FOREWORD	iii
ACKNOWLEDGMENTS.	v
CONTENTS	vii
SYMBOLS	xi
PHYSICAL CONSTANTS	xv
 Chapter 1 INTRODUCTION	1
 Chapter 2 MOLECULAR STRUCTURE AND SPECTRA OF OH	7
Electronic States Involved in Radiative Transitions	7
The State $X^2\Pi_1$	7
The State $^2\Sigma^+$	15
Spectral Features of Band Structure in Different Radiative Transitions	17
$^2\Sigma - ^2\Sigma$ Transitions	17
$^2\Sigma - ^2\Pi$ Transitions	22
$^2\Sigma - ^2\Pi(a)$	22
$^2\Sigma - ^2\Pi(b)$	22
$X^2\Pi - X^2\Pi$ Transitions	24
 Chapter 3 OBSERVED SPECTRA OF OH	27
Electronic Spectra	27
System A: $A^2\Sigma^+ \leftrightarrow ^2\Pi_{3/2, 1/2}$ (4107-2444A)	27
OH Lines in the Solar Spectrum	31
System B: $B^2\Sigma^+ - A^2\Sigma^+$ (5660-4216 \AA)	35
	vii

System C': C $^2\Sigma^+$ - A $^2\Sigma^+$ (2600-2249 \AA)	38
System C: C $^2\Sigma^+$ - X $^2\Pi_1^{\circ}$ (1990-1770 \AA)	41
VUV Absorption Band: $^2\Sigma^-$ - X $^2\Pi_1^{\circ}$ (1221 \AA)	42
Rotation-Vibration Spectra.	45
Meinel Bands: X $^2\Pi_1^{\circ}$ - X $^2\Pi_1^{\circ}$ (44745-3810 \AA)	45
Rotational and Sub-Rotational Spectra	54
Pure Rotational Spectrum: X $^2\Pi_1^{\circ}$ - X $^2\Pi_1^{\circ}$ (20.4 - 15 μ)	54
OH Infrared Laser Oscillations.	55
OH Spectra in Microwave and Radiofrequency Regions	59
Microwave Spectrum.	59
Electron Paramagnetic Resonance Spectrum. .	63
OH Radiation in Interstellar Space.	65
OH Microwave Absorption in Interstellar Space	65
OH Microwave Emission from Galactic Sources	68
Chapter 4 DISSOCIATION AND IONIZATION PROCESSES IN OH	73
Dissociation Energies and Limits.	73
Predissociation and OH Spectrum	76
Molecular Ionization Potential	84
Chapter 5 INTENSITY PARAMETERS OF OH.	87
Franck-Condon Factors and \bar{r} -Centroids	88
Oscillator Strengths.	100

Chapter 6 IONIZED RADICAL OH ⁺ AND ITS BAND SPECTRA.	111
Band Structure of A ³ Π - ³ Σ Transitions	111
Observed Spectra of OH ⁺	115
A ³ Π _i → X ³ Σ ⁻ (3983-3332Å) Bands.	115
OH ⁺ Radical in Interstellar Space	119
APPENDIX A	123
APPENDIX B	149
REFERENCES	163

SYMBOLS

\AA	Angström
A	Constant related to ionization energy by hca (Eq. 4-1)
A	Spin coupling constant
a, b, c, d	Magnetic hyperfine interaction constant (Table 3-18)
a	Spin-orbit interaction constant
A_{mn}	Einstein coefficient for spontaneous emission
B_v	Rotational constant for a given vibrational level and is expressed as $B_v = B_e - \alpha_e (V + 1/2)$, where B_e is a rotational constant in the equilibrium position and α_e is an interaction constant between rotational and vibrational energies.
B_{eff}	Effective B value for different multiplet components
B_{mn}	Einstein coefficient for induced absorption
c	Velocity of light
C_1, C_2	Λ -type doubling constant
D_0°	Dissociation energy of the molecule in the ground electronic state
D_e	Dissociation energy referred to the minimum of the potential curve
D_v	Rotational constant involving centrifugal distortion and is expressed as $D_v = D_e + \beta_e (V + 1/2)$, where D_e is another rotational constant and β_e is another interaction constant.
D_{eff}	Effective D value for different multiplet components
D, D_n, δ	Centrifugal distortion constant (Table 3-18)
e	Charge of an electron
E_J	Rotational energy of a molecule

E_{nm}	Energy of radiation associated with the transition n-m.
f_{mn}	Oscillator strength of a transition m-n
$F_v(J)$	Rotational term in a given vibrational level and is given as $F_v(J) = E_J/hc$
ΔF	Term value interval
g	Degeneracy factor
h	Planck's constant
H, P	Higher order rotational constant (Table 3-15)
I_e	Moment of inertia of the molecule in equilibrium position (Table 6-6)
I_{nm}	Intensity of radiation involved in the transition n-m
$I_o(nm)$	Intensity of incident radiation at ν_{nm}
J	Quantum number of the total angular momentum
ΔJ	Change in rotational quantum number
k	Boltzmann constant
l_0	Layer thickness of the absorbing species reduced to 0° C and 1 atm.
m_e	Mass of an electron
M_e	Electric dipole moment arising due to orbital electrons in a molecule
M_J	Magnetic quantum number
ΔM_J	Change in M_J - quantum number
N	Quantum number of the total angular momentum of the molecule apart from spin
ΔN	Change in N-quantum number
N_n	Number of molecules in the upper state - n
N_m	Number of molecules in the lower state - m

n_o	Loschmidt number
P_o	Standard pressure 760 mm-Hg)
P	Pressure at a temperature T
$Q_{v',v''}$	Franck-Condon factor for the (v',v'') band
R	Rydberg constant (Eq. 4-1)
R	Gas constant
R	Quantum number of the angular momentum of nuclear rotation (Chapter 2)
$\bar{r}_{v',v''}$	\bar{r} -centroid for the (v',v'') band
r	Internuclear distance
r_e	Equilibrium internuclear distance
S	Quantum number of the resultant spin
ΔS	Change in spin quantum number
S_{nm}	'Transition Strength' of the transition $n-m$
$S_{v',v''}$	'Band Strength' for the (v',v'') band
T_o	Standard temperature (0° C or 273.15° K)
T_e	Electronic energy term value and is expressed as $T_e = T_o + A\Lambda\Sigma$, where T_o is the electronic energy term value if spin is neglected, A is the spin-coupling constant, Λ and Σ quantum numbers
$U(E)$	Potential energy function for a molecule
V	Vibrational quantum number
ΔX	Thickness of the absorbing layer
Y_v	A coupling parameter signifying the ratio A/B_v , where A is a spin-coupling constant and B_v is a rotational constant
α	Correction term (Eq. 4-1)
α_e	Interaction constant which accounts for the interaction between rotational and vibrational energies

α_λ	Absorption coefficient at wavelength λ (cm^{-1})
α_ν	Absorption coefficient at wavenumber ν (cm^{-1})
β_e	Another interaction constant similar to α_e
γ	Spin rotation coupling constant for multiplet Σ states
δ	Centrifugal distortion constant (Table 3-18)
δ	A constant (Eq. 5-22)
ε	Shape factor (Eq. 5-21)
λ	Wavelength in $\text{\AA}^{\circ\circ}$
λ	Spin-coupling constant (Table 6-6)
Λ	Quantum number of the component of the resultant electronic orbital angular momentum of the molecule along the internuclear axis
$\Delta\Lambda$	Change in Λ -quantum number
μ	Reduced mass
μ	Micron (10^{-4} cm)
ν	Wavenumber (cm^{-1})
ν_e	Wavenumber of the pure electronic jump; origin of the band system
ν_{nm}	Wavenumber of the radiation associated with the transition $n-m$
$\Delta\nu$	Wavenumber interval
σ_λ	Absorption cross section at wavelength λ (cm^2)
Σ	Quantum number of the component of the resultant electronic spin of the molecule along the internuclear axis
$\Delta\Sigma$	Change in Σ -quantum number
τ	Mean lifetime for a radiative transition
ψ	Wavefunction

ψ^*	Complex conjugate wavefunction
ω_e	Vibrational constant; vibrational frequency that an anharmonic oscillator should have for an infinitesimal amplitude (cm^{-1})
ω_{eXe}	Vibrational constant; a constant involving anharmonicity
Ω	Quantum number of the total electronic angular momentum of the molecule along the internuclear axis
$\Delta\Omega$	Change in Ω -quantum number

PHYSICAL CONSTANTS

Speed of light:

$$C = 2.997930 \times 10^{10} \text{ cm sec}^{-1}$$

Electron charge:

$$e = 1.60206 \times 10^{-19} \text{ coulomb}$$

Electron rest mass:

$$\begin{aligned} m_e &= 0.510976 \text{ MeV} \\ &= 9.1083 \times 10^{-28} \text{ gram} \end{aligned}$$

Planck constant:

$$\begin{aligned} h &= 4.1354 \times 10^{-15} \text{ eV sec} \\ &= 6.62517 \times 10^{-27} \text{ erg sec} \end{aligned}$$

Boltzmann constant:

$$\begin{aligned} k &= 8.6164 \times 10^{-5} \text{ eV K}^{-1} \\ &= 1.38044 \times 10^{-16} \text{ erg K}^{-1} \end{aligned}$$

Gas constant:

$$R = 8.3170 \times 10^7 \text{ erg K}^{-1} \text{ mole}^{-1}$$

Loschmidt number:

$$n_0 = 2.68714 \times 10^{19} \text{ cm}^{-3}$$

Standard pressure:

$$P_0 = 1.013250 \text{ dyn cm}^{-2}$$

Standard temperature:

$$T_0 = 273.150^\circ\text{K}$$

INTRODUCTION

Band spectroscopy of the free hydroxyl radical has long been of considerable scientific interest. Its significance in both theory and various applications is well recognized. Though this molecule is composed of two simple and most abundant atoms, O and H, it presents more than the usual structural complexity expected of a normal diatomic molecule. A closer perusal of its molecular spectrum reveals many of the internal interactions characteristic of the diatomic structures. It exhibits the existence of a strong magnetic coupling leading to an inverted multiplet, large Lambda-type doubling, presence of numerous satellites, and unlike most diatomics, an almost complete transformation from Hund coupling case (a) to case (b). Also, the OH molecule provides very useful information toward the understanding of various photochemical and combustion processes. OH exists either as an essential bi-product or as an impurity in all types of combustion processes like flames; gas discharges; sparks, etc. An insight into the excitation, dissociation, and ionization mechanisms of this molecule is, therefore, very helpful in determining the energy contents and thereby the spectroscopic temperatures in flames and other radiative and non-radiative systems.

Knowledge of the detailed vibrational and rotational structure of OH is important to studies of the planetary atmospheres and various other astrophysical and aeronomical

applications. Numerous OH rotational lines have been identified in the spectra of night airglow, dayglow, and twilight; solar spectra; stellar spectra; and the spectra of comets and different galactic sources. OH happens to be the first gaseous diatomic molecule ever discovered in interstellar space by way of microwave emission. It may be recalled that this discovery later proved to be the boon that ushered in a new era of modern radioastronomy. The mystery of anomalous behavior of OH emission in interstellar space is not yet clearly understood. OH is potentially important from the viewpoint of environmental studies, such as air pollution. The role of OH in photochemical smog is well known and OH may play a useful role in different remote sensing applications for such purposes. Development of hydroxyl radical infrared lasers is another significant application of the radiative behavior of this molecule. The new lasers may prove to be valuable in probing OH concentrations in various chemically active systems including the earth's atmosphere. Last but not least, OH still owes its unique position to being the most prospective molecular entity that one would search for in any system where life might be postulated.

OH thus occupies a significant position in the molecular world, both from the viewpoint of academic interest as well as its potentiality as an application molecule. There exist quite a few scattered technical reports and reviews, apart from a host of research articles which are devoted to spe-

cific areas of OH spectroscopy. Spectroscopic numerical data pertaining to OH were compiled by various authors (Herzberg, 1950; Wallace, 1962a; Pearse and Gaydon, 1965; and Rosen, 1970, 1973). Dieke and Crosswhite (1948) also presented a detailed analysis of OH spectra but it is primarily devoted to only one of the electronic band systems, namely, the $A^2\Sigma^+ - X^2\Pi_1$. But, in spite of the wide applicability of the spectroscopic information about this molecule, there exists no single broad-based document which might give a reasonable coverage to the various aspects of the spectroscopy of this molecule. Also, with the advent of more sophisticated experimental techniques, our knowledge about this molecule has increased tremendously in recent years and thus more and more reliable spectroscopic data are now available. Recognizing the pressing need to fill these gaps, it was decided to make an endeavor to review the observed OH spectra, critically evaluate the available spectroscopic data, and present the same with a short background discussion on the theoretical principles involved. The present monograph is the outcome of such an attempt.

To make the subject matter coherent and comprehensive, the text has been divided into three sections:

Molecular Structure and Spectra of OH

Dissociation and Ionization Processes in OH

Intensity Parameters in OH

MOLECULAR STRUCTURE AND SPECTRA OF OH

This section incorporates an exhaustive account of the various radiative electronic, rotation-vibrational, and pure rotational molecular transitions so far identified in the case of the free gaseous radical OH. Multiplet structures as evidenced through microwave, radiofrequency and electron paramagnetic resonance spectra are included. OH transitions relevant to different astrophysical observations such as spectra of the sun, comets, interstellar space, and various galactic sources are discussed in the proper context. Molecular transitions of relevance to the development of OH infrared lasers are introduced.

Necessary data have been evaluated and presented in respect to each spectrum except for the $A\ 2\Sigma^+ - X\ 2\Pi$ ultraviolet electronic system for which an exhaustive compilation already exists (Dieke and Crosswhite, 1962).

DISSOCIATION AND IONIZATION PROCESSES IN OH

This section deals with the dissociation energies and dissociation limits and also the molecular ionization potentials of the free molecule OH. The phenomena of predissociation is discussed at length. Preceding the presentation of data in respect to the dissociation energies and their limits for the various electronic states, a brief survey has been made to highlight the various merits and demerits of different

methods adopted to determine this important molecular parameter. Data on ionization potential are provided with brief introductory remarks.

INTENSITY PARAMETERS IN OH

This section mainly speaks of the intensity considerations in various OH transitions. The significance of molecular intensity parameters, such as Franck-Condon factors, \bar{r} - centroids, oscillator strengths, absorption cross sections, and the lifetimes in understanding aeronomical conditions, are spelled out and discussed. Also, the relevant data are provided.

Data on the spectra and structure of OH⁺ are incorporated. Although the structural features of OH⁺ spectra differ significantly from those of OH, it is very likely that one may identify some OH⁺ transitions in certain extreme cases of aeronomical conditions. In fact a few OH⁺ transitions have already been identified in certain cometary spectra. On the other hand, discussion and presentation of data in respect to the isotopic molecule OD are excluded because it is less likely that the appreciable amount of OD may be present in interstellar space so as to be easily detected by spectroscopic techniques.

The theoretical outlines of the different relevant spectroscopic phenomena are provided at appropriate places, in order to make the subject matter self-contained and comprehensible even to a non-specialist engaged

in the pursuit of studies on planetary aeronomy and astrophysics.

While every effort has been made to cover the data up to 1974 and thus make the monograph up-to-date, the authors would be glad to consider all comments with regard to omissions necessary to improve upon the text and its presentation.

MOLECULAR STRUCTURE AND SPECTRA OF OH

OH radical is a paramagnetic diatomic molecule involving one unpaired electron in its ground state electronic configuration. According to the Wigner - Witmer correlation rules the four electronic states, namely, $^2\Pi$, $^2\Sigma^-$, $^4\Sigma^-$, and $^4\Pi$ for $O(^3P)H(^2S)$ molecule are feasible from the ground state configuration $K(2s\sigma)^2 (2p\sigma)^2 (2p\pi)^3$. The next excited states $^2\Sigma^+$ and $^2\Delta$ are possible according to the first excited electron configuration $K(2s\sigma)^2 2p\sigma (2p\pi)^4$. The radiative transitions so far observed are those between pure rotation and rotation-vibration levels in the ground $X\ ^2\Pi_i$ state and the electronic transitions $A\ ^2\Sigma^+ \leftrightarrow X\ ^2\Pi_i$, $B\ ^2\Sigma^+ - A\ ^2\Sigma^+$, $C\ ^2\Sigma^+ - A\ ^2\Sigma^+$, $C\ ^2\Sigma^+ - X\ ^2\Pi_i$, and a recently observed transition $^2\Sigma^-(R) \leftarrow X\ ^2\Pi_i$ (Douglas, 1974) in the vacuum ultraviolet. A schematic of the molecular states and electronic transitions is shown in figure 2-1. This figure also gives the values of various spectroscopic constants. The electronic transition $B\ ^2\Sigma^+ - X\ ^2\Pi_i$ has not been identified so far, perhaps because of the overlapping of the spectrum of water vapor in the spectral region around 1200\AA .

ELECTRONIC STATES INVOLVED IN RADIATIVE TRANSITIONS

The state $X\ ^2\Pi_i$: $^2\Pi_i$ symbolizes the ground electronic state of this molecule. It is the lowest in the term manifold arising out of the electron configuration $K(2s\sigma)^2$

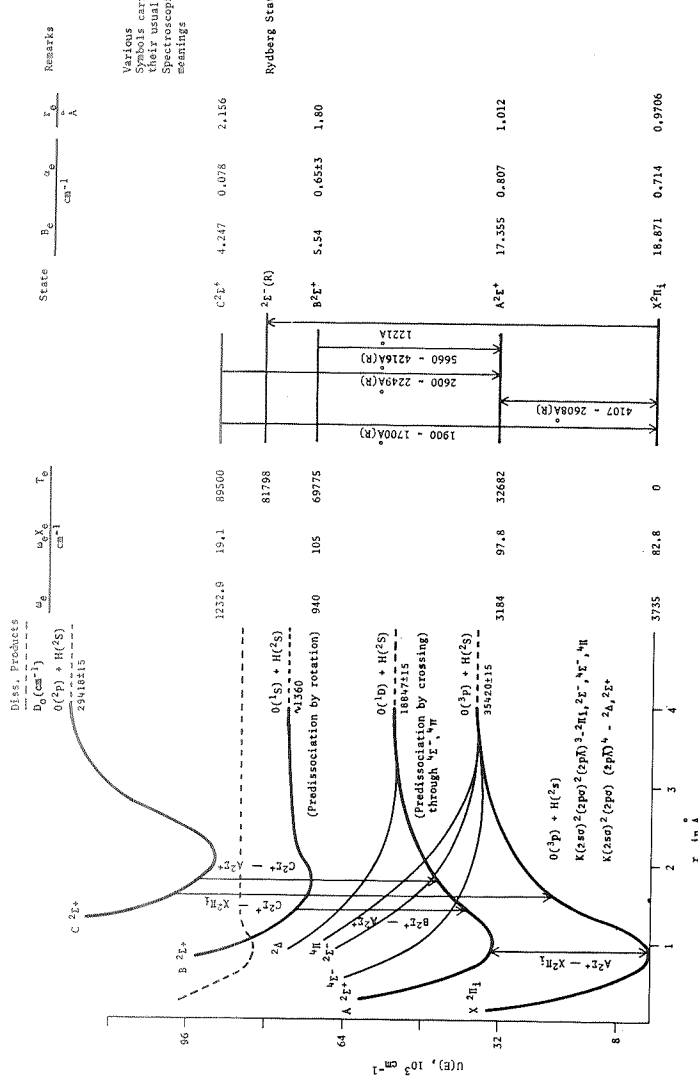


Figure 2-1 Various electronic states and the observed electronic transitions in OH. The values of the various spectroscopic constants (Rosen, 1970; Carlone and Dalby, 1969a; Douglas, 1974) are also shown. The identity of dashed electronic state is uncertain.

$(2p\sigma)^2 (2p\pi)^3$, as applied to this case. Structurally, it is an inverted doublet with F_1 components, ($J = N^+ + 1/2$) lying at a lower energy level than the F_2 components, ($J = N - 1/2$). This multiplet structure, commonly known as spin-splitting, arises as a result of interaction between the electron spin vector and the orbital electronic angular momentum vector along the internuclear axis. In Hund case (a) both the spin vector and the orbital electronic momentum vector are coupled strongly to the internuclear axis. The interaction of nuclear rotation with electronic motion (spin as well as orbital) is very weak. The result is that even in the rotating molecule the electronic angular momentum quantum number Ω , where $\Omega = \Lambda + \Sigma$, is well defined. The angular momentum of the nuclear rotation R and Ω form the resultant J which represents the total angular momentum of the molecule given by $J = \Omega, \Omega + 1, \Omega + 2, \dots$. Here Ω is integral or half-integral depending on whether the number of electrons in the molecule is even or odd. Further, since Ω is the component of J , J is integral when Ω is integral and half integral when Ω is half integral. Naturally, J cannot be smaller than its component Ω . Therefore, the levels with $J < \Omega$ do not occur. In a ${}^2\Pi_i$ state, such a spin-splitting manifests itself in an appreciable two-fold degeneracy resulting in two sub-

[†]Following a decision of the Joint Commission for Spectroscopy in 1952 (see J. Opt. Soc. Amer. 43, 425, 1953), the symbol K has been replaced by N. The symbol K is used for symmetric top molecules.

states $^2\Pi_{3/2}$ and $^2\Pi_{1/2}$. The rotational energy in Hund case

(a) takes the form

$$F_v(J) = B_v [J(J+1) - \Omega^2] - D_v J^2 (J+1)^2 + \dots, \quad (2-1)$$

where the terms $F_v(J)$, B_v and D_v carry their usual spectroscopic meanings. As long as the rotations are small, the Hund case (a) is operative and the electron spin continues to be coupled to the internuclear field. The energy of separation between the corresponding F_1 and F_2 components is larger than the energy separation between the adjacent rotational levels. As molecular rotations become faster, the spin uncouples from the orbital angular momentum and becomes coupled to the field generated by the molecular rotation. Here the molecule enters the domain of Hund case (b). The spin vector S is not coupled to the internuclear axis at all. This means that Ω is no longer well defined. The angular momenta Λ and R form a resultant which is defined by N given as

$$N = \Lambda, \Lambda + 1, \Lambda + 2, \Lambda + 3 \dots, \quad (2-2)$$

where N is the total angular momentum of the molecule apart from spin. In this situation the angular momenta N and S form a resultant J , the total angular momentum including spin, and may be expressed by the relation

$$J = (N + S), (N + S - 1), \dots |N - S|. \quad (2-3)$$

The energy of the levels here is mainly determined by N and the spin causes a small splitting of the levels into sub-levels. The rotational energy takes the form

$$F_v(N) = B_v [N(N+1) - \Lambda^2] + \text{small terms due to spin-splitting} \quad (2-4)$$

In fact, in most of the actual cases $^2\Pi$ states are close to Hund case (a) for slow rotations and close to case (b) for fast rotations. Incidentally, OH represents a typical case where one finds a rapid transition from case (a) to case (b) while going to higher rotational levels.

The rotational term values of spin components of a $^2\Pi$ state for an intermediate case or, in other words, for any magnitude of spin-orbit-coupling have been calculated theoretically by Hill and Van Vleck (1928). In the case of the $^2\Pi_{3/2}$ and $^2\Pi_{1/2}$ states, the respective relations according to Herzberg (1950) are

$$F_1(J) = B_v \left[(J + 1/2)^2 - 1 - 1/2 \left\{ 4(J + 1/2)^2 - 4 \left(\frac{A}{B_v} \right) + \left(\frac{A}{B_v} \right)^2 \right\}^{1/2} \right] - D_v J^4, \quad (2-5)$$

$$F_2(J) = B_v \left[(J + 1/2)^2 - 1 + 1/2 \left\{ 4(J + 1/2)^2 - 4 \left(\frac{A}{B_v} \right) + \left(\frac{A}{B_v} \right)^2 \right\}^{1/2} \right] - D_v (J + 1)^4. \quad (2-6)$$

If, however, these relations are expressed in terms of N and neglecting the centrifugal force term D_V , we get

$$F_1(N) = B_V \left[(N + 1)^2 - 1 - 1/2 \left\{ 4(N + 1)^2 + Y_V (Y_V - 4) \right\}^{1/2} \right]$$

... (2-7)

$$F_2(N) = B_V \left[N^2 - 1 + 1/2 \left\{ 4N^2 + Y_V (Y_V - 4) \right\}^{1/2} \right],$$

... (2-8)

where $Y_V = A/B_V$. Here Y_V represents the coupling constant and other symbols have their usual spectroscopic meanings. When there is a large spin-orbit uncoupling [Hund case (b)], Y_V is too small, and the square root term in the above relations can be replaced by

$$2(J + 1/2) = \frac{Y_V (Y_V - 4)}{4(J + 1/2)} . \quad (2-9)$$

Substituting this value and also $J = N + 1/2$ and $N = 1/2$, the respective terms become

$$F_1(N) = B_V N(N + 1) - 1 + \frac{Y_V (4 - Y_V)}{8(N + 1)} + \dots , \quad (2-10)$$

$$F_2(N) = B_V N(N + 1) - 1 - \frac{Y_V (4 - Y_V)}{8N} . \quad (2-11)$$

When Y_v is too large in the case of strong spin-orbit coupling [Hund case (a)], these two formulas may be combined giving the expression

$$F(J) = B_{\text{eff}} J (J+1) - D_v J^2 (J+1)^2, \quad (2-12)$$

where B_{eff} is slightly different for the two multiplets.

According to Mulliken (1931), B_{eff} for these doublet states is

$$B_{\text{eff}} = B [1 \pm B_v / A + \dots]. \quad (2-13)$$

Using the above formulas, one can determine the spin multiplet separations whatever the coupling conditions might be.

In addition to spin multiplet structure arising out of spin-orbit interactions there exists yet another splitting of each spin component of a $^2\Pi$ state. Both $F_1(J)$ and $F_2(J)$ states are two-fold degenerate. This degeneracy arises out of the interaction between the nuclear rotation and the orbital angular momentum which gives each spin-split level a positive or negative symmetry. This is known as Λ - doubling. The two Λ - components are characterized by opposite symmetry with respect to inversion at the origin of the coordinates (π_i^+ and π_i^-). Such a splitting manifests itself appreciably well, particularly for greater speeds of rotation or, in other words, at higher J values. In Hund case (a), when the spin doublets of a $^2\Pi$ state are quite far apart, Λ -doubling in the

$^2\Pi_{1/2}$ component varies with the first power of J while in the $^2\Pi_{3/2}$ component, it is relatively very small. It is only in a higher order approximation that the $^2\Pi_{3/2}$ component exhibits a Λ -splitting proportional to J^3 . According to Kovacs (1969), in the Hund case (a) the Λ -separations can be expressed as

$$\Delta\nu(^2\Pi_{3/2}) = 2 \frac{C_1}{Y_V^2} + \frac{C_2}{Y_V} (J - 1/2) (J + 1/2) (J + 3/2), \quad (2-14)$$

and

$$\Delta\nu(^2\Pi_{1/2}) = 2 (C_1 + C_2) (J + 1/2) \quad (2-15)$$

whereas in the Hund case (b)

$$\Delta\nu(^2\Pi_{3/2}) = C_2 (N + 1) N + C_1 (N + 1), \quad (2-16)$$

and

$$\Delta\nu(^2\Pi_{1/2}) = C_2 (N + 1) N - C_1 N \quad (2-17)$$

where C_1 , C_2 and Y_V are the parameters involving different coupling constants.

In the case of $^2\Pi_{1/2}$ state of OH, a reversal is observed for a Λ -doubling between $N = 4$ and $N = 5$ as one would expect on the basis of the relative values of C_2 and C_1 as applied to OH. Mulliken and Christy (1931) have studied the changes in C_1 and C_2 as a function of J for increasing rotations.

In addition, the nuclear spin of the molecule induces further splittings in these lambda-components, thereby causing what is known as "hyperfine multiplet structure." Interaction with an external magnetic field results in further split-up of the hyperfine structure. Such a set of levels is encountered in the study of microwave zeeman effect or the electron spin resonance spectrum of this molecule. Figure 2-2 depicts all such multiplet structures.

The state $^2\Sigma^+$: In such an electronic state, the molecule possesses no resultant orbital angular momentum along the internuclear axis ($\Lambda = 0$) and the electron spin S is always coupled to the rotation axis of the molecule. The Hund case (b) applies to all N values. The lowest rotational level is $J = 0$, rather than 1 as in the case of a $^2\Pi$ state. However, if N is not equal to zero, there exists a Λ -type doubling due to magnetic coupling of the spin and the momentum due to rotation. The two doublet components F_1 and F_2 are coincident for $N = 0$. The rotational energy terms for F_1 and F_2 are expressed as

$$F_{J=1/2}(N) = F_1(N) = B_V N(N + 1) -$$

$$D_V N^2(N + 1)^2 + 1/2 \gamma N, \quad \dots \quad (2-18)$$

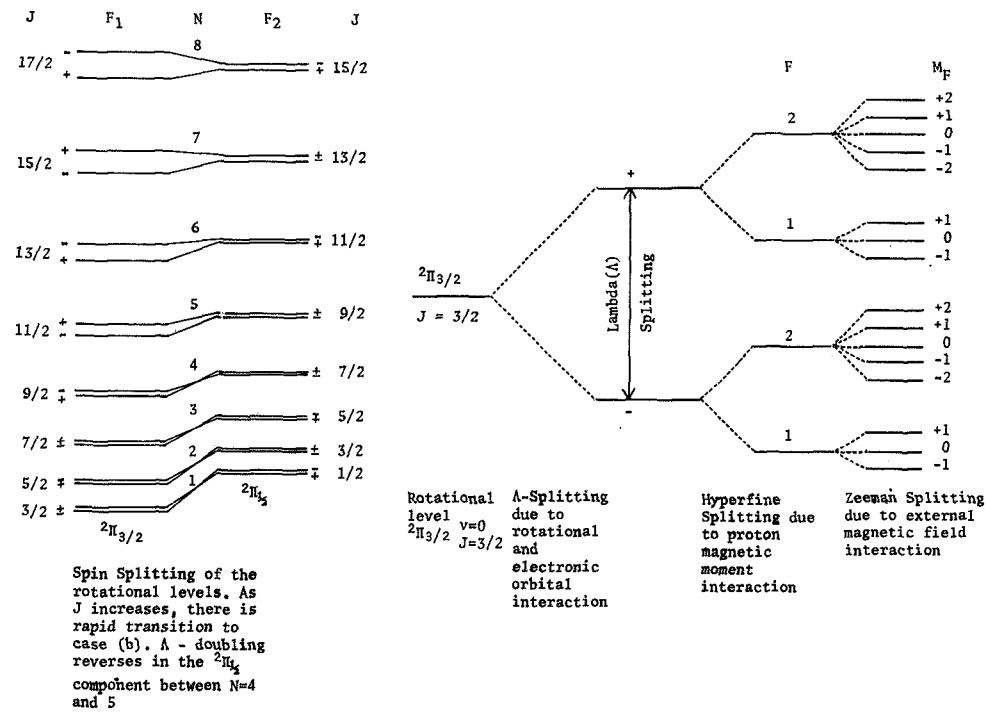


Figure 2-2 Spin splitting of the rotational levels is shown in the left side. The splittings of a single rotational level due to various interactions are shown in the right.

and

$$F_{J+1/2}(N) = F_2(N) = B_v N(N+1) - D_v N^2(N+1)^2 - 1/2 \gamma (N+1). \quad (2-19)$$

From these above expressions the doublet splitting can be derived as

$$\Delta F_{12}(N) = \gamma(N+1/2). \quad (2-20)$$

The splitting constant γ is very small compared to B_v and is usually, though not necessarily, positive. As a matter of fact, both the quantities D_v and γ are so small that the deviations caused by them are observable only at higher rotational quantum numbers.

SPECTRAL FEATURES OF BAND STRUCTURE IN DIFFERENT RADIATIVE TRANSITIONS

Three groups of rotational structures corresponding to the three types of electronic transitions, $^2\Sigma - ^2\Sigma$, $^2\Sigma - ^2\Pi_i$, and $^2\Pi - ^2\Pi$, have been identified in OH spectra.

$^2\Sigma - ^2\Sigma$ Transition: Rotational structure in the bands arising out of the electronic transition $^2\Sigma - ^2\Sigma$ is characterized by single P and R branches quite similar to the simplest type of $^1\Sigma - ^1\Sigma$ transition. Each of these lines are further resolved into two strong components and one weak

satellite. Thus, the R-branch consists of R_1 , R_2 , and R_{21} and P of P_1 , P_2 , and P_{12} . The lines $R_2(0)$, $P_2(1)$, and all $P(0)$ lines are missing. All such branches are shown in figure 2-3. Since $^2\Sigma$ state always belongs to Hund case (b), only the selection rule $\Delta N = \pm 1$ holds. $\Delta N = 0$ is not valid in a $^2\Sigma - ^2\Sigma$ transition; consequently, Q branches are missing. The separation of the two sub-levels with $J = N + 1/2$ and $J = N - 1/2$ for a given N is, in general, quite small as compared to the separation between successive rotational levels. Under normal instrumental resolutions one, therefore, gets the same band structure as for $^1\Sigma - ^1\Sigma$ bands except that the lines are now to be numbered by N instead of J. If the indices 1 and 2 correspond to $J = N + 1/2$ and $J = N - 1/2$ respectively, one gets six branches (4 main and 2 satellite) given in table 2-1.

The rotational terms for spin multiplets of a $^2\Sigma$ state are given below.

$$F_1(N) = B_v N(N + 1) + 1/2 \gamma N - D_v N^2 (N + 1)^2 ,$$

... (2-21)

and

$$F_2(N) = B_v N(N + 1) - 1/2 \gamma (N + 1) - D_v N^2 (N + 1)^2 ,$$

... (2-22)

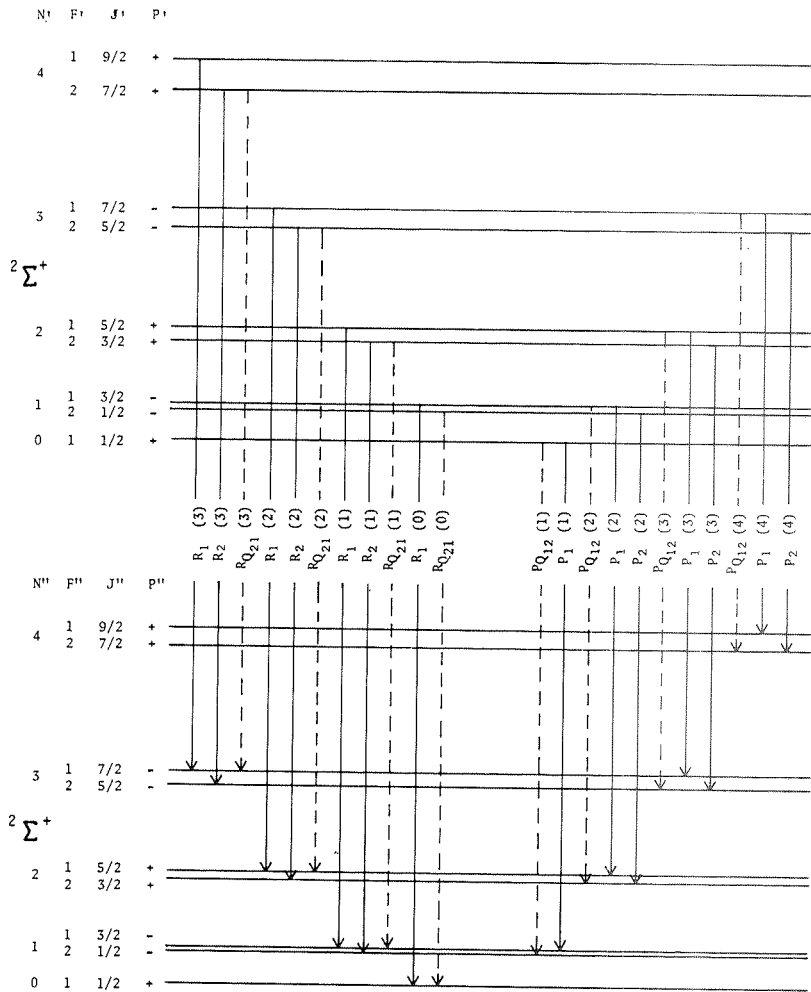


Figure 2-3 Schematic of the various branches in the rotational structure of OH expected in an electronic transition $^2\Sigma^+ - ^2\Sigma^+$.

TABLE 2-1 TERM VALUE DIFFERENCES AND SELECTION RULES
FOR $^2\Sigma - ^2\Sigma$ TRANSITIONS

Nomenclature	Term Value Differences $\nu \text{ cm}^{-1}$	Selection Rules ΔN	Selection Rules ΔJ	Remarks
P_1	$F'_1 (N - 1) - F''_1 (N)$	-1	-1	
R_1	$F'_1 (N + 1) - F''_1 (N)$	+1	+1	
P_2	$F'_2 (N - 1) - F''_2 (N)$	-1	-1	Main Branches
R_2	$F'_2 (N + 1) - F''_2 (N)$	+1	+1	
$R_{Q_{21}}$	$F'_2 (N + 1) - F''_1 (N)$	+1	0	Satellites
$P_{Q_{12}}$	$F'_1 (N - 1) - F''_2 (N)$	-1	0	

where γ represents the spin-splitting constant.

From the above, one can determine the spin doubling as follows:

$$\Delta\nu_{1,2}(P) = (P_1 - P_2) = (\gamma' - \gamma'') N - 1/2 (\gamma' - \gamma'')$$

... (2-23)

and

$$\Delta\nu_{1,2}(R) = (R_1 - R_2) = (\gamma' - \gamma'') N + 1/2 (3\gamma' - \gamma'')$$

... (2-24)

The splitting of lines in the branches increases linearly with N , the magnitude depending essentially on the difference of the splitting factors in the upper and the lower states.

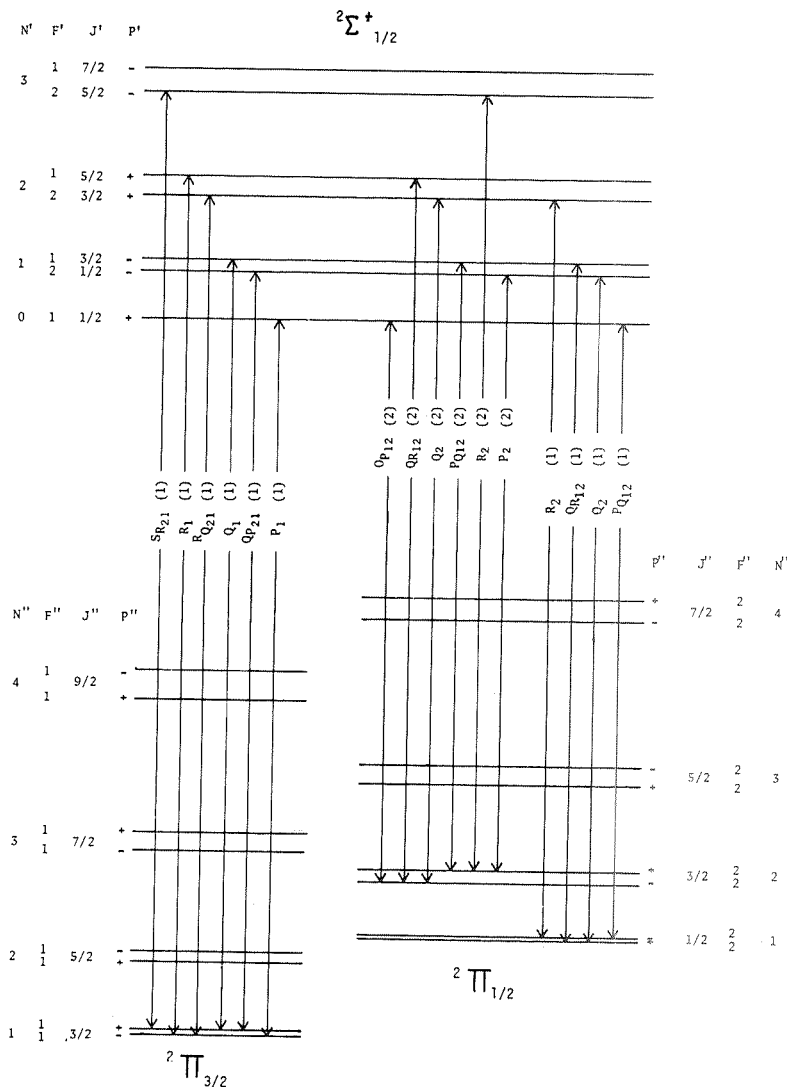


Figure 2-4 Schematic of the various branches in the rotational structure of OH expected in an electronic transition $^2\Sigma^+ - ^2\Pi$.

$^2\Sigma - ^2\Pi$ Transition: The appearance of $^2\Sigma - ^2\Pi$ bands differs considerably according to whether the state $^2\Pi$ belongs to Hund case (a) or (b) or intermediate between (a) and (b), and to the magnitude of spin doubling of the rotational levels in the state $^2\Sigma$. The band structure characteristics arising from the different nature of the $^2\Pi$ state are briefly discussed below.

$^2\Sigma - ^2\Pi$ (a): When the state $^2\Pi$ belongs to Hund case (a), the spin-orbit coupling is strong and there exist two distinct sub-bands $^2\Sigma - ^2\Pi_{3/2}$ and $^2\Sigma - ^2\Pi_{1/2}$. Each sub-band has six branches (3 main branches and 3 satellites) making 12 branches in all. These are identified as

$^2\Sigma - ^2\Pi_{3/2}:$	P_1	Q_1	R_1	main branches
	Q_P	P_Q	Q_R	satellites
	$_{12}$	$_{12}$	$_{12}$	

$^2\Sigma - ^2\Pi_{1/2}:$	P_2	Q_2	R_2	main branches
	Q_P	R_Q	S_R	satellites
	$_{21}$	$_{21}$	$_{21}$	

and are depicted schematically in figure 2-4. Here the satellites are of almost the same intensity as the main branches. The term values of these 12 branches are presented in table 2-2.

$^2\Sigma - ^2\Pi$ (b): When the spin-orbit coupling gets progressively weaker, the state $^2\Pi$ moves towards Hund case (b). While the main six branches continue to be strong, the

TABLE 2-2 TERM VALUE DIFFERENCES AND SELECTION RULES
FOR $^2\Sigma - ^2\Pi(a)$ TRANSITIONS

Nomenclature	Term Value Differences $\nu \text{ cm}^{-1}$	Selection Rules		Remarks
		ΔN	ΔJ	
P_1	$F'_1 (N - 1) - F''_1 (N)$	-1	-1	
Q_1	$F'_1 (N) - F''_1 (N)$	0	0	
R_1	$F'_1 (N + 1) - F''_1 (N)$	+1	+1	
P_2	$F'_2 (N - 1) - F''_2 (N)$	-1	-1	Main Branches
Q_2	$F'_2 (N) - F''_2 (N)$	0	0	
R_2	$F'_2 (N + 1) - F''_2 (N)$	+1	+1	
$Q_{P_{21}}$	$F'_2 (N) - F''_1 (N)$	0	-1	
$R_{Q_{21}}$	$F'_2 (N + 1) - F''_1 (N)$	+1	0	
$S_{R_{21}}$	$F'_2 (N + 2) - F''_1 (N)$	+2	+1	
$P_{Q_{12}}$	$F'_1 (N - 1) - F''_2 (N)$	-1	0	Satellites
$Q_{R_{12}}$	$F'_1 (N) - F''_2 (N)$	0	+1	
$O_{P_{12}}$	$F'_1 (N - 2) - F''_2 (N)$	-2	-1	

satellites get weaker and weaker and finally become extinct when the coupling becomes insignificant and the state $^2\Pi$ conforms exclusively to Hund case (b). At such a stage only the six strong branches are observed.

In intermediate stages of coupling when the state $^2\Pi$ approaches to Hund case (b), two outer satellites $(O_{P_{12}}$ and $S_{R_{21}}$) are entirely absent ($\Delta N \neq \pm 2$) and the remaining four

$\left(Q_{P_{21}}, P_{Q_{12}}, R_{Q_{21}}, Q_{R_{12}} \right)$ are also very weak and fall off rapidly as N increases.

$X^2\Pi - X^2\Pi$: The fine structure of infrared rotation-vibration bands of OH is characteristic of a $^2\Pi - ^2\Pi$ transition. Here the rotation-vibration transitions take place within the same ground electronic state $^2\Pi$.

In Hund case (a) the selection rule $\Delta\Sigma = 0$ holds and as a result each $X^2\Pi - X^2\Pi$ band splits into two sub-bands

$^2\Pi_{1/2} - ^2\Pi_{1/2}$ and $^2\Pi_{3/2} - ^2\Pi_{3/2}$. Each of these sub-bands should have six branches forming three close pairs, namely, 2 P, 2 Q, and 2 R. Since Q branches are very weak and each sub-band has only one head, apparently each band has only two heads. These two sub-bands, however, differ in the number of missing lines at the beginning of the branches and in the magnitude of the Λ -type doubling, which is appreciably greater for $^2\Pi_{1/2}$ than for the $^2\Pi_{3/2}$.

In Hund case (b), the selection rule $\Delta N = 0, \pm 1$ holds and the rule that branches corresponding to $\Delta N \neq \Delta J$ are very weak also holds. There are again twelve branches which correspond completely to those of case (a) except that now they do not form two separate sub-bands. Since in such a condition, there is an appreciable amount of Λ -doubling, each spin component is once more split into two components. The additional 12 satellite branches with $\Delta N \neq \Delta J$ are usually not observed, although theoretically predicted. These would make the total number of possible branches as much as 24.

The rotational line strengths for the $^2\Pi - ^2\Pi$ bands of OH with intermediate coupling have been evaluated theoretically by Benedict, Plyler, and Humphreys (1953). According to their estimations, the vibration-rotation bands of OH exhibit a series of lines grouped in sets of four. These groups consist of the pairs of spin doublets whose separation decreases with increasing N. Each component of the spin doublet is itself a Λ -doublet whose separation increases with increasing N. The term values for various branches of $^2\Pi - ^2\Pi$ transitions are given in table 2-3 and schematically depicted in figure 2-5.

TABLE 2-3 TERM VALUE DIFFERENCES AND SELECTION RULES
FOR $^2\Pi - ^2\Pi$ TRANSITIONS

<u>Nomenclature</u>	<u>Term Value Differences</u> ν (cm^{-1})	<u>Selection Rules</u>		<u>Remarks</u>
		ΔN	ΔJ	
P_1	$F'_1(N-1) - F''_1(N)$	-1	-1	
Q_1	$F'_1(N) - F''_1(N)$	0	0	
R_1	$F'_1(N) - F''_1(N-1)$	+1	+1	Main Branches
P_2	$F'_2(N-1) - F''_2(N)$	-1	-1	
Q_2	$F'_2(N) - F''_2(N)$	0	0	
R_2	$F'_2(N) - F''_2(N-1)$	+1	+1	
Q_{21}	$F'_2(N) - F''_1(N)$	0	-1	
R_{21}	$F'_2(N) - F''_1(N-1)$	+1	0	
$S_{R_{21}}$	$F'_2(N) - F''_1(N-2)$	+2	+1	Satellites
$P_{Q_{12}}$	$F'_1(N-1) - F''_2(N)$	-1	0	
$Q_{R_{12}}$	$F'_1(N) - F''_2(N)$	0	+1	
$O_{P_{12}}$	$F'_1(N-2) - F''_2(N)$	-2	-1	

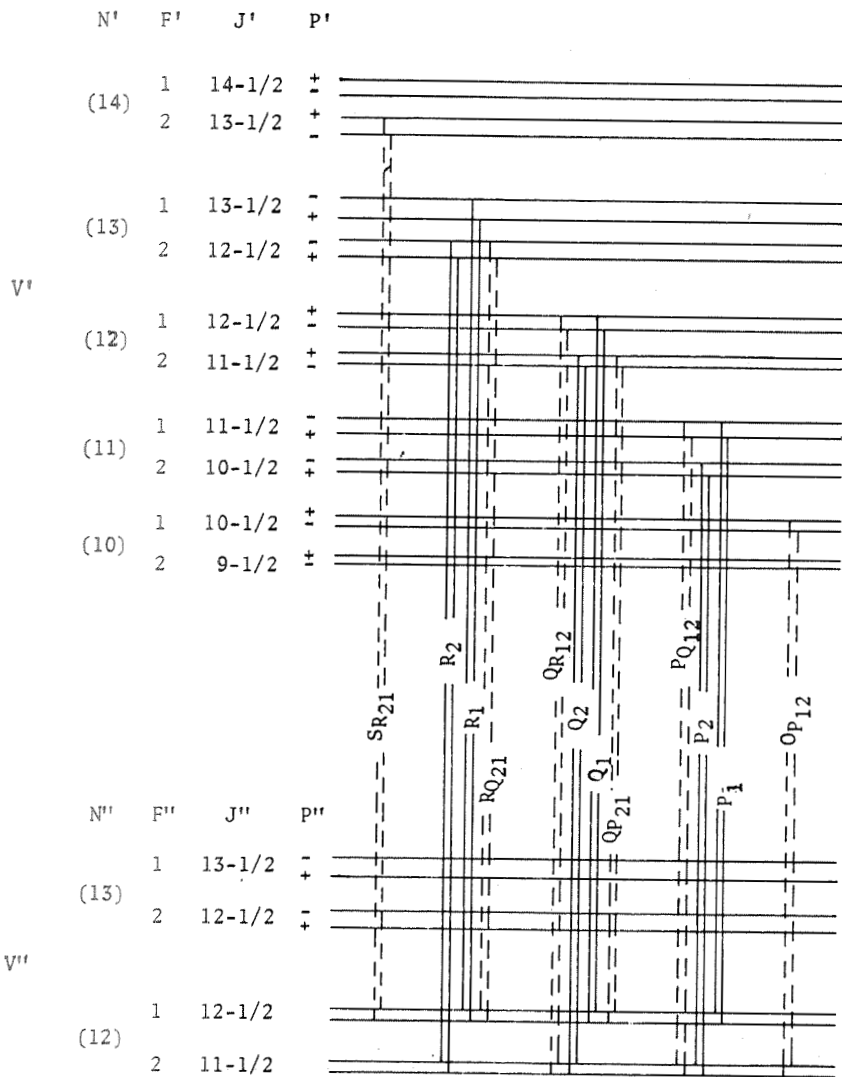


Figure 2-5 Schematic of the rotation-vibration transitions of OH in the ground electronic state for Hund case (b).

OBSERVED SPECTRA OF OH

The observed spectra of the OH radical cover an extensive spectral region, from vacuum ultraviolet to the radiofrequencies. Depending upon the nature of the transitions involved, these spectra can be classified in the following three broad categories.

Electronic Spectra

Rotation-Vibration Spectra

Rotational and Sub-Rotational Spectra.

ELECTRONIC SPECTRA

This class of spectra is characterized by radiative transitions between various electronic states of diatomic OH. In this category five electronic radiative transitions have been observed and identified.

System A

$A^2\Sigma^+ \leftrightarrow X^2\Pi_{3/2, 1/2}$ (4107 - 2444 \AA): This group of bands is perhaps the most easily excitable band system of the OH molecule and consequently observed even if water vapor is present as a minor impurity in any discharge. The well known "water vapor bands" known to be among the earlier observed, one time assigned to H_2O or O_2 , were eventually identified with this band system of OH. Most of the system lies in the ultraviolet region and has been extensively studied both in absorption and

emission from a variety of sources. Grebe and Holtz (1912) were perhaps the first to measure the rotational lines of the 3064\AA band which is the strongest one in the system. Heurlinger (1917) gave a formal classification to these lines but the significance of this classification could not be recognized in the absence of any plausible theory of the band spectra in those days. Further progress in this area was characterized by the measurements and analyses of the additional bands by various authors [Watson (1924); Dieke (1925); Jack (1927, 1928 a, b); Tanaka and Siraishi (1933); Tanaka and Koana (1933, 1934); Dawson and Johnston (1933); Chamberlain and Cuther (1933); Johnston, Dawson and Walker (1933)]. Because these measurements were made utilizing low dispersion instruments, the results reported by different workers varied quite often in their details. Another series of investigations on OH spectra dealt with the behavior of OH bands in different light sources, namely, flames and chemiluminescence (Oldenberg, 1935; Frost and Oldenberg, 1936 a, b; Oldenberg and Rieke, 1938 a, b, c). The latest exhaustive work on the ultraviolet bands of OH is that of Dieke and Crosswhite (1948, 1962) and is undoubtedly superior to the work reported earlier. These authors used the bluish outer cone of an oxyacetylene flame to produce these bands and recorded the spectrum on a 21-foot concave grating spectrograph in the second order (linear dispersion $\sim 0.6 \text{\AA/mm}$). There have been, however, a few subsequent additions to these data character-

ized by the identification of the additional sequences. For instance, Stoebner and Delbourgo (1967) identified the $\Delta v = -2$ band sequence using an oxygen hydrogen reaction in a flow system under low pressure in a Geissler discharge tube. Later, Bass and Broida (1953) published a spectrographic atlas showing the intensity distribution of these bands. The Deslandres scheme, showing the wavelengths and intensity estimates for the band-heads of different OH bands in this system so far reported, is presented in table 3-1.

TABLE * 3-1 THE DESLANDRES SCHEME OF A $^2\Sigma^+$ \leftrightarrow X $^2\Pi_g$

v'	0	1	2	3	4	5
0	<u>3064</u>	3428	3843			
	10	7				
1	2811	3122	3484	3898		
	9	9	6			
2	2609	2875	3185		3959	
	4	9	6			
3	2444	2677	2945	3254		
	1	5	6	4		
4		2517	2753	3022	3331	
		2	4	5	4	

* Rosen (1970)

Note - Underlined band is the most characteristic in A-X system.

This band system is allowed by the change in electric dipole moment which results from the electronic transition $A\ ^2\Sigma - X\ ^2\Pi$. There are only six allowed branches, namely, P_1, Q_1, R_1 , and P_2, Q_2, R_2 corresponding to the transitions $A\ ^2\Sigma^+ - X\ ^2\Pi_{3/2}$ and $A\ ^2\Sigma^+ - X\ ^2\Pi_{1/2}$, respectively. Yet, when the $^2\Pi$ states belong to Hund case (a), the spin-orbit-coupling is large leading to a large separation between the multiplets $^2\Pi_{3/2}$ and $^2\Pi_{1/2}$; the selection rule $\Delta N = 0, \pm 1$ no longer holds, and all the transitions follow the selection rule $\Delta J = 0, \pm 1$ and $+ \leftrightarrow -$. In addition, there are satellite branches for which $\Delta J = \Delta N$ and the intensity decreases rapidly with increasing N . These satellites have the same form as the six main branches. For a small doublet-splitting of the $^2\Sigma^+$ state, these lines lie very close to the corresponding lines of the main branches. This description is applicable only for lower J quantum numbers. For higher J values ($J \geq 4$) when the Hund case (b) becomes important, the satellites are seldom observed. Figure 2-4 represents all such possible transitions.

As mentioned in Chapter 1, a comprehensive report on the various vibrational and rotational transitions involving the electronic $A\ ^2\Sigma^+$ and $X\ ^2\Pi_i$ was presented by Dieke and Crosswhite (Bumblebee Series Report No. 87, 1948). This document has also appeared in its original form without any updating or modifications as an open literature article (Dieke and Crosswhite, 1962). The report presents the useful and reliable structural data on nine bands of this system along with

the combinational differences for the various vibrational and rotational transitions involved. It also presents computed values for the various transition probabilities. Because this publication is almost complete in its scope and has been the subject of frequent citations, the data given have not been reproduced in the present monograph. As mentioned earlier, however, Stoebner and Delbourgo (1967) identified three additional bands in the region $3844 - 4107\text{\AA}$ forming a new sequence $\Delta v = -2$ in this system. They presented a rotational analysis for these new vibrational transitions (0,2), (1,3) and (2,4), and determined the values of the rotational displacements, ΔF_J ($v' = 4$), for the level $v'' = 4$ which were hitherto undetermined. They also obtained the value of the coupling constant "a" ($a = -8.547$ for $v'' = 4$). These observations were taken under relatively low dispersion (Hilger quartz/glass spectrograph) compared to those of Dieke and Crosswhite (21-foot grating; second order). Therefore, the rotational displacements for the levels $v' = 0, 1, 2$ and $v'' = 2, 3$ determined by these authors on the basis of these new bands cannot be regarded as more accurate compared to those reported by Dieke and Crosswhite. Because of this, only wavelength data for P, Q, and R branches of these three new bands for $v'' = 4$ are presented in tables 3-2, 3-3 and 3-4.

OH Lines in the Solar Spectrum: A large number of rotational lines belonging to the OH bands in the ultraviolet system $A\ 2\Sigma^+ - X\ 2\Pi_i$ have been identified in the solar spectrum.

TABLE[†] 3-2 OBSERVED WAVENUMBERS OF THE A $^2\Sigma^+$ - X $^2\Pi_g$ SYSTEM
(0, 2) BAND

N	P ₁	Q ₁	R ₁	P ₂	Q ₂	R ₂
1	25469.8	25503.3	2570.0	25343.8	* 25375.3	* 25444.1
2	426.0	493.2	595.0	320.5	388.3	488.3
3	* 384.3	485.2	620.3	294.0	395.7	530.4
4	* 343.8	478.6	647.5	* 266.2	--	* 570.0
5	305.3	472.0	* 675.2	236.7	--	606.7
6	* 266.2	466.7	702.5	205.6	407.3	641.7
7	228.6	460.8	729.9	173.6	407.3	* 675.2
8	191.1	* 455.7	757.8	140.9	407.3	706.8
9	154.2	450.0	784.5	107.7	--	738.0
10	117.4	* 444.1	810.4	073.8	--	767.0
11	080.2	437.2	835.8	039.5	--	794.6
12	043.6	* 430.8	859.2	* 005.7	395.7	821.1
13	* 005.7	424.0	882.9	* 24970.1	389.9	845.8
14	* 24970.1	415.4	904.9	* 934.6	--	869.1
15	* 934.6	* 406.5	925.5	899.0	* 375.3	890.5
16	896.9	397.4	* 943.5	* 863.4	367.4	910.1
17	859.1	--	959.9	827.8	357.2	927.5
18	822.1	373.6	974.7	790.2	* 345.9	* 943.5
19	783.9	* 360.3	987.9	753.1	334.1	957.9
20	745.3	* 345.9	998.3	--	320.4	968.5
21	706.1	330.4	26006.9	--	--	* 976.7
22	666.0	313.3	* 011.6	--	287.6	983.7
23	625.5	--	015.1	597.0	--	987.3
24	583.1	--	015.1	556.5	* 250.4	987.3
25	540.9	* 248.2	* 011.6	511.5	* 228.6	982.1
26	498.3	223.2	* 006.9	470.0	* 205.6	976.7
27		453.8		25994.2		

[†]Stoebner and Delbourgo (1967)

*The lines which have not been resolved completely or which correspond to a number of theoretical transitions.

TABLE[†] 3-3 OBSERVED WAVENUMBERS OF THE A $^2\Sigma^+$ - X $^2\Pi_1$ SYSTEM
(1,3) BAND

N	P ₁	Q ₁	R ₁	P ₂	Q ₂	R ₂
1	--	25250.4	25316.4	*25095.1	25123.0	25192.4
2	*25176.4	240.0	338.6	069.6	134.3	231.2
3	* 134.3	* 231.2	360.3	043.6	140.9	--
4	* 095.1	224.3	384.8	* 017.3	--	305.3
5	056.7	216.0	--	24987.3	147.2	339.7
6	* 017.3	* 208.1	433.5	* 956.2	147.2	371.4
7	24980.1	201.4	--	924.5	146.2	401.7
8	942.1	193.4	--	891.3	--	--
9	904.2	185.2	503.3	856.8	--	455.7
10	866.2	* 176.4	* 524.7	822.1	* 134.3	480.3
11	* 827.8	167.0	544.9	788.2	* 128.3	--
12	788.2	156.3	563.8	* 750.5	* 119.5	* 524.7
13	* 750.5	* 146.2	581.5	712.7	109.9	543.9
14	711.1	* 134.3	--	674.3	100.5	560.8
15	671.2	* 119.5	--	--	088.5	577.0
16	631.1	105.8	623.6	597.0	--	590.5
17	589.6	092.9	633.6	557.0	059.7	600.0
18	548.3	--	--	516.6	--	609.0
19	506.0	* 059.7	646.5	475.2	022.0	615.0
20	463.1	--	646.5	433.4	24996.0	--
21	417.3	* 022.0	--	389.1	966.6	--
22				345.4		616.0

[†]Stoebner and Delbourgo (1967)

*The lines which have not been resolved completely or which correspond to a number of theoretical transitions.

TABLE[†] 3-4 OBSERVED WAVENUMBERS OF THE A 2Σ⁺ - X 2Π_i SYSTEM

N	(2, 4) BAND					
	P ₁	Q ₁	R ₁	P ₂	Q ₂	R ₂
1	*24934.6	*24966.6	25025.4	*24807.8	24837.8	—
2	894.1	*956.2	49.0	786.4	847.4	24938.4
3	853.9	*944.7	68.0	761.9	853.9	975.5
4	815.4	938.9	88.5	734.7	857.7	—
5	776.4	925.7	*	706.1	857.7	*25039.5
6	736.9	918.0	130.1	674.3	857.7	*
7	698.4	907.9	*150.3	—	853.9	*
8	659.1	*	899.0	—	608.0	92.9
9	620.1	887.4	—	572.5	—	118.6
•10	580.7	875.3	202.9	535.9	842.8	*
11	539.2	*	864.7	—	—	140.9
12	498.6	—	*	498.6	—	—
13	458.8	837.8	—	460.6	—	—
14	*	417.3	—	420.2	*	193.4
15	*	803.7	253.7	380.5	786.4	—
					769.3	—

[†]Stoebner and Delbourgo (1967)

*The lines which have not been resolved completely or which correspond to a number of theoretical transitions.

In the (0,0), (1,1), and (2,2) bands, a total of 175 solar lines are ascribed to OH unblended and 124 have OH as a partial contributor. A list of such OH lines and other relevant data are presented in Appendix A for ready reference (Moore and Broida, 1959).

System B' (Intercombinational)

$B\ 2\Sigma^+ \rightarrow A\ 2\Sigma^+$ (5660 - 4216 Å): Schuler and Woeldike (1943)

were probably the first to identify these bands in the spectrum obtained in water vapor discharge. The system was further studied by Schuler, Reinebeck, and Michel (1954); Benoist (1955); Barrow (1956); Barrow and Downie (1956); and Herman, Felenbok, and Herman (1961). However, Felenbok (1963) re-investigated the OH bands in emission from a tungsten-water surface spark source. Using such a source he investigated (0,6), (0,7), (0,8), and (1,9) bands of the system and reported their rotational analysis with precision. Also, the spin doubling in the (0,6), (0,7), and (0,8) bands was measured and a breaking-off was observed for the rotational lines P(16) and R(14) for the band (0,7) and P(9), and R(7) for the bands (1,6) and (1,9), respectively. This breaking-off phenomenon was interpreted as due to the predissociation by the rotation of the upper state. Recently, Czarny and Felenbok (1968) made a high resolution study of these bands using a high frequency excited water vapor jet. They identified the satellite line $P_{Q_{12}}$ and observed the perturbations, namely, (a) the change of γ sign between $v'' = 5$ and $v'' = 6$; (b) the

rotational line half width variation for the bands (0,8), (0,7) and (0,6); and (c) the increase in the half width for $N \geq 6$ in the (0,8) band. Carloni and Dalby (1969a) also carried out a similar investigation of OH and observed an additional band (1,4) but they failed to observe (1,7) band. The rotational analysis of this system is presented in table 3-5.

TABLE* 3-5 OBSERVED WAVENUMBERS OF THE $B^2\Sigma^+$ - $A^2\Sigma^+$ SYSTEM

N	R ₂	R ₁	P ₂	P ₁
(1,9)				
0	18058.76			
1	18063.57	18063.30	18038.72	
2	18064.76	18064.30	18024.05	18023.57
3	18062.59	18062.00	18006.05	18005.42
4	18057.54	18056.80	17985.60	17984.79
5	18050.14	18049.18	17963.43	17962.45
6	18041.14	18039.99	17940.66	17939.44
7	18031.72	18030.24	17918.62	17917.25
8	18021.44	18019.80	17899.87	17898.38
(0,8)				
0	18238.46			
1	18242.14		18211.56	
2	18239.50	18239.21	18188.80	18188.45
3	18230.53	18230.07	18159.67	18159.16
4	18215.53	18214.90	18124.67	18124.02
5	18194.81	18194.14	18084.20	18083.40
6	18168.94	18168.03	18038.81	18037.88
7	18138.48	18137.45	17989.15	17988.08
8	18104.29	18103.03	17935.88	17934.64
9	18067.22	18065.83		
(0,7)				
0	19512.3			
1	19512.3		19481.9	
2	19502.5		19451.5	
3	19482.8		19411.9	
4	19453.3		19362.4	
5	19414.5	19413.9	19303.9	19303.1
6	19366.2		19256.2	19235.5
7	19309.2	19308.5	19160.1	19158.9
8	19243.1		19075.2	

* Carloni and Dalby (1969b, Depository of Unpublished Data of NRC Library, Canada).

TABLE 3-5 (Continued)

N	R ₂	R ₁	P ₂	P ₁
(0,6)				
0	21136.8			
1	21134.4		21103.8	
2	21119.3		21068.3	
3	21091.4		21020.4	
4	21051.0		20960.2	
5	20998.4	20997.8	20888.1	
6	20933.8	20932.8	20803.7	20802.6
7	20856.6	20856.1	20707.4	20706.6
8			20600.2	20598.8
(1,6)				
0	21795.2			
1	21788.1		21763.2	
2	21766.9		21726.1	
3	21730.6		21674.1	
4	21679.9		21607.6	
5	21612.6		21527.1	
6			21432.1	
(0,5)				
0	23048.5			
1	23047.2		23016.6	
2				
3	22993.5		22922.9	
4	22944.4		22853.6	
5	22880.6		22769.6	
6	22801.3		22671.8	
			22559.7	
(1,5)				
0	23710.6			
1	23701.9		23676.8	
2	23676.8		23635.4	
3	23633.8		23577.2	
4	23573.7			
5	23495.4		23409.3	
6			23301.3	
(1,4)				
1	25862.40		25838.02	
2	25832.88		25792.09	
3	25784.36	25783.92	25727.77	25727.24
4	25716.78	25715.91	25644.65	25643.88
5			25542.86	25541.94

In the electronic transition $B\ 2\Sigma^+ \rightarrow A\ 2\Sigma^+$ proposed for this system, the state $A\ 2\Sigma^+$ is the upper state of the well known ultraviolet system $A\ 2\Sigma^+ - X\ 2\Pi_g$. The state $B\ 2\Sigma^+$ correlates with $O(^1S)H(^2S)$ molecule and its potential energy curve is very shallow. The bands observed correspond to the transitions of high vibration levels $4 \leq v'' \leq 9$ of $A\ 2\Sigma^+$ and $v' = 0,1$ of the upper state $B\ 2\Sigma^+$. So far, only single-headed-red degraded bands belonging to this system have been identified, and are arranged in the Deslandres scheme in table 3-6.

TABLE 3-6 THE DESLANDRES SCHEME OF $B\ 2\Sigma^+ \rightarrow A\ 2\Sigma^+$

v''	0	--	4	5	6	7	8	9
0			4337	4730	<u>5124</u>	<u>5480</u>		
			4	6	8	8		
1			3866*	4216	4587	4957		5534
			4	4				4

^{*}(1,4) band at 3866 \AA was observed by Carbone and Dalby (1969a). However, they did not observe (1,7) band at 4957 \AA which was earlier reported by Felenbok (1963).

Note - Underlined bands are the most characteristic in the B-A system.

System C' (Intercombinational)

$C\ 2\Sigma^+ \rightarrow A\ 2\Sigma^+$ (2600 - 2249 \AA): This is an intercombinational system of OH bands lying in the ultraviolet region. A few bands now unequivocally identified as belonging to this system

were observed earlier (Chamberlain and Cuther, 1933; Benoist, 1955; Schuler and Michel, 1956). It was Michel (1957) who first studied this spectrum in greater detail. He observed four bands at 2249, 2334, 2465 and 2545 \AA and classified them as (1,6), (1,7), (0,7), and (0,8), respectively. Felenbok (1963) confirmed the investigations made by Michel (1957) regarding these four bands and reported two additional bands at 2600 \AA and 2455 \AA which fitted nicely into Michel's analysis as (0,9) and (1,9) bands. He also conducted rotational analysis for the two new bands but the dispersion of his instrument in the region of interest was not sufficient to claim any high order of precision.

Carlone and Dalby (1969a) reinvestigated this system under better dispersion using a Jarell-Ash 3.4 m Ebert spectrograph (Dispersion 0.4 $\text{\AA}/\text{mm}$). They reported six bands in all; four of these bands were the same as reported by Michel (1957), one at 2600 \AA was the same as additionally reported by Felenbok and classified as the (0,9) band in Michel's analysis, and another sixth band at 2685 \AA . Felenbok's sixth band was at 2455 \AA and he did not observe any band at 2685 \AA . Carlone and Dalby (1969a) presented a modified analysis on the basis of their observations and obtained a different set of vibrational and rotational constants. On the basis of isotopic relations, these authors concluded that the v -numbering of the earlier analysis (Michel, 1957; Felenbok, 1963) was incorrect. Carlone and Dalby emphasized

that what those authors actually observed were the (3,6), (3,7), (1,7), (1,8), and (1,9) transitions of the C-A system. Table 3-7 provides the band-origin data in the form of the Deslandres scheme. It may be pointed out that Wallace (1962a) has reported 11 bands belonging to this system. Out of these, only six bands have been observed and identified. The wavelengths of five additional bands at 2155.9, 2161.1, 2267.1, 2370.3, and 2405.9 \AA as tabulated by Wallace appear to be the computed values. This was mentioned in the reference (Herman et al 1961) cited by Wallace.

TABLE* 3-7 THE DESLANDRES SCHEME OF C $^2\Sigma^+$ - A $^2\Sigma^+$

v'	5	6	7	8	9
0				2685	
				9	
1			<u>2465</u>	<u>2545</u>	2600
				8	9
2					
3		2249	2334		

* Carbone and Dalby (1969a)
Note - Underlined bands are the most characteristic in C-A system.

The state C has been found to possess a number of remarkable characteristics. Although it has a relatively large dissociation energy, its internuclear distance (r_e) is about double and its fundamental vibration frequency less than half

that of the low-lying states of both OH and OH⁺. All these characteristics are that of a strongly ionic state. It seems likely that it may correspond to an ionic state (presumably H⁺O⁻) and would, but for the non-crossing rule, dissociate into ions. If this hypothesis is true, one would expect the C-state to possess a very large electric dipole moment. Another remarkable features of this C-state is its very large spin-splitting constant [$\gamma = (0.25)$ B].

System C

$C\ 2\Sigma^+ \rightarrow X\ 2\Pi_i$ (1990 - 1770 \AA): Felenbok and Czarny (1964) identified this system comprised of red-degraded bands with weak vibrational structure, in the vacuum ultraviolet region. The spectrum was produced by a high frequency discharge in water vapor at low pressures. The observed bands have been classified as involving only two low-lying vibrational levels $v' = 0, 1$ of the C $2\Sigma^+$ state and $v' = 10$ to 16 of the X $2\Pi_i$ state. The last band observed was the (0,16) band which lies very close to the limit of dissociation of the X $2\Pi_i$ state. The wavelengths of the band-heads in the Deslandres scheme are presented in table 3-8.

TABLE * 3-8 THE DESLANDRES SCHEME OF $C\ 2\Sigma^+ \rightarrow X\ 2\Pi_i$

v'	0	10	11	12	13	14	15	16
0		1635	1686	1734	1777	1813	<u>1839</u>	<u>1854</u>
1		1578	1624	1668	1708	1741	<u>1765</u>	1779

* Felenbok and Czarny (1964)

Note - Underlined bands are the most characteristic of C-X system.

VUV Absorption Band

$^2\Sigma^- \leftarrow X^2\Pi_i$ (1221 \AA): Recently Douglas (1974) has reported a strong absorption band due to OH around 1221 \AA . From the analysis of high resolution records obtained on a 10 m concave grating vacuum spectrograph in the ninth order (reciprocal dispersion 0.2 $\text{\AA}/\text{mm}$), he concluded that this band is most probably due to the transition $^2\Sigma^- \leftarrow X^2\Pi_i$ in which $^2\Sigma^-$ is a Rydberg state.

OH spectra around 1200 \AA were explored earlier too, but all such attempts proved futile, particularly because of the strong overlapping absorption due to H_2O and the vibrationally excited H_2 . Discharge through water vapor provides a copious quantity of OH radical which is evinced by the appearance of strong OH absorption bands due to $A^{\Sigma^+} - X^2\Pi$. But side by side, there exists an abundance of H_2O molecules in the system giving relatively strong absorption near 1200 \AA . Douglas also produced OH by a condenser discharge but through a mixture of O_2 , H_2 and He. By reducing the time delay between the discharge through the absorption column and the continuum flash, he was able to record a new band due to OH at 1221 \AA . The identity of the absorbing molecule was established by replacing H_2 by D_2 in the system and observing the corresponding isotopic shifts. H_2O bands under such conditions were not so interfering as otherwise. It may be remarked here that such an experimental condition also does not favor the appearance of the well known $A^{\Sigma} \leftrightarrow X^2\Pi_i$ band of OH or OD.

The new band has been classified as the (0,0) band of a new electronic transition $^2\Sigma^- \leftarrow ^2\Pi_i$. It has the open structure characteristic of a hydride band which comprises all of the six branches, $P_{1,2}$, $Q_{1,2}$, and $R_{1,2}$ expected for a $^2\Sigma - ^2\Pi$ transition.

The wavenumber list of the different rotational lines is presented in table 3-9. Analysis of the data indicates that P and R branch transitions terminate on the same lower state levels as the Q branches of the A $^2\Sigma^+ - X ^2\Pi_i$ transition. Since it is well established that the A state is a $^2\Sigma^+$ state, the new excited state must be a $^2\Sigma^-$ state. Further, since no $^2\Sigma^-$ states are expected to arise from the basic orbital configurations of OH, it could be that the new $^2\Sigma^-$ state might result from σ - Rydberg orbitals built on the $^3\Sigma^-$ core of the radical OH⁺. The state $^2\Sigma^-$ can thus be classified as a Rydberg state having B - value of 15.216 cm^{-1} and $\Delta G(1/2)$ value of approximately 2750 cm^{-1} . These values are comparable with the corresponding values for the $^3\Sigma^-$ state of OH⁺. This hypothesis is further borne out by the theoretical calculations of Rydberg terms by Lefebvre-Brion (1971) and Easson and Pryce (1973).

The transition probability of this new system ($^2\Sigma^- - ^2\Pi_i$) must be quite high since the (0,0) band can be observed in absorption even when the number density of OH in the absorption tube is so small that it is not possible to get the otherwise most readily observable OH system A $^2\Sigma^+ - X ^2\Pi$.

TABLE[†] 3-9 WAVENUMBERS OF THE LINES OF THE $^2\Sigma^-$ - A $^2\Pi$ BAND OF OH (0 0) BAND

J	P ₁ (J)	Q ₁ (J)	R ₁ (J)	P ₂ (J)	Q ₂ (J)	R ₂ (J)
0.5						
1.5	81 797.86*				81 702.27*	81 763.55
2.5	745.60	81 805.62*	81 889.07*	81 641.27	702.27*	794.14*
3.5	686.70	778.29		600.97		813.71
4.5	624.19	745.60		551.66	672.60	824.87*
5.5	556.24	708.82	889.07*	494.08	645.74	
6.5	483.04	665.82	874.79	429.58*	610.66	821.71
7.5	404.22	617.74*	855.00	356.80	568.53	808.29
8.5	319.39*	562.85		277.59	519.15	787.45
9.5	229.48	502.44	790.75*		462.97	758.83*
10.5	133.58	435.98	758.06*	001.00	399.79	723.79
11.5	031.76	363.28	712.04	80 896.10	330.09	681.62
12.5	80 924.42*	284.76	659.73	785.22*	254.09	632.83*
13.5	811.51				171.80	576.07
14.5	693.02*	109.74*			083.27	512.81
15.5		013.45			80 988.35	442.94
16.5		80 910.95			887.30	
17.5		801.93*			780.16	

* Overlapped lines.

† Douglas (1974)

It may, therefore, be possible that at least three strong rotational lines of this electronic transition, namely, 1221.166\AA (R_1) 1222.071\AA (Q_1) and 1222.524\AA (P_1) might be observed in absorption in interstellar space where the OH number density is expected to be low.

ROTATION-VIBRATION SPECTRA

This spectrum is characterized by the radiative transitions between various vibrational levels of the ground electronic state $^2\Pi_1$ of the molecule OH.

Meinel Bands

$X^2\Pi_1 - X^2\Pi_1$ ($44745 - 3810\text{\AA}$): These bands were first observed and identified by Meinel (1950a, b) in the spectrum of night airglow. Later on these bands were detected in other natural radiative phenomena such as day airglow and twilight, etc., as well as in a number of laboratory sources. Because this discovery by Meinel proved crucial in establishing the correct identity of quite a few of the astral radiations, this group of OH bands is also termed as 'Meinel bands'. For example, an emission around 6500\AA in the night airglow spectrum, once considered presumably due to H_α (Elvey, 1950), was in fact due to OH. The airglow emission near 10440\AA , which was designated by Swings and Meinel (1951) as the $(0,0)$ band of the first positive system of N_2 , was also in reality the OH emission.

Night airglow happens to be one of the most efficient sources of rotation-vibration emission of OH. Using high

altitude balloon-borne instruments, this system of bands has been scanned up to 36000\AA in the airglow. (MacDonald et al, 1968; Moreels et al, 1970; Pick et al, 1971; Bunn and Gush, 1972; Lowe and Lytle, 1973). It may, however, be pointed out that although this system has actually been found to extend throughout the spectral region $44745-3810\text{\AA}$ as evidenced through laboratory studies, airglow OH bands could so far be identified up to 36000\AA . As a matter of fact, though the nature of the transitions involved in this spectrum is such that a major part of the total emission energy should be confined to the bands lying above 2800\AA (Wallace, 1962b), the strong background intensity due to thermal emission from the lower strata of the atmosphere starts creating difficulty in the investigation of the airglow spectrum from 25000\AA onward. It is only through airborne high altitude experiments that it has been possible to identify OH bands up to 36000\AA , and that too only a few members of the $\Delta v = 1$ sequence (1-0, 2-1, 3-2, and 4-3). (Lowe and Lytle, 1973)

In laboratory, this system of OH bands has been quite extensively studied by many workers. Dejardin, Janin, and Peyron (1953) and Herman and Hornbeck (1953) obtained these bands using oxyacetylene flames. McKinley et al (1955) and Bass and Garvin (1962) investigated these bands in the spectrum of chemiluminescence produced by the reaction of atomic hydrogen and ozonized oxygen at low pressures. The bands with $v \geq 10$ could not be observed either in the laboratory

sources or in the airglow. Meinel (1950 a,b) was the first to note the abrupt decrease in intensity of the OH airglow bands for $v > 9$ which corresponds to the vibrational energy equal to 3.3 eV. This discontinuity is a characteristic feature of the OH rotation-vibration bands emitted by the known laboratory sources as well. A schematic of the transitions involving $v = 9$ is shown in figure 3-1.

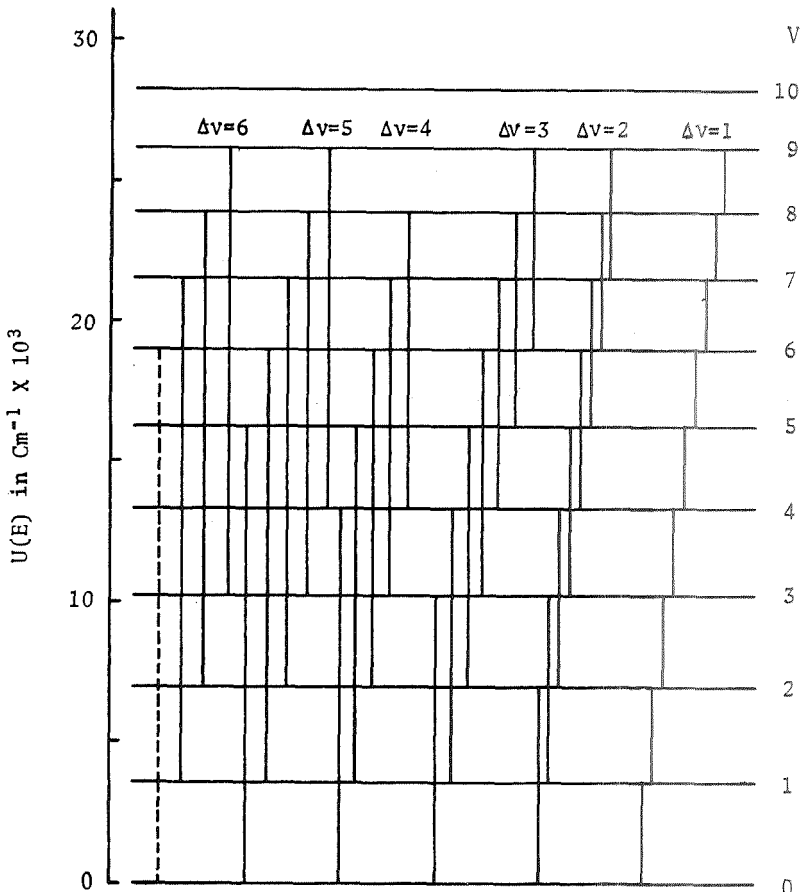


Figure 3-1 Schematic of the observed rotation-vibration bands in the ground electronic state of OH.

Each band has distinct P, Q, and R branches. The R-lines form the band-heads. Since $^2\Pi_1$ is a doublet composed of $^2\Pi_{3/2}$ and $^2\Pi_{1/2}$, $^2\Pi_{3/2}$ lies approximately 140 cm^{-1} below $^2\Pi_{1/2}$, two sets of P, Q, and R lines are obtained. One set P_1 , Q_1 , and R_1 corresponds to $^2\Pi_{3/2}$ and the other P_2 , Q_2 , and R_2 to $^2\Pi_{1/2}$. The P_2 , Q_2 , and R_2 lines are weak compared to P_1 , Q_1 , and R_1 as the latter group of lines corresponds to a more populated $^2\Pi_{3/2}$ state. Consequently there is an alteration of intensity between P_1 and P_2 and so on for each band. The Q branch in each case forms an unresolved line-like structure near the center of each band and has an appreciable intensity only for the lower J values. There is also a Λ -doubling which has been identified in the high resolution laboratory spectra (Bass and Garvin, 1962) but not in the airglow. The wavelengths of the bandheads in the Deslandres scheme are given in table 3-10.

TABLE* 3-10 ROTATION-VIBRATION BANDS OF X $^2\Pi_1$ STATE OF OH
R-BRANCH FORMS BAND-HEAD FOR N < 7 AND Q BRANCH FOR N \geq 7

v''	0	1	2	3	4	5	6	7	8
v'									
1	28016								
2	14342	29380							
3	9791	15052	30862						
4	7461.4	10286	15830	32495					
5	6136.7	7849.3	10684	16690	34308				
6	5253.9	6463.6	8278.3	11285	17647	18734			
7	4627.4	5542	6827	8758	11961		38668		
8	4163.9	4890	5865.4	7238.6	9305	12743	20003	41440	
9	3809.7	4409.3	5187.5	6234.4	7712	9942	13662	21514	44745

*Rosen (1970)

Chamberlain (1961) in his book 'Physics of the Aurora and Airglow' has compiled the wavelengths for 45 band origins along with their branches. These wavelengths were computed from the energy levels tabulated by Chamberlain and Roesler (1955) and rotational and spin constants reported by Herman and Hornbeck (1953). It may be mentioned that the most accurate wavelengths measured on airglow spectra are probably those of Kvifte (1959a, b) for 5-0, 6-1, 8-2, and 9-3 (photographed at 35\AA/mm); Chamberlain and Roseler (1955) for the P-branch lines of 5-1 and 6-2 (70\AA/mm); Wallace (1960) for 8-3 and 9-4 (30\AA/mm); and Wallace and Jones (1955) for 3-0, 4-1, 5-2, 8-4, and 9-5 (85\AA/mm). Moreover, the most accurate wavelengths on laboratory spectra are probably those measured by Herman and Hornbeck (1953); Dejardin, Janin, and Peyron (1953); and Bass and Garvin (1962). Bass and Garvin (1962) carried out an extensive study of the rotation-vibration spectrum photographed in the region $3900-11500\text{\AA}$ in the $\text{H} + \text{O}_3$ reaction. They presented a rotational analysis of the bands up to $v = 9$. For band involving $v' = 10$, they extrapolated the data of $v' = 9$ assuming that the rotational energy level scheme for higher levels vary so slowly as to be ignorable. The rotational analysis for observed bands is presented in table 3-11.

TABLE* 3-11 WAVENUMBERS OF LINES IN THE HYDROXYL RADICAL ROTATION-VIBRATION BANDS, 4000 \AA - 11000 \AA OBSERVED IN THE $\text{H} + \text{O}_3$ REACTION

Line	V	V'	8 - 0	9 - 1	7 - 0	8 - 1	9 - 2	6 - 0
R head					21595.0		19267.8	
R ₁ (5)								
R ₂ (5)								
R ₁ (4)							19248.9	
R ₂ (4)							R ₁ (4)	
R ₁ (3)						R ₂ (2)		
R ₂ (3)						R ₂ (2)		
R ₁ (2)			R ₁ (1)			20442.7		
R ₂ (2)			R ₂ (1)			20432.9		
R ₁ (1)			22669.0					9-2 P ₁ (4)
R ₂ (1)			659.8					9-2 P ₁ (4)
Q (1)			617.4		21536.9	386.4	19217.4	9-2 P ₁ (5)
Q (2)			596.1			364.7	190.7	18933.3
Q (3)								18908.0
Q (4)							126.0	
Q (5)								
P ₂ (2)			22558.6			331.4	161.5	883.0
P ₁ (2)			538.9		21451.9	303.2	136.7	864.9
P ₂ (3)			505.5			272.8	106.9	839.2
P ₁ (3)	23813.4		479.2		393.1	248.5	083.1	815.2
P ₂ (4)	765.5		433.5		354.7	207.3	043.5	774.5
P ₁ (4)	741.3		409.0		334.7	184.1	19022.4	755.0
P ₂ (5)	686.2		345.7			131.7	18968.4	704.9
P ₁ (5)	658.1		327.0		263.4	110.7	948.5	687.6
P ₂ (6)	591.4		254.2			047.6	6-0 P ₂ (2)	626.0
P ₁ (6)	566.1		236.6		176.5	20029.0	6-0 P ₁ (2)	613.7
P ₂ (7)	484.9		156.1			19951.7	18790.3	539.5
P ₁ (7)	467.7		135.1		21082.3	934.8	6-0 P ₂ (4)	525.7
P ₂ (8)			032.4			847.0	6-0 P ₁ (5)	
P ₁ (8)	354.2		22018.5		20986.7	832.1	18671.2	9-2 P ₁ (10)
P ₂ (9)			21898.9			733.5	574.2	
P ₁ (9)	238.9		886.3		883.2	718.8	556.2	
P ₂ (10)						605.3	451.9	
P ₁ (10)			770.0			594.8	437.9	224.5
P ₂ (11)						473.1		113.9
P ₁ (11)			743.9		615.8	463.4		103.7
P ₂ (12)							174.1	
P ₁ (12)						332.5	163.9	

* Bass and Garvin (1962)

TABLE 3-11 (Continued)

Line	V' - V''	7 - 1	8 - 2	5 - 0	9 - 3	6 - 1	7 - 2
R, head		18042.1	17043.6	16290.2	16035.0	15466.5	14639.6
R ₁ (5)			17018.8				
R ₂ (5)					16003.0		
R ₁ (4)			R ₁ (1)	head			
R ₂ (4)			R ₂ (1)				
R ₁ (3)			head	head			
R ₂ (3)			R ₁ (1)			R ₁ (2)	head
R ₁ (2)			head	16284.2		15460.5	head
R ₂ (2)	18036.1		R ₁ (1)	R ₁ (1)		R ₁ (1)	14629.8
R ₁ (1)			17039.6	16272.2	head	449.1	R ₂ (2)
R ₂ (1)	18021.0		17027.1	254.5	16020.9	433.5	14615.0
Q (1)	17973.2		16976.1	202.8	15976.3	382.6	565.0
Q (2)	955.8		957.6	188.6	958.0	369.0	550.1
Q (3)	930.1		936.1	167.1		348.1	528.6
Q (4)	17896.9		P ₁ (2)			319.3	501.6
Q (5)							
P ₂ (2)	917.5	16927.0	16144.3	925.4	15528.4	511.9	
P ₁ (2)	892.3	902.0	118.7	900.6	303.2	486.4	
P ₂ (3)	864.3	873.3	091.6	876.2	276.5	461.9	
P ₁ (3)	841.6	852.3	16069.2	852.3	255.1	439.7	
P ₂ (4)	803.4	815.0	9-3 head	816.1	219.5	406.1	
P ₁ (4)	782.3	793.5	16014.5	795.3	200.3	385.6	
P ₂ (5)	732.8	746.5	15967.0	748.6	155.3	342.6	
P ₁ (5)	713.9	727.3	950.0	730.0	138.7	325.2	
P ₂ (6)	655.2	670.4	15895.1	670.9	084.0	272.2	
P ₁ (6)	640.6	652.7	9-3 P ₂ (3)	654.1	069.0	257.7	
P ₂ (7)	569.5	584.6		587.4	15006.6		
P ₁ (7)	555.7	570.0	15804.4	571.9	10-4 R ₁ (1)	195.4	
P ₂ (8)	472.9	492.2	9-3 P ₁ (5)	494.6	14924.4		
P ₁ (8)	460.0	478.5	15714.2	480.3	912.6	111.4	
P ₂ (9)	371.6	390.7	638.8	15394.2	834.0		
P ₁ (9)	358.2	378.4	629.7	6-1 Q(1)	824.6	14022.8	
P ₂ (10)	261.2		541.3	15286.7	737.4		
P ₁ (10)	250.3		527.3	6-1 P ₂ (3)	726.3	13928.8	
P ₂ (11)	144.3			15170.3			
P ₁ (11)	135.6	16155.8					
P ₂ (12)				15045.2			
P ₁ (12)				15034.6			

TABLE 3-11 (continued)

Line	V' - V''	8 - 3	4 - 0	9 - 4	5 - 1	6 - 2	7 - 3
R head	13812.2	13397.2		12958.7	12735.2	12072.4	11410.7
R ₁ (5)					725.37	R ₁ (2)	R ₁ (2)
R ₂ (5)						064.4	11404.5
R ₁ (4)						R ₁ (1)	
R ₂ (4)						048.5	390.9
R ₁ (3)	head						
R ₂ (3)							
R ₁ (2)	head						
R ₂ (2)	13802.6	365.3			707.5	R ₁ (1)	
R ₁ (1)	R ₂ (2)					048.5	372.9
R ₂ (1)	13786.1	337.1		12944.6	688.5	12032.6	
Q (1)	742.3	287.5		899.5	636.5	11983.2	326.5
Q (2)	726.6			887.2	621.0	969.5	315.3
Q (3)				865.0	606.2	953.7	298.0
Q (4)	709.9						
Q (5)							
P ₂ (2)	689.8	236.17		848.8	579.7	928.8	276.7
P ₁ (2)	666.8	202.4		830.0	549.3	903.8	250.2
P ₂ (3)	644.4	181.3		804.8	531.8	881.3	228.7
P ₁ (3)	621.3	157.4		783.1	508.3	860.4	208.7
P ₂ (4)	589.6	125.0		751.9	475.5	827.9	180.7
P ₁ (4)	569.6	106.2		5-1 head	455.5	808.6	160.3
P ₂ (5)	526.8	065.6		5-1 R ₂ (1)	415.9	770.1	122.9
P ₁ (5)	507.6	13046.8		672.7	401.1	756.2	106.8
P ₂ (6)	459.2	12996.9		5-1 Q(2)	352.8	709.1	062.6
P ₁ (6)	442.6	985.5		5-1 Q(3)	338.5	694.1	11047.9
P ₂ (7)	383.6	927.7		5-1 P ₁ (2)	284.2	641.1	10995.7
P ₁ (7)	4-0 R ₂ (2)	915.8		5-1 P ₂ (3)	270.8	630.3	983.6
P ₂ (8)	13302.2	9-4 P ₂ (2)		465.4	208.7	569.8	924.8
P ₁ (8)	4-0 Q(1)			5-1 P ₁ (4)	199.8	557.0	914.0
P ₂ (9)	214.8			378.7	130.8	493.1	848.9
P ₁ (9)	4-0 P ₁ (2)			365.6	119.8	480.1	838.3
P ₂ (10)				5-1 P ₂ (7)	6-2 R ₂ (2)		767.1
P ₁ (10)				5-1 P ₁ (7)	6-2 R ₂ (1)		756.7
P ₂ (11)	13008.6			180.6			680.8
P ₁ (11)				167.6			
P ₂ (12)							
P ₁ (12)							

TABLE 3-11 (continued)

Line	V' - V''	8 - 4	3 - 0	9 - 5	4 - 1	5 - 2
R head	10738.1	10357.7	10051.5	9849.5	9360.7	
R ₁ (5)		351.3				head
R ₂ (5)						
R ₁ (4)		340.6				9352.0
R ₂ (4)						
R ₁ (3)					831.1	337.1
R ₂ (3)		318.7				
R ₁ (2)		309.6	3-0 P ₂ (4)	812.8	324.9	
R ₂ (2)	R (1)	299.6	3-0 P ₁ (4)	R ₁ (1)	310.2	
R ₁ (1)	723.2	289.5	3-0 P ₁ (4)	794.5	304.1	
R ₂ (1)	707.1		10023.3	775.4	286.0	
Q (1)	663.7	209.6	9984.3	719.3	236.2	
Q (2)	651.2		973.2	711.7	228.5	
Q (3)	634.3		9954.5	699.5	214.9	
Q (4)		171.2		682.6	198.8	
Q (5)						
P ₂ (2)	612.8	10149.5	937.6	662.9	181.9	
P ₁ (2)	592.6	124.8	916.0	639.6	158.4	
P ₂ (3)	572.4	103.3	893.4	617.4	137.4	
P ₁ (3)	550.1	081.9	873.8	597.1	117.4	
P ₂ (4)	522.3	051.5	4-1 head	568.6	090.1	
P ₁ (4)	503.5	10038.4		551.1	072.7	
P ₂ (5)	467.2	9997.2		515.8	037.5	
P ₁ (5)	450.8	9-5 Q(1)	4-1 R ₂ (1)	502.2	9022.8	
P ₂ (6)	407.3	9-5 P ₂ (2)	9734.4	459.0	8980.7	
P ₁ (6)	393.2	9926.8		447.4	968.6	
P ₂ (7)	3-0 R(4)			398.6	921.3	
P ₁ (7)	329.9			388.9	910.2	
P ₂ (8)	272.6					
P ₁ (8)	216.5					
P ₂ (9)	195.0			9269.6		
P ₁ (9)	110.5			9260.2		
P ₂ (10)						
P ₁ (10)						
P ₂ (11)						
P ₁ (11)						
P ₂ (12)						
P ₁ (12)						

Identified lines in the P and R branches are unresolved lambda doublets.
 Q branch lines are unresolved spin doublets.

ROTATIONAL AND SUB-ROTATIONAL SPECTRA

This class of spectra is characterized by radiative transitions between numerous rotational levels and their lambda and magnetic hyperfine components studied in the laboratory and in the extra-terrestrial sources.

Pure Rotational Spectrum

$X^2\Pi_g^- - X^2\Pi_g$ (20.4 - 15 μ): Pure rotational lines of the OH molecule were first satisfactorily investigated by Madden and Benedict (1955). Using oxyacetylene flame and an Ebert grating - Goley cell scanning unit, they scanned the OH rotational spectrum in emission in the wavelength region 15-20.4 μ .

Plyler and Humphreys (1948) and Silverman and Herman (1949) had earlier used prism spectrometers to explore these spectral lines. Since the resolution of their instruments was not sufficient to distinguish the OH lines from the stronger overlapping lines due to H_2O , no satisfactory results could be obtained.

The observed rotational lines, with $N'' = 13$ to 18 fall in groups of 4 due to Λ and spin doubling. The groups characterized by $N'' = 13$ (near 498 cm^{-1}) and $N'' = 14$ (near 531 cm^{-1}) are particularly found free from distortion by the water spectrum. All possible OH lines from $N'' = 13$ to 18 lie almost at the same frequencies as computed and tabulated by Dieke and Crosswhite (1948), the error being $\pm 0.2 \text{ cm}^{-1}$ which is within

the accuracy limit of the experiment. For ready reference, these wave numbers are presented in table 3-12.

TABLE* 3-12 PURE ROTATION BAND

N	R ₁		R ₂		N	R ₁		R ₂	
	cm ⁻¹		cm ⁻¹			cm ⁻¹		cm ⁻¹	
1	83.70		61.28		12	465.88		463.88	
	3.87		1.35			6.97		4.79	
2	118.20		101.30		13	498.77		497.17	
	8.47		1.36			9.70		7.89	
3	153.19		140.44		14	531.10		529.67	
	3.50		0.40			2.18		30.61	
4	188.45		178.70		15	562.83		561.62	
	8.95		8.93			3.85		2.40	
5	223.91		216.34		16	593.74		592.70	
	4.35		6.60			5.01		3.82	
6	259.24		253.39		17	624.26		623.26	
	9.93		3.71			5.28		4.16	
7	294.56		289.76		18	653.78		652.88	
	5.14		90.19			4.99		4.00	
8	329.49		325.59		19	682.69		681.98	
	30.26		6.17			3.94		2.94	
9	364.24		361.11		20	710.73		710.13	
	5.03		1.61			2.01		1.24	
10	398.53		395.89		21	738.07		737.40	
	9.52		6.59			9.28		8.56	
11	432.50		430.31		22	764.44		764.04	
	3.31		0.91			5.73		5.11	

*Dieke and Crosswhite (1962)

OH Infrared Laser Oscillations: Several rotation-vibration laser lines have been observed in the case of the OH radical by Callear and Van Den Bergh (1971). Mixtures of O₃ and H₂ were flashed in a laser cavity and induced infrared emission

was detected in the 3μ region. The observed stimulated radiation was identified as involving P_1 transitions of the $v = 3 \rightarrow 2$, $2 \rightarrow 1$ and $1 \rightarrow 0$ fundamentals of the OH rotation-vibration spectrum. The relevant data are presented in table 3-13.

TABLE 3-13* ASSIGNMENT OF THE TRANSITIONS
OF THE $O_3 - H_2$ LASER

Observed Frequencies (cm^{-1})	Frequencies The OH Radical (cm^{-1})	v
3407 ± 2	3407.94 (P_1)	$1 \rightarrow 0$
3368 ± 2	3367.01 (P_1)	$1 \rightarrow 0$
3249 ± 2	3248.05 (P_1)	$2 \rightarrow 1$
3210 ± 2	3208.55 (P_1)	$2 \rightarrow 1$
3168 ± 2	3167.59 (P_1)	$2 \rightarrow 1$
3092 ± 2	3090.09 (P_1)	$3 \rightarrow 2$
3054 ± 2	3052.01 (P_1)	$3 \rightarrow 2$

* Callear and Van Den Bergh (1971)

Recently, Ducas et al (1973) observed laser action in pure rotational transitions in both OH and OD. The experiment consisted of a pulsed discharge through a flowing mixture of SF_6 , H_2 and O_2 . The optimum partial pressures of the three gases for maximum laser action were typically in the ratio 4:2:6 and the pulses originated from a $0.1\mu F$ condenser bank charged to about 15 KV. Forty-four lines were seen in the $12-20\mu$ region and have been assigned to the rotational transitions within $v' = 0, 1, 2$ levels of the ground electronic state $^2\Pi_{3/2}$. The study provided more accurate values of the

higher order rotational constants for the molecule OH. Data for the observed laser lines are presented in table 3-14.

TABLE* 3-14 OH ROTATIONAL LINES†

v	Assignment	ν (cm ⁻¹) Observed	Intensity (Arbitrary units)
1	R ₂ (14)	508.91	15.0
1	R ₂ '(14)	509.70	1.4
1	R ₁ (14)	510.37	16.0
1	R ₁ '(14)	511.32	1.0
2	R ₂ (15)	517.56	2.0
2	R ₁ (15)	518.86	2.1
0	R ₂ (14)	529.72	2.0
0	R ₂ '(14)	530.54	3.8
0	R ₁ (14)	531.12	10.0
0	R ₁ '(14)	532.26	4.0
1	R ₂ (15)	539.62	3.0
1	R ₂ '(15)	540.49	0.5
1	R ₁ (15)	540.77	7.0
1	R ₁ '(15)	541.85	1.5
0	R ₂ (18)	653.04	81.0
0	R ₁ (18)	653.86	85.0
0	R ₂ '(18)	654.07	8.4
1	R ₂ (19)	654.69	14.1
1	R ₁ (19)	655.48	19.6
1	R ₂ (20)	681.70	42.0
0	R ₂ '(19)	682.04	97.0
1	R ₁ (20)	682.35	5.7
0	R ₁ '(19)	682.78	55.0
0	R ₂ (19)	683.07	28.0
0	R ₁ (19)	683.99	112.0
1	R ₂ (21)	707.76	98.0
1	R ₁ (21)	708.32	141.0
0	R ₂ (20)	710.20	325.0
0	R ₁ (20)	710.88	337.0
0	R ₂ '(20)	711.30	80.0
0	R ₁ '(20)	712.08	84.0
1	R ₂ (22)	733.04	10.7
1	R ₁ (22)	733.55	15.4
0	R ₂ (21)	737.64	224.0
0	R ₁ (21)	738.19	140.0
0	R ₂ '(21)	738.68	14.0
0	R ₁ '(21)	739.37	8.4

TABLE 3-14 (continued)

v	Assignment R(N)	ν (cm ⁻¹) Observed	Intensity (Arbitrary Units)
0	R ₂ (22)	764.03	84.0
0	R ₁ (22)	764.59	84.0
0	R ₂ (22)	764.91	0.5
0	R ₂ (23)	789.72	14.0
0	R ₁ (23)	790.14	22.4
0	R ₂ (24)	814.43	8.0
0	R ₁ (24)	814.79	14.0

*Ducas et al (1973)

[†]The quartet grouping of the laser lines indicates splitting of each rotational level into four closely spaced levels due to Λ and spin splitting.

Molecular rotational parameters were determined from these laser frequencies, using the relations

$$E_J = 1/4 [F_2^{\prime} (J) + F_2^{\prime\prime} (J) + F_1^{\prime} (J) + F_1^{\prime\prime} (J)], \quad (3-1)$$

where F_1^{\prime} , $F_1^{\prime\prime}$ and F_2^{\prime} , $F_2^{\prime\prime}$ signify Λ -doublets of the spin-multiplets corresponding to $J = N + 1/2$ and $J = N - 1/2$, respectively, and

$$(E_J - E_{J-1}) = 2 B_{\text{eff}} J - 4 D_{\text{eff}} J^3 + H(6J^5 + 2J^3) - 8P (J^7 + J^5). \quad (3-2)$$

Here, B_{eff} is essentially the rotational constant B , D_{eff} represents the influence of centrifugal force, and H & P are higher order terms for the vibrating rotor. These relations are due to Mizushima (1972). These rotational parameters for OH are tabulated in table 3-15.

TABLE 3-15 ROTATIONAL PARAMETERS OF OH IN π STATES

v	Parameter	Mizushima (1972) (cm ⁻¹)	Ducas et al (1973) (cm ⁻¹)
0	B_{eff}	18.5315	
0	D_{eff}	1.9074×10^{-3}	
0	H	$(1.4074 \pm 0.070) \times 10^{-7}$	$(1.347 \pm 0.083) \times 10^{-7}$
0	P	$(1.23 \pm 0.31) \times 10^{-11}$	$(1.04 \pm 0.37) \times 10^{-11}$
1	B_{eff}	17.8208	
1	D_{eff}	1.8696×10^{-3}	
1	H	1.3883×10^{-7}	
1	P	$(1.68 \pm 1.28) \times 10^{-11}$	$(1.65 \pm 0.44) \times 10^{-11}$

OH SPECTRA IN MICROWAVE AND RADIOFREQUENCY REGIONS

Microwave Spectrum: The microwave absorption spectrum of the free hydroxyl radical was first investigated in the laboratory by Dousmanis, Sanders, and Townes (1955). OH radicals were produced by a high frequency discharge in water vapor and the absorption spectrum was studied in a flow system using a conventional type of microwave spectrometer. Microwave absorption lines corresponding to radiative transitions between a number of hyperfine sub-levels* of the Λ -doublets

* OH has, in total, nine orbital electrons and thus it has one unpaired electron in its electronic structure with two-fold spatial distribution in terms of its spin. In a non-rotating molecule, these two configurations have the same energy but when rotations set in, appreciable spin-rotation interaction forces come into play giving the two distributions slightly different energies. This is known as ' Λ -doubling' resulting in the splitting up of each rotational level into a doublet.

In addition, the nuclear magnetic moment of hydrogen in OH also interacts with the internal magnetic field of the molecule and different energies result from different orientations of this magnetic moment relative to the molecular magnetic

for both the ground electronic state components $^2\Pi_{3/2}$ and $^2\Pi_{1/2}$ were identified at frequencies ranging from 7000 MHz to 24000 MHz. Poynter and Beaudet (1968) reinvestigated microwave absorption of this molecule employing better experimental conditions and presented much improved data on the different radiative hyperfine transitions reported earlier. Later a number of workers using more sophisticated and improved experimental techniques, such as a highly sensitive superheterodyne cavity spectrometer, a servo-tuned cavity spectrometer, and a stark modulation spectrometer, etc., identified many more microwave absorption lines involving J values up to 13/2 for the states $^2\Pi_{3/2}$ and $^2\Pi_{1/2}$ (Radford, 1968; Ter Meulen and Dymanus, 1972; Ball et al, 1970; Ball et al, 1971; Turner et al, 1970; Destombes et al, 1974). Table 3-16 presents a consolidated report on the various microwave frequencies so far identified through laboratory experiments. Table 3-17 provides a list of different frequencies computed by Destombes et al (1974) using the constants given in table 3-18.

It may be pointed out that laboratory data in respect to these hyperfine OH transitions have been of great value in identifying a number of interstellar and galactic radiations

field. Since only two orientations of this nuclear magnetic moment are possible in OH, such a Λ sub-level is further split into two hyperfine sub-levels.

A schematic of these component energy levels for a typical rotational level is presented in figure 2-2.

TABLE 3-16 MICROWAVE FREQUENCIES OBSERVED IN THE LABORATORY

J	F + F'	State $^2\Pi_{1/2}$ (Frequencies, MHz)	References	State $^2\Pi_{3/2}$ (Frequencies, MHz)	References
1/2	1 → 0	4 660.242 ± 0.003	Radford (1968)		
	1 → 1	4 750.656 ± 0.003			
	0 → 1	4 765.562 ± 0.003			
3/2	2 → 1	7 749.909 ± 0.005	Ball et al (1970)	1 612.231 ± 0.0002	Ter Meulen and Dymanus (1972)
	1 → 1	7 761.747 ± 0.005		1 665.401 ± 0.0001	
	2 → 2	7 820.125 ± 0.005		1 667.359 ± 0.0001	
	1 → 2	7 831.962 ± 0.005		1 720.530 ± 0.0001	
5/2	3 → 2	8 118.052 ± 0.005	Ball et al (1971)	6 016.746 ± 0.008	Radford (1968)
	2 → 2	8 135.868 ± 0.005		6 030.739 ± 0.005	
	3 → 3	8 189.586 ± 0.005		6 035.085 ± 0.005	
	2 → 3	8 207.401 ± 0.005		6 049.084 ± 0.008	
7/2	3 → 4				
	3 → 3			13 434.608	Poynter and Beaudet (1968)
	4 → 4			*13 441.371	
	4 → 3				
9/2	4 → 5			23 805.13 ± 0.01	Poynter and Beaudet (1968)
	4 → 4			23 817.64 ± 0.01	
	5 → 5			23 826.62 ± 0.01	
	5 → 4			23 838.46 ± 0.01	
11/2	5 → 5			36 983.47 ± 0.03	Poynter and Beaudet (1968)
	6 → 6			36 994.43 ± 0.05	
13/2	6 → 6			52 722.01 ± 0.17	Destombes et al (1974)
	7 → 7			52 734.46 ± 0.17	

* $^2\Pi_{3/2}$, J = 7/2 (4 → 4) line at 13441.371 MHz was detected in the galactic source W_3 by Turner, Palmer and Zuckerman (1970) using 140 ft telescope at National Astronomy Observatory, West Virginia.

TABLE * 3-17 COMPUTED MICROWAVE FREQUENCIES

J	F → F'	State $^2\Pi_{1/2}$	State $^2\Pi_{3/2}$
		(Frequencies, MHz)	(Frequencies, MHz)
7/2	3 → 4	5 548.32	13 434.04
	3 → 3	5 473.87	13 434.54
	4 → 4	5 524.40	13 441.29
	4 → 3	5 449.95	13 441.79
9/2	4 → 5	191.05	23 805.54
	4 → 4	162.51	23 817.53
	5 → 5	114.55	23 826.52
	5 → 4	86.01	23 838.51
11/2	5 → 6	8 607.42	36 963.95
	5 → 5	8 575.39	36 983.47
	6 → 6	8 529.57	36 994.43
	6 → 5	8 497.54	37 013.95
13/2	6 → 7	19 587.67	52 697.19
	6 → 6	19 553.04	52 721.90
	7 → 7	19 509.00	52 734.54
	7 → 6	19 474.37	52 759.26
15/2	7 → 8	32 942.08	70 815.49
	7 → 7	32 905.50	70 843.92
	8 → 8	32 862.96	70 857.98
	8 → 7	32 826.38	70 886.41
17/2	8 → 9	48 504.49	91 152.88
	8 → 8	48 466.44	91 184.05
	9 → 9	48 425.16	91 199.33
	9 → 8	48 387.11	91 230.50

* Destombes et al (1974)

TABLE * 3-18 CENTRIFUGAL DISTORTION AND MAGNETIC HYPERFINE INTERACTION CONSTANTS

Constants	Frequencies (MHz)	Remarks
D	117.4 ± 0.1	Centrifugal Distortion Constants
D_n	108.8 ± 0.5	
δ	-50.7 ± 0.3	
a	85.7 ± 0.1	Magnetic Hyperfine Interaction Constants
b	-116.8 ± 0.3	
c	144.5 ± 0.3	
d	56.4 ± 0.2	

* Destombes et al (1974)

in astrophysics and radioastronomy. This will be discussed in the "OH Radiation in Interstellar Space" Section.

Electron Paramagnetic Resonance Spectrum: Radford (1961) was the first to investigate the electron paramagnetic resonance spectrum of OH. The products of a microwave electric discharge in water vapor at low pressure were pumped continuously through the microwave cavity of a Varian V-4500 EPR spectrometer where the microwave absorption by the vapor around a 3 cm wavelength was measured as a function of magnetic field strength. The dimensions of the cavity were chosen to make it resonate in the TE mode. In these early experiments (Radford, 1961, 1962) only the electric dipole type transitions between various Λ -doublet components could be identified. Later, however, more sophisticated instrumentation led to the detection of a number of magnetic dipole and quadrupole transitions in addition to many other electric dipole transitions (Churg and Levy, 1970; Carrington and Lucas, 1970). In EPR, the applied magnetic field removes the $(2J + 1)$ degeneracy of the total angular momentum J and as a result each Λ -doublet is split into $(2J + 1)$ levels with a very small proton hyperfine splitting further superimposed. The schematic shown in figure 3-2 depicts the strongest paramagnetic resonance transitions, electric dipole type, identified for ^{16}OH hyperfine zeeman sub-levels in the $J = 3/2$ level of $^2\Pi_{3/2}$ state. These transitions follow the selection rules $\Delta M_J = \pm 1$, $\Delta F = 0$, and $+\leftrightarrow-$. The corresponding magnetic dipole transitions which are weaker

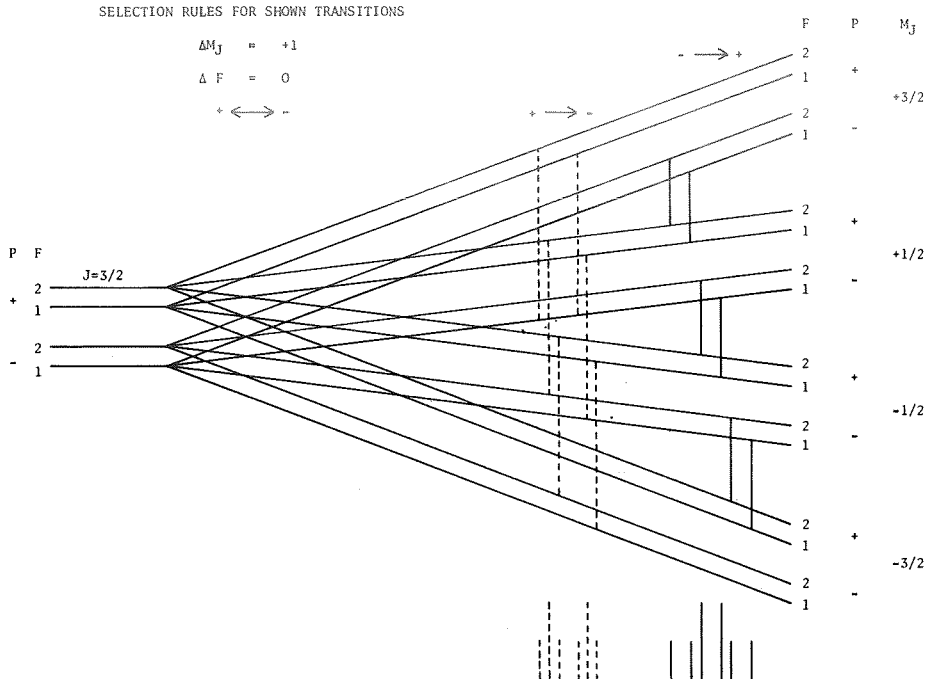


Figure 3-2 Schematic of the OH electric dipole transitions observed in the presence of external applied magnetic field for a rotational level corresponding to $J = 3/2$. In the bottom of the figure are shown two groups of lines which are observed at different magnetic fields.

($+\rightarrow+$, $- \rightarrow -$; $\Delta F = 0$) are not shown in figure 3-2. It may be pointed out that higher order transitions ($\Delta M_J = \pm 1$; $\Delta F = \pm 1$) by nature are very weak. The electric dipole transitions shown in the figure may form two groups corresponding to $+\rightarrow-$ and $- \rightarrow +$, respectively. The proton hyperfine coupling produces a further doublet splitting. Radford (1961) also observed resonance absorption in several rotational levels of both the $^2\Pi_{1/2}$ and $^3\Pi_{3/2}$ states. Radford's measurements confirmed many aspects of the earlier analysis of the pure microwave spectrum, provided 'g' values for the various rotational levels, and led to a more complete analysis of the hyperfine coupling. The magnetic resonance spectrum of the $^2\Pi_{3/2}$ $J = 3/2$ rotational level of the $v = 1$ vibrational state was also studied and frequencies corresponding to zero-field Λ -doublet transitions of $^2\Pi_{3/2}$ ($J = 3/2$; $v = 1$) were determined. These were the first microwave measurements of the excited vibrational levels of this radical (Churg and Levy, 1970).

OH RADIATION IN INTERSTELLAR SPACE

The hydroxyl radiation in microwave region has been observed both in absorption and emission in interstellar space.

OH Microwave Absorption in the Interstellar Space: OH as a free radical in interstellar space was first detected by Weinreb et al (1963) through microwave absorption. Using an 84-foot radiotelescope at M.I.T. and looking in the direction of the

strong galactic source Cassiopeia - A, these authors detected a significant microwave absorption at 1667 MHz which was attributed to OH. It was the fateful evening of 15 October 1963. Hardly a month after the M.I.T. discovery, on 20 November 1963, Bolton et al (1964), in Australia detected hydroxyl absorption at two frequencies 1665 and 1667 MHz in the direction of another strong galactic source - Sagittarius using a 210-foot radiotelescope. Three weeks later Dieter and Ewen (1964) of Harvard, using the U.S. Air Force 84-foot radio-telescope confirmed the presence of OH in both the directions of Cassiopeia and Sagittarius. In the same week, Weaver and Williams (1964) at Berkeley observed hydroxyl absorption in the direction of the galactic center. As soon as the OH absorptions at 1665 and 1667 MHz were discovered, efforts were made to detect absorptions at the other two radio lines at 1612 and 1720 MHz in OH. In April 1964, both these lines were actually detected in the direction of Sagittarius by an Australian group. During the same period while surveying the hydroxyl absorption in the direction of Sagittarius over a wider frequency range, Goldstein et al (1964) had also identified the higher frequency line, 1720 MHz. All these four frequencies correspond to the OH electric dipole transitions. Table 3-19 provides the laboratory data of these lines.

These new discoveries brought to light a new anomaly. Theoretical calculations and later laboratory measurements, given in table 3-19 showed that the relative intensity of

TABLE * 3-19 LABORATORY DETERMINATIONS
OF OH REST FREQUENCIES

Transition	Frequency (MHz)	Relative Intensity
$F = 1 \rightarrow 2$	1612.231±2	1
$F = 1 \rightarrow 1$	1665.401±2	5
$F = 2 \rightarrow 2$	1667.358±2	9
$F = 2 \rightarrow 1$	1720.533±2	1

* Radford (1964)

absorption at the four OH lines are in the ratio 1:5:9:1 for the lines at 16112, 1665, 1667 and 1720 MHz, respectively. The actual absorptions recorded put the intensity ratios at 1:2; 2:2 and 7:1 of the respective lines 1612/1665, 1665/1667 and 1667/1720 for the strong Sagittarius absorption. These ratios are incompatible with simple self-absorption effects and imply unusual physical conditions at the galactic center. Also, it was found that the ratios vary in different parts of the galaxy (Gardner et al, 1964; McGee et al, 1965). OH is now known to be extremely widespread and prolific within the galaxy and to exist outside. It has been seen in absorption in the cool neutral hydrogen of H I regions and both in absorption and emission in the hotter ionized H II regions of the spiral arms. It is also present in many dark dust clouds where it is more abundant than hydrogen. A recent survey (Turner 1972) has added about 180 new sources comprising 424 clouds from 264 directions searched.

OH Microwave Emission for Galactic Sources: Hydroxyl microwave emission from galactic sources was first observed in June 1964 by Australian astronomers (McGee et al 1965). It was a narrow intense microwave emission line to the side of an absorption line at 1665 MHz. The effect, however, was apparently thought to be an instrumental effect and was not flashed immediately. Later, this emission was confirmed by the Harvard and Berkeley groups in U.S.A. [Gundermann (1965) - Harvard; Weaver et al (1965) - Berkeley.]

The characteristic features of this emission were so unexpected that the Berkeley astronomers nicknamed the line 'Mysterium' in order to dramatize its importance. Out of the four OH transitions identified in galactic absorption, the emission line at 1665 MHz was a narrow strong line and the other three emission lines were unexpectedly much weaker. Departures by several orders of magnitude from the expected intensity ratios were noted. Another curious fact about this OH emission was its location within the galaxy. It was heavily biased by the observational selection. It was not widely distributed throughout the galaxy as is the case with the 21 cm line of atomic hydrogen. It was found only in isolated positions near H II regions. In H II regions which are around the hot stars, the hydrogen is almost completely ionized. Such regions are closely confined to the galactic equator. At the sites of OH emission, the medium is very intense by interstellar standards. These seem to be confined to the atmosphere's

cool-young-stars or the proto-stars on their way to becoming stars.

The radiation shows strong linear polarization and in some cases circular polarization. The peculiar behavior of the OH emission lines with regard to their intensity ratio and the state of polarization have presented many new questions about the constitution and state of excitation of molecules in interstellar space. No thermal emission from OH emission galactic sources has so far been detected. It is only the non-thermal emission with most curious properties both with regard to intensity as well as polarization that has been seen in the direction of a score of galactic sites. Dickinson and Turner (1972) have attempted to propose a broad classification of the various OH galactic sources.

Most attempts to explain the OH observational results have centered around some kind of population inversion of the energy levels, and various pumping mechanisms have been invoked in an attempt to devise a hypothetical celestial OH maser to explain the observations. The suggested schemes for radiation pumping include the use of ultraviolet (Cook, 1966; Perkins et al, 1966; Litvak et al, 1966); infrared (Shklovskii, 1966; Litvak, 1969); and radio (Rogers, 1967) radiations as a means of creating population inversions. None of these schemes, however, can satisfactorily account for all the observed results with regards to anomalies of both the intensity and polarization. Pertinent data about the excited states of

OH and their sources of emission in interstellar space as summarized by Litvak (1972) are presented in table 3-20 for ready reference.

For the most comprehensive study of the radiative processes of OH in interstellar space and other galactic sources, the readers are referred to a few review articles (Cook, 1969; Litvak, 1972; Robinson and McGee, 1967; and Barrett, 1967).

TABLE* 3-20 SUMMARY OF DATA FOR OH EMISSION IN INTERSTELLAR SPACE

OH excited state	Energy above ground state (cm ⁻¹)	Frequency (MHz)	Relative line strength	Signal strength (f.u.)	Source	Models Considered
$^2\Pi_{3/2}(J = 5/2)$	84					Zeeman splitting $B = 10^{-2}$ G. Population ≈ 0.1 x ground state population.
F = 3+3	6035.085+0.005	20	79,20 2,47	W3(OH), W75B W49, NGC 6334N		Far IR + near UV pumping ($N_{OH} \approx 10^{16} \text{ cm}^{-2}$)
			4,3	Sgr B ₂ , NML Cyg		
2+2	6030.749+0.005	14	26,2	W3(OH), NGC 6334N		Collisional excitation of rotation ($T_k \approx 100^\circ\text{K}$, emitting area 1.7 arcsec^2 ; $N_{OH} \approx 10^{17} \text{ cm}^{-2}$).
2+3	6016.741+0.008	1				Far IR coupling of ground state and excited state population inversions.
3+2	6049.084+0.008	1				
$^2\Pi_{1/2}(J = 1/2)$ F = 1+1	126	4750.656	2			Far IR + near UV pumping (correlation of 4765 and 1720 MHz emission).
1+0	4765.562	1	3,1, 0.7,0.3	W3(OH), W49, Sgr B ₂ , NGC 6334N ²		
0+1	4660.242	1	0.7	Sgr B ₂		Far IR coupling
$^2\Pi_{1/2}(J = 3/2)$	188			Not detected yet		Collisional excitation of rotation, anti-inversion of doublet.
F = 2+2	7820.125+0.005	9	<0.2	W3(OI)		
1+1	7761.747	5				
1+2	7831.962	1				
2+1	7749.909	1				
$^2\Pi_{3/2}(J = 7/2)$ F = 4+4	202	13441.371	35	19	W3(OII)	Collisional excitation of rotation ($T_k > 100^\circ\text{K}$), far IR coupling to $^2\Pi_{3/2}(J = 5/2)$, F = 3+3) population inversion.
3+3	13434.608	27				Far IR pumping (153 cm^{-1}) via $^2\Pi_{3/2}(J = 9/2)$, overlap of hyperfine split IR lines in upper doublet only.
3+4	13441.963	1				
4+3	13434.015	1				
$^2\Pi_{1/2}(J = 5/2)$	289			Not detected yet		Collision excitation of rotation-anti-inverted doublet.
F = 3+3	8189.586+0.005	20	<0.3	W3(OH)		
2+2	8135.868	14				
2+3	8118.052	1				
3+2	8207.401	1				
$^2\Pi_{3/2}(J = 9/2)$ F = 5+5	355	23826.6	54	Not		
4+4	23817.6	44	detected yet			
5+4	23805.4	1				
4+5	23838.8	1				
Vibrationally-excited (v = 1) $^2\Pi_{3/2}(J = 3/2)$	3568					Near infrared pumping.
F = 2+2	1538.80	9				
1+1	1537.06	5				
2+1	1586.76	1				
1+2	1489.10	1				

*Litvak (1972)

DISSOCIATION AND IONIZATION PROCESSES IN OH

The significance of dissociation energies and ionization potentials of diatomic molecules is well recognized in the domain of planetary optics and a variety of other applied disciplines of science. These values are, in a way, the building bricks with which more complex structures may be built. Ionization of molecules without dissociation has a simplicity comparable with atomic ionization. Once the molecular bonds are broken, the processes, and their interpretation become more complex.

Predissociation is another important spectroscopic phenomenon which in some cases precedes dissociation. It causes intensity anomalies in the spectral features which in turn have strong bearing on the relative disposition of various electronic states of the molecule concerned.

In what follows, we discuss the salient features of these phenomena in general in the beginning and thereafter with special reference to OH.

DISSOCIATION ENERGIES AND LIMITS

Accurate determination of the dissociation of diatomic molecules is of fundamental importance in many applications. These values are really useful in formulating reaction schemes representing various radiative or non-radiative phenomena. The dissociation energy of a diatomic molecule (D_0°) is the energy required to dissociate the molecule into normal atoms

from the lowest rotation-vibration level ($J = \Omega$; $v = 0$) of the ground electronic state. This term, as such, can be applied to all other stable electronic states as well. Thus, every state has a unique dissociation energy which represents the energy required to dissociate the molecule in that electronic state ($v = 0$; $J = \Omega$) into the two constituent atoms. In general, the precise value of dissociation energy of a molecule is more difficult to determine than the ionization potential. This is mainly because of the problems associated with the experiment and the interpretation. The method usually employed to determine dissociation energy values of the various molecules are summarized in table 4-1.

TABLE 4-1 METHODS OF DETERMINATION OF
DISSOCIATION ENERGIES OF MOLECULES

Spectroscopic Methods	Non-Spectroscopic Methods
Continuous Spectra & Band Convergence Limit	Thermal and Thermochemical
Birge-sponer Extrapolation	Electron-Impact and Mass
Predisociation Limit	Spectrometric
Atomic Fluorescence	
Photodissociation	

Although the non-spectroscopic methods are not primarily spectroscopic, the thread of spectroscopy does run through practically all the interpretations. In electron impact methods, one uses the Franck-Condon principle and has to

deal with the potential energy curves and also the excitation state of the dissociation products. In thermal and mass spectrometric work, one needs the statistical weights of the atomic and molecular states. In some of the thermal methods quantitative spectroscopic methods are used to determine concentrations of molecular species. For a detailed account of the applicability and the relative merits and demerits of these different techniques one is referred to the book

Dissociation Energies by Gaydon (1968).

Dissociation energies of the different electronic states of the OH molecule have been determined primarily by employing spectroscopic techniques, and it would be possible to estimate only the approximate values in the absence of any apparent convergence limits. The following D_0° values, however, may be regarded as more reliable (Carlone and Dalby, 1969a) and are summarized in table 4-2.

TABLE 4-2* DISSOCIATION ENERGIES AND DISSOCIATION LIMITS OF ELECTRONIC STATES OF OH

Electronic States	Dissociation Energies (D_0°) (cm^{-1})	Dissociation Limits (cm^{-1})	Dissociation Products
$C^2\Sigma^+$	29418 ± 15	117679	$O(^2P) + H(^2S)$
$B^2\Sigma^+$	1360^+	69212.3 ± 15	$O(^1S) + H(^2S)$
$A^2\Sigma^+$	18847 ± 15	51287.6 ± 15	$O(^1D) + H(^2S)$
$X^2\Pi_i (X^2\Pi_{3/2})$	35420 ± 15	35419.9 ± 15	$O(^3P) + H(^2S)$

* Carlone and Dalby (1969a)

[†] In view of the fact that the B state is very shallow and the isotope relations are invoked, it has been difficult to assess the range of error.

PREDISSOCIATION AND OH SPECTRUM

Predissociation, in a way, is the molecular analogue of "Auger Process"** in atomic spectroscopy. Although the appearance of this effect is not frequent, at least in the spectra of diatomics, it is significant in its own way both theoretically and from a practical viewpoint. Observations of predissociation quite often lead to very precise estimations of dissociation energies and in almost all cases, they at least set maximum limits for the D_0° values of the molecules. The appearance of predissociation in the spectral structure enables us to have a better insight into the interaction of different energy states of a molecule. Predissociation data have been used to determine the actual forms of repulsive electronic states in a number of cases. Predissociation transition probabilities and lifetimes can be converted into the respective oscillator strengths and thereby, could be useful to understand different radiative processes in planetary atmospheres. Predissociation normally manifests itself in an actual spectrum either as an abrupt breaking off or termination of the band structure beyond a certain stage in the system in the case of emission. Also, the predissociation causes the diffuseness or blurring in the

* "Auger Process" signifies a phenomenon in atomic spectra when a radiationless process takes place from a discrete energy state into the continuum of almost the same energy, leading to a radiationless decomposition of the atom into a positive ion and an electron.

band structure beyond a certain stage in the system in the case of absorption. The former, however, is a more reliable test for the occurrence of the phenomenon of predissociation.

In theoretical framework, this phenomenon is understood in terms of radiationless (or non-adiabatic) transition from a stable excited state of the molecule into a continuum of another unstable state of almost the same energy. This leads the molecule to a spontaneous dissociation. If this transition occurs in a lifetime that is of the order of the rotational period (say 10^{-11} sec), the rotational energy which controls the rotational structure no longer remains strictly quantized and the rotational structure becomes ill-defined. Because, however, vibrational frequencies are normally 10 to 100 times greater than the rotation frequencies, the vibrational energies which determine the gross structure of the system remain unaffected and the vibrational structure of the system remains intact. In borderline cases the rotational lines are simply broadened and the predissociation effect may not be clearly evident from the spectrum. Therefore, for a nice manifestation of predissociation effect, the radiationless transition should occur rapidly enough to give sufficient line broadening. Yet, even if this radiationless transition occurs at say 10 times the rate of spontaneous emission, most of the molecules in the first excited state will pass over the second state and become dissociated. Although in such a case there may not be any apparent diffuseness in

the absorption bands, emission bands will be drastically reduced in intensity since most of the molecules will not survive in the first excited state long enough to radiate spontaneously. Thus, breaking off the bands in the emission spectrum is more sensitive a test of predissociation than is diffuseness in absorption. It may be pointed out, however, that there will be no such breaking off in the thermal emission bands even though predissociation may be present. In thermal equilibrium, the population of the rotational levels of the upper state is also determined by the Boltzmann factor and so the number of predissociating molecules is exactly compensated by an equal number of new molecules formed by the inverse process. There is however, a broadening of rotational structure just as in absorption. Similar effects are observed at sufficiently high pressures. In such circumstances, there is no thermal equilibrium. The breaking-off of the band structure is suppressed due to quenching by the non-predissociated molecules by collisions. These considerations indicate that in order to detect weak predissociations, it is necessary to investigate discharge spectra at low pressures. Also, the energy considerations suggest that the possibility of predissociation occurring for all the discrete molecular states that lie above the lowest dissociation limit is not a relatively frequent phenomenon, especially in diatomics. This is most probably because the probability of a radiationless transition into the dissociating state

is usually so small that long before the decomposition would have taken place, the molecule has already passed into a lower lying discrete state with the emission of radiation. For the radiationless transition probability to be large enough to make predissociation feasible, there are certain selection rules which must be satisfied. In addition to the selection rules given below, the conditions of energy discussed above should also be met. The selection rules for the two participating states, known as Kronig's selection rules, for any coupling condition are

$$\Delta J = 0, + \not\leftrightarrow - \text{ and } S \not\leftrightarrow a.$$

In Hund case (a) and (b), the additional selectional rules,

$$\Delta S = 0 \text{ and } \Delta \Lambda = 0, \pm 1,$$

have to be satisfied. If both states belong to Hund case (a) or both to case (b), the respective selection rules are

$$\Delta \Sigma = 0 \text{ and } \Delta N = 0.$$

In Hund case (c) the rules $\Delta S = 0$ and $\Delta \Lambda = 0, \pm 1$. are replaced by $\Delta \Omega = 0, \pm 1$. Further, although the Kronig's selection rules restrict the possibility of considerable occurrence of predissociation, they are not sufficient to exclude the theoretical possibility of its occurrence in all cases. The Franck-Condon principle plays an equally important role in this context. According to this principle, predissociation

is more probable if the potential curves of the participating states intersect or at least come very close to one another. Then it is only in such a case that a transition to the dissociating state is possible without an appreciable alteration of position and momentum, thus allowing a decomposition of the molecule to take place. Naturally the transition does take place only when the molecule is in the neighborhood of the point of intersection. Summarizing, it is combined effect of the three factors, proximity of energy, selection rules, and the Franck-Condon principle that determines the occurrence of predissociation. Corresponding to the three forms of energy of a molecule, three cases of predissociation are possible.

Case 1 - Predissociation by electronic transition

Case 2 - Predissociation by vibration

Case 3 - Predissociation by rotation

Case 1 - Predissociation by Electronic Transition: The radiationless transition takes place between the discrete levels of one electronic state and the dissociation continuum belonging to another electronic state. This type of predissociation is the most commonly observed in diatomics and applies whenever the band structure becomes diffuse or breaks off at a distance from the point of convergence of the band system.

Case 2 - Predissociation by Vibration: This applies only to polyatomic molecules and has been of considerable importance in that area. Most unimolecular decompositions belong to this

case. Here a radiationless transition takes place in the continuum associated with a different vibration within the same electronic state.

Case 3 - Predissociation by Rotation: This is applicable to both types of molecules but so far it has been observed only in certain cases of diatomics. It occurs for those vibrational levels of an electronic state that lie in the neighborhood of the dissociation limit, since the higher rotational levels of such vibrational levels can lie above the dissociation limit. This case is most readily observed when the dissociation energy of the state is quite small. It may be pointed out that sometimes it is not possible to distinguish between Case 1 and 3.

In a stable type electronic state of a diatomic molecule, the potential curves without rotation shows a pronounced minimum. This minimum becomes less and less marked and finally disappears altogether for the higher rotational levels. The electronic state will not have a minimum corresponding to such higher J values and will be rotationally unstable. Excitation to such higher rotational levels may thus lead to dissociation of the molecule. The onset of the predissociation of the molecule by rotation, therefore, does not correspond to the dissociation limit.

In the case of the electronic spectrum of OH, the following three cases of predissociation have been reported.

- I. A sudden decrease in the intensity of emission lines originating from higher J levels of $v \geq 2$ in the system

$A\ ^2\Sigma^+$ - $X\ ^2\Pi_i$. The F_1 spin component was more strongly affected than the other component F_2 for both the vibrational levels $v' = 0$ and $v' = 1$. The predissociation effect sets in around $v' = 2$. This was first reported by Gaydon and Wollfran (1951). II. Of the eight bands (1,4), (1,5), (1,6), (1,9), (0,5), (0,6), (0,7), and (0,8) photographed (Carlone and Dalby, 1969a) in the system $B\ ^2\Sigma^+$ - $A\ ^2\Sigma^+$, only (1,4), (0,8), and (1,9) appeared sharper; the rest appeared diffused. The rotational lines were found to be much increased in width which could not be accounted for by temperature, collision, stark broadening, or some peculiar mode of formation of OH. The predissociation effect was found to set in around $v' = 5$ and was reported first by Carlone and Dalby (1969a). III. In system $B\ ^2\Sigma^+$ - $A\ ^2\Sigma^+$, a breaking-off was observed of the rotational levels at P(16) and R(14) for the band (0,7) and P(9), and R(7) for the band (1,6) and (1,9), respectively. This was reported by Felenbok (1963).

In the predissociation cases I and II cited above, the state $A\ ^2\Sigma^+$ is the common state. The predissociation in the $A\ ^2\Sigma^+$ must be caused by a molecular state arising from the normal atoms $O(^3P)$ and $H(^2S)$. In the ground state configuration, according to Winger and Witner rules, the only possible states are $^2\Pi$, $^2\Sigma^-$, $^4\Pi$, and $^4\Sigma^-$. The $^2\Pi$ state is the ground state and its potential curve does not cross that of $A\ ^2\Sigma^+$, $^4\Pi$, and $^2\Sigma^-$. Consequently, only weak effects are expected. In these circumstances the interaction of the $^4\Sigma^-$ state, the

closest among the three with $X^2\Pi$ near $v' = 2$ at $r > r_e$, appears to be responsible for the weak predissociation reported by Gaydon and Kopp (1971); and Sutherland and Anderson (1973). This also accounts for the different strengths of the levels from the F_1 and F_2 components. Michels and Harris (1969) have used configuration - interaction calculations to obtain potential energy curves of OH for all states arising from normal atoms. They found that the order of the states in increasing energy is $4\Sigma^- < 2\Sigma^- < 4\Pi$ and the $4\Sigma^-$ state crosses the state $2\Sigma^-$ on the outer limb at a point somewhere above the level $v' = 2$. To account for the stronger predissociation as reported by Carbone and Dalby (1969a), the following three hypothesis have been put forward.

a. Since none of the 4Π , $2\Sigma^-$, or $4\Sigma^-$ can account for the strong predissociation, the ground state 2Π could also be involved since interaction between $2\Sigma^+$ and 2Π is expected to lead to strong effects.

b. Predissociation might occur in two steps: first through the 2Π state and then to the $2\Sigma^-$ state. It is possible that the $X^2\Pi$ state comes sufficiently close to A $2\Sigma^+$ near $v' = 5$ at $r < r_e$ and the predissociation takes place through the $X^2\Pi$ state. However, in the case when 2Π is a predissociation state, a linear dependence on J is expected which is not actually observed. Alternatively, may be the 4Π state whose interaction with the A $2\Sigma^+$ around $v' = 5$ at $r > r_e$ might cause strong predissociation.

Interaction with $^2\Sigma^-$ is less probable since $^4\Pi$ state is believed to be the least stable (Czarny et al, 1971). The contention of Czarny et al that this stronger predissociation is caused by the interaction with the $^4\Pi$ state is based on the comparison between observed and calculated line widths.

c. In this case, the predissociation as reported by Felenbok (1963) comes under the category 'Predissociation by Rotation'. Breaking-off of the rotational lines of the $B\ 2\Sigma^+ - A\ 2\Sigma^+$ system was observed at P(16) and R(14) for the band (0,7) and at P(9) and R(7) for the bands (1,6) and (1,9), respectively. All the selection rules of Kronig are applicable to this case, as is usually the case in "Predissociation by Rotation."

Molecular Ionization Potential

A precise knowledge of the ionization potentials of molecules is quite often very useful in understanding aeronautical as well as many physical and chemical problems. The term signifies the difference in energy between the ground state of the molecular ion ($v = 0, J = \Omega$) and the ground state of the neutral molecule.

It is also possible for molecules to become ionized and to a first approximation, this is equivalent to the process of ionizing an atom. An infinite number of electronic states exist for each electron in a molecule and the transition to these states gives rise to a Rydberg series which is represented in wavenumber by the relation (Bauman, 1966)

$$v = A - \frac{R}{(n+\alpha)^2}, \quad (4-1)$$

where, hcA is the ionization energy, n is a running index (or principal quantum number of electrons), and α is a correction term. Such Rydberg series generally fall in the vacuum ultraviolet region for diatomics and are not observed. They may be hidden by a continuum arising from dissociation of the molecule in one of the low lying states.

Molecular ionization potentials are normally determined experimentally by electron impact, photoionization, and spectroscopic methods. The precision of ionization potential determinations by electron impact methods rarely exceeds ± 0.1 eV, due mostly to the rather large energy spread in the ionizing electron beams used in these experiments. In photoionization methods, the precision normally attained is ± 0.01 eV corresponding approximately to an exit beam half width $\sim 1\text{\AA}$. These techniques are, however, being improved. While the spectroscopic methods are capable of greatly improved accuracy, usually of the order of ± 0.001 eV, and depend on the identification of Rydberg series limit, no spectroscopic value of ionization potential of OH is known. The currently accepted value of 13.17 ± 0.1 eV for the first ionization potential of OH is based on the electron impact data and tabulated in the Handbook of Chemistry and Physics (Weast, 1970). By mass spectrometry, however, the reported value is 13.18 eV (Foner and Hudson, 1956).

INTENSITY PARAMETERS IN OH

Solution to many aeronomical problems is sought through the diagnostic study of upper atmospheres by using the methods of quantitative spectroscopy. A wide range of aeronomical phenomena, for example, cold air absorption, hot air absorption, aurora, dayglow, nightglow, and twilight, etc., have been investigated through these channels. In recent years the increased use of rocket, balloon, and satellite techniques has immensely extended the applicability and efficacy of these methods to other planetary atmospheres.

Intensity of absorption or emission at different frequencies is the basic observable quantity in all such investigations. Theoretically, the most dominating parameter in controlling the intensity of a radiative molecular transition, apart from the molecular population factor, is the transition strength matrix element S . This parameter is the main connecting link of other useful molecular parameters like Einstein A and B coefficients, linear absorption cross sections, photon mean free paths, optical paths, oscillator strengths, and radiative lifetimes which are frequently used diagnostically to determine the aeronomical conditions.

Franck-Condon Factors ($Q_{v'v''}$), \bar{r} -centroids ($\bar{r}_{v'v''}$) and Hönl-London factors $S_{v''}^{J'}$ are the theoretically computable quantities which determine the "transition strengths" of the molecular features. In the analysis of data on molecular band systems such computations have already provided a fund

of useful physical information for the understanding of many aeronomical and astrophysical problems.

The present section deals with brief outlines of the basic theory of molecular absorption, relative importance of the different molecular parameters controlling the intensities of molecular transitions, and the relevant data in respect to all these parameters as applied to the molecule OH.

FRANCK-CONDON FACTORS AND \bar{r} -CENTROIDS

The "probability" or "strength" of a radiative transition in a molecule is a very fundamental molecular parameter, significant in both theory and application. The property is as important in the domain of molecular quantum theory as it is useful in the application of quantitative spectroscopic data to various radiative phenomena. "Transition probabilities" must be known in any treatment involving radiative transfer properties. A knowledge of these values in respect to different transitions is quite useful in determining relative abundances of different atomic and molecular species in a system and their concentrations in specific quantum states under non-equilibrium conditions such as in flames, discharges, hot blasts and stellar atmospheres, etc. They are equally useful in determining different "spectroscopic temperatures". The reliable values of transition probabilities are crucially important in cases where one is interested in the competition between different radiative and

non-radiative processes such as collisional deactivation, predissociation, and chemical reaction.

Transition probabilities are closely linked with various other important molecular parameters, namely, Einstein A-coefficient of spontaneous emission; Einstein B-coefficient for induced absorption as well as induced or stimulated emission ($B_{12} = B_{21}$); linear absorption coefficient; molecular or atomic absorption cross section; photon flux or intensity; optical path of absorption; oscillator strength; and radiative lifetimes. Once we know the "transition probability" or the "transition strength", we can calculate all the other parameters and use them in different contexts. As a matter of fact, all these spectroscopic parameters have proved diagnostically very useful, at one stage or the other, in determining numerous aeronomical conditions and combustion processes. According to quantum mechanical formulation, the intensity of a spectrum line due to a transition $n \rightarrow m$ can be expressed as follows (Herzberg, 1950):

$$I_{nm} \left(\begin{smallmatrix} \text{spontaneous} \\ \text{emission} \end{smallmatrix} \right) = N_n h c \nu_{nm} A_{nm} , \quad (5-1)$$

where N_n is the total number of molecules or atoms in the initial upper state n , $h c \nu_{nm} = E_{nm}$ is the energy involved in the transition $n \rightarrow m$, and A_{nm} is the radiative transition probability for spontaneous emission ($n \rightarrow m$) or Einstein A-coefficient. For a dipole transition,

$$A_{nm} = \frac{64\pi^4}{3h} \cdot v_{nm}^3 | \langle n | M_e | m \rangle |^2 , \quad (5-2)$$

where $|\langle n | M_e | m \rangle|$ is called matrix element of the electric dipole moment M_e ^{*}. Combining (5-1) and (5-2) we get,

$$I_{nm} \left(\begin{array}{l} \text{spontaneous} \\ \text{emission} \end{array} \right) = \frac{64\pi^4}{3h^4 c^3} N_n E_{nm}^4 | \langle n | M_e | m \rangle |^2$$

$$= H N_n E_{nm}^4 S_{nm} \quad (5-3)$$

Here, H is a constant and S_{nm} is called the "transition strength" of the transition $n \rightarrow m$.

Similarly, for absorption, we can obtain the expression (Herzberg, 1950)

$$I_{nm} \text{ (absorption)} = I_{0(nm)} N_m \Delta x h v_{nm} B_{mn} , \quad (5-4)$$

where $I_{0(nm)}$ is the intensity of the incident radiation at v_{nm} , N_m is the total number of molecules in the initial lower state m , v_{nm} is the wavenumber of the absorption line, Δx is the thickness of the absorbing layer, and B_{mn} is the radiative transition probability for the induced absorption ($m \rightarrow n$) or Einstein B-coefficient.

^{*}The total electric dipole moment M of a molecule can be resolved into two contributions M_e and M_n , one arising from the molecular electrons and the other arising from nuclei such that $M = M_e + M_n$.

Again, for a dipole transition

$$B_{mn} = \frac{8\pi^3}{3h^2c} |\langle n | M_e | m \rangle|^2, \quad (5-5)$$

where $|\langle n | M_e | m \rangle|$ has the same concept as in emission.

Substituting this value of B_{mn} in equation (5-4), we get

$$\begin{aligned} I_{nm} \text{ (absorption)} &= \frac{8\pi^3}{3h^2c^2} I_{o(nm)} \Delta x N_m E_{nm} |\langle n | M_e | m \rangle|^2 \\ &= K N_m E_{nm} S_{nm}, \end{aligned} \quad (5-6)$$

where K is another constant involving $I_{o(nm)}$ and the geometry of the system. Under normal conditions $N_n \ll N_m$ and therefore, the contribution of stimulated emission is insignificant while considering these intensity parameters.

From the above discussion, it is evident that the most dominant parameter controlling a radiative transition, whether absorptive or emissive, is the transition strength S_{nm} . In the case of molecules, because a number of internal degrees of freedom exist that can influence the "transition strength" of a molecular spectral feature, S_{nm} actually should cover all the different energy states. Therefore,

$$S_{nm} = S_{(nv'J'L'M', \; mv''J'L'M'')} \quad (5-7)$$

where n and m represent the upper and lower electronic states, v' and v'' are the vibrational quantum numbers, J' and J'' are the quantum numbers of the component of electronic angular momentum along the internuclear axis, and M' and M'' are the magnetic quantum numbers and refer to the component of J in the direction of an externally applied magnetic field. (In all these quantum numbers, single primes refer to the upper levels and double primes to the lower levels.)

Now,

$$\begin{aligned}
 S_{(nv'J'A'M', \; mv''J''A''M'')} &= \left| \langle nv'J'A'M' | M_e | mv''J''A''M'' \rangle \right|^2 \\
 &= \left| \int \psi_n^* \frac{\psi_{v'}}{r} \psi_{J'A'M'} M_e \psi_m \frac{\psi_{v''}}{r} \psi_{J''A''M''} dr \right|^2 \quad (5-8)
 \end{aligned}$$

Furthermore, when it is possible to average this expression over the rotational sub-structure of a (v', v'') band, as is usually the case in astrophysical observations, the transition strength of a (v', v'') electronic band or the "Band Strength" can be expressed as:

$$\begin{aligned}
 S_{(nv', \; mv'')} \text{ or Simply } S_{v'v''} &= \left| \int \psi_n^* \frac{\psi_{v'}}{r} M_e \psi_m \frac{\psi_{v''}}{r} dr \right|^2 \\
 &= \left| \int \psi_{v'} \psi_n^* M_e \psi_m dr \right|^2 \\
 &= \left| \int \psi_{v'} R_e(r) \psi_{v''} dr \right|^2, \quad (5-9)
 \end{aligned}$$

where $R_e(r) = \int \psi_n^* M_e \psi_m d\tau_e$, and ψ_n and ψ_m are the electronic wavefunctions of the electric dipole moment M_e . If $R_e(r)$ is independent of r , equation (5-9) becomes

$$S_{v'v''} = R_e^2 \left| \int \psi_{v'} \psi_{v''} dr \right|^2. \quad (5-10)$$

In a realistic case, $R_e(r)$ may vary with r in a polynomial fashion,

$$R_e(r) = \sum_n a_n r^n.$$

$$\text{Then } S_{v'v''} = \left| \int \psi_{v'} \sum_n a_n r^n \psi_{v''} dr \right|^2 \quad (5-11)$$

Now, if we introduce a term $\bar{r}_{v'v''}$ characterized by the following relations obtained by the \bar{r} -centroid approximation (Fraser, 1954a, b; Drake and Nicholls, 1969):

$$\bar{r}_{v'v''} = \frac{\int \psi_{v'} \psi_{v''} r dr}{\int \psi_{v'} \psi_{v''} dr}, \quad (5-12)$$

and

$$\left(\bar{r}_{v'v''} \right)^n = \frac{\int \psi_{v'} r^n \psi_{v''} dr}{\int \psi_{v'} \psi_{v''} dr}, \quad (5-13)$$

then, Equation (5-11) takes the form

$$\begin{aligned} S_{v'v''} &= \left| \sum a_n \left(\bar{r}_{v'v''} \right)^n \right|^2 \left| \int \psi_{v'} \psi_{v''} dr \right|^2 \\ &= R_e^2 \left(\bar{r}_{v'v''} \right) Q_{v'v''}. \end{aligned} \quad (5-14)$$

In this expression for the "Band Strength" of a $(v'v'')$ band, the quantities $\bar{r}_{v'v''}$ and $Q_{v'v''}$ are called the \bar{r} -centroid and Franck-Condon factor for a $(v'v'')$ transition, respectively. The term $\bar{r}_{v'v''}$ represents the average characteristic internuclear separation associated with a particular transition $(v'v'')$ or in other words, it is the weighted average with respect to $\psi_v' \psi_v''$ of the range of r values experienced by a molecule in both the states of (v', v'') transition. It is also the \bar{r} -coordinate of the centroid of the area represented by the overlap integral from which its nomenclature is derived. The term $Q_{v'v''}$ signifies the extent of overlap of the two vibrational wavefunctions involved in a (v', v'') transition or in other words, it is a measure of the relative probability that a $(v'v'')$ transition would take place. The Franck-Condon principle predicts a particular $(v'v'')$ transition to be more probably on the basis of the extent of such a vibrational function overlap. It is because of this close association with the Franck-Condon principle that $Q_{v'v''}$ values are termed as Franck-Condon factors.

Felenbok (1963) calculated both the Franck-Condon factors and the \bar{r} -centroids in respect to various electronic transitions for OH and OD. Arrays of these parameters for all the known band systems of OH are presented in tables 5-1 through 5-8. Morse wavefunctions have been assumed as valid in the case of all the involved electronic states.

TABLE 5-1 FRANCK-CONDON FACTORS OF THE TRANSITION A $^2\Sigma^+$ - X $^2\Pi_g$ OF OH

v'	0	1	2	3	4	5	6	7	8	9	10	11	12
0	9.0701-1	8.9339-2	3.5776-3	5.1921-5	3.5662-8	1.7989-7	7.9590-8	3.3621-8	7.5067-8	2.7997-8	2.7582-8	5.7817-8	2.0284-7
1	8.5972-2	7.1375-1	1.8624-1	1.3193-2	2.4916-4	2.6760-6	3.5312-6	1.5470-6	3.8349-6	1.4150-6	1.3587-6	2.8447-6	8.9651-6
2	6.4934-3	1.7059-1	5.0663-1	2.7732-1	2.9868-2	4.9747-4	1.6402-5	2.5229-5	5.6927-5	2.0741-5	2.0827-5	4.2857-5	5.3737-5
3	4.7662-4	2.3134-2	2.4057-1	3.0142-1	3.3666-1	5.2108-2	1.7373-3	3.2821-4	3.0753-4	1.0631-4	1.0676-4	2.1762-4	2.3480-3
4	3.4233-5	2.7996-3	5.1213-2	2.8298-1	1.2942-1	3.6481-1	1.0114-1	1.1113-2	1.0941-3	1.1387-4	1.4134-4	2.7941-4	1.2859-1
5	2.5425-6	3.1533-4	9.3200-3	9.1037-2	2.6538-1	3.6066-2	3.9766-1	1.7901-1	1.9969-2	5.5177-4	5.1223-7	1.4010-6	3.8747-1
6	2.0513-7	3.2628-5	1.7150-3	2.1188-2	1.4327-1	1.8688-1	3.1728-4	3.3027-1	2.3842-1	4.3720-2	2.5235-3	8.0913-5	1.1592-2
7	1.0268-8	4.1338-6	2.7491-4	5.3001-3	4.7228-2	1.5382-1	1.2347-1	2.8219-2	2.3786-1	3.2251-1	7.5513-2	4.8425-3	5.6196-2
8	1.6181-10	9.1823-7	3.1172-5	1.6350-3	1.2047-2	8.4521-2	1.4160-1	3.8054-2	8.5514-2	1.1038-1	3.6025-1	1.3944-1	1.010-14
9	8.9524-10	2.3040-7	2.9493-6	4.9919-4	3.2148-3	3.7085-2	9.2622-2	1.0139-1	1.5256-3	1.3407-1	2.4486-2	3.4662-1	8.6493-2
10	1.6267-10	2.1680-8	9.4972-7	1.1039-4	1.2502-3	1.3546-2	5.1729-2	9.7926-2	4.4208-2	1.8050-2	1.2780-1	2.6846-3	6.1089-2

Note: $a \cdot b \cdot x = a \cdot b \cdot x \cdot 10^{-x}$

TABLE 5-2 \bar{r} -CENTROIDS OF THE TRANSITION $A\ ^2E^+$ - $X\ ^2\bar{E}_1$ OF OH

v^1	0	1	2	3	4	5	6	7	8	9	10	11	12
v^1	0.008	1.261	1.447	1.745	3.026	1.338	1.393	1.385	1.400	1.399	1.392	1.393	1.371
0	0.796	1.044	1.286	1.473	1.794	0.801	1.352	1.394	1.393	1.391	1.397	1.395	1.380
1	0.571	0.849	1.081	1.314	1.504	1.956	0.819	1.436	1.395	1.395	1.395	1.394	0.931
2	0.306	0.648	0.904	1.118	1.344	1.545	1.931	1.666	1.423	1.394	1.396	1.395	1.917
3	-0.066	0.439	0.719	0.963	1.151	1.380	1.571	1.750	1.683	1.292	1.395	1.395	1.550
4	-0.599	1.625	0.543	0.798	1.012	1.207	1.421	1.596	1.819	2.140	4.600	1.429	1.383
5	-1.344	-0.282	0.385	0.608	0.893	1.050	1.378	1.468	1.643	1.836	2.010	0.874	1.106
6	-3.676	-0.739	0.118	0.469	0.743	0.938	1.128	1.309	1.520	1.681	1.894	2.153	1.156
7	1.935	0.755	0.568	0.431	0.525	0.857	1.002	1.183	1.366	1.594	1.734	1.923	1.013
8	5.070	-0.765	-2.034	0.376	0.298	0.773	0.897	1.080	1.303	1.432	1.709	1.796	0.916
9	5.922	-2.370	-2.008	0.094	0.250	0.646	0.816	0.997	1.167	1.320	1.506	1.293	0.856

Note: Negative \bar{r} -values are the numerically calculated values. They do not convey any physical meaning.

TABLE 5-3 FRANCK-CONDON FACTORS OF THE TRANSITION $B\ 2\Sigma^+ - A\ 2\Sigma^+$ OF OH

v'	0	1	2	3	4	5	6	7	8	9	10
0	6.6958-8	3.3916-6	7.3813-5	9.0559-4	6.9010-3	3.3981-2	1.0879-1	2.2205-1	2.7656-1	1.9941-1	8.2266-2
1	1.9974-7	9.3133-6	1.8251-4	1.9522-3	1.2352-2	4.6533-2	9.7795-2	9.0936-2	8.8559-3	6.7029-2	2.8623-1

Note: $a \cdot b \cdot x = a \cdot b \cdot x \cdot 10^{-X}$ TABLE 5-4 \bar{r} -CENTROIDS OF THE TRANSITION $B\ 2\Sigma^+ - A\ 2\Sigma^+$ OF OH

v'	0	1	2	3	4	5	6	7	8	9	10
0	1.386	1.425	1.466	1.513	1.565	1.624	1.691	1.770	1.867	1.994	2.156
1	1.377	1.414	1.454	1.497	1.545	1.599	1.657	1.718	1.705	1.987	2.037

TABLE 5-5 FRANCK-CONDON FACTORS OF THE TRANSITION C $2\Sigma^+$ \rightarrow A $2\Sigma^+$ OF OH

v'	0	1	2	3	4	5	6	7	8	9	10
0	6.4865-19	5.1761-16	1.7571-13	3.3269-11	3.8669-9	2.2609-7	1.3524-5	4.0002-4	7.0584-3	6.8231-2	3.0971-1
1	6.9080-18	5.0053-15	1.5190-13	2.5236-10	2.5139-8	1.5456-6	5.8156-5	1.2831-3	1.5146-2	7.8703-2	1.0087-1
2	3.9526-17	2.6289-14	7.2270-12	1.0709-9	9.3388-8	4.9100-6	1.5321-4	2.6857-3	2.3621-2	8.2098-2	5.6090-2
3	1.6089-16	9.9120-14	2.4950-11	3.3401-9	2.5904-7	1.1879-5	3.1523-4	4.5345-3	3.0882-2	7.3161-2	1.7135-2

Note: a.b.x = a.b x10^{-x}TABLE 5-6 \bar{r} -CENTROIDS OF THE TRANSITION C $2\Sigma^+$ \rightarrow A $2\Sigma^+$ OF OH

v'	0	1	2	3	4	5	6	7	8	9	10
0	1.813	1.835	1.858	1.883	1.910	1.938	1.968	2.001	2.037	2.078	2.128
1	1.797	1.816	1.837	1.859	1.882	1.905	1.929	1.953	1.974	1.989	1.960
2	1.782	1.800	1.819	1.838	1.858	1.879	1.899	1.919	1.937	1.952	1.972
3	1.770	1.785	1.802	1.820	1.838	1.856	1.874	1.891	1.906	1.918	1.906

INTENSITY PARAMETERS

TABLE 5-7 FRANCK-CONDON FACTORS OF THE TRANSITION C $2\Sigma^+$ - X $2\Pi_1$ OF OH

v'	0	1	2	3	4	5	6	7	8	9	10	11	12
0	5.0830-23	2.4063-20	8.2728-18	1.6648-15	2.1901-13	1.9892-11	1.2825-9	5.9370-8	1.9715-6	4.6413-5	7.5691-4	8.2345-3	5.6344-2
1	4.0851-22	2.9991-19	9.0261-17	1.7892-14	2.1473-12	1.7541-10	9.9987-9	4.0058-7	1.1197-5	2.1360-4	2.6685-3	2.0333-2	8.2409-2
2	2.8320-21	1.9711-18	5.5467-16	1.0289-13	1.1370-11	8.4439-10	4.3116-8	1.5196-6	3.6523-5	5.8093-4	5.7904-3	3.2796-2	8.6493-2
3	1.3674-20	9.0700-18	2.5876-16	4.1966-13	4.3036-11	2.9325-9	1.3557-7	4.2578-6	8.9375-5	1.2088-3	9.8537-3	4.2892-2	7.5585-2

Note: $a \cdot b \cdot x = a \cdot b \cdot 10^{-x}$

TABLE 5-8 \bar{r} -CENTROIDS OF THE TRANSITION C $2\Sigma^+$ - X $2\Pi_1$ OF OH

v'	0	1	2	3	4	5	6	7	8	9	10	11	12
0	1.758	1.774	1.792	1.811	1.832	1.855	1.879	1.904	1.931	1.960	1.992	2.026	2.0651
1	1.747	1.762	1.778	1.796	1.815	1.835	1.857	1.879	1.902	1.926	1.951	1.976	1.993
2	1.738	1.751	1.766	1.782	1.800	1.818	1.837	1.857	1.878	1.899	1.920	1.940	1.956
3	1.730	1.742	1.755	1.770	1.786	1.802	1.820	1.838	1.857	1.876	1.894	1.911	1.926

OSCILLATOR STRENGTHS

Electronic transition probabilities are often expressed in terms of another molecular parameter called "Oscillator Strength" or the f -value. The term " f " (oscillator strength) owes its genesis to the classical dispersion theory of molecular refraction but in the context of radiative energy transfer it is defined as the ratio of the experimental value of the transition probability for a particular transition to a certain reference ideal value of transition probability. For an electronic transition, this reference value is taken to be the value predicted on the assumption that a single electron bound in a spherically symmetrical field of an ideal molecule undergoes radiative transition under the influence of an appropriate electromagnetic radiation, and the wavefunctions for the electron in various states are those of a harmonic oscillator. In such an idealized situation an exact calculation of the transition moment is possible and it can be used as a reference standard.

Let us assume that m and n represent the lower and the upper states respectively of an electronic transition, then for an ideal case,

$$|\langle n | M_e | m \rangle|^2_{\text{ideal}} = \left[\frac{3\hbar e^2}{8\pi^2 c m_e v_{mn}} \right], \quad (5-15)$$

where ν_{mn} is the wavenumber of the radiation involved in the transition and $|\langle n | M_e | m \rangle|$ is the matrix element of the electric dipole moment M_e , c is the velocity of light, e and m_e are the respective charge and the mass of an electron and h is the Planck constant. By definition, the oscillator strength for the transition $m \rightarrow n$ can be expressed as

$$f_{mn} = \frac{|\langle n | M_e | m \rangle|^2}{|\langle n | M_e | m \rangle|_{\text{ideal}}^2} = \frac{8\pi^2 m_e c \nu_{mn}}{3h e^2} |\langle n | M_e | m \rangle|^2$$

(5-16)

where the value of $|\langle m | M_e | m \rangle|^2$ should be determined from the experimental data. Depending then upon the methods of determining $|\langle m | M_e | m \rangle|^2$ values, there exist a number of ways to determine f -values. Generally f -values are determined either through integrated absorption cross section measurements or through direct measurements of radiative lifetimes under conditions of sharply defined excitations. The first method, while widely used, suffers from two general difficulties, namely,

1. to measure the true absorption coefficient over a line or a band, one needs very high resolution,
2. to know the molecular population in a particular energy state of a molecule, particularly in the case of a reactive molecule like OH, one often resorts to producing the molecules under thermal

equilibrium and, this requires very accurate thermodynamic data.

Moreover, the determination of absorption coefficients is dependent on the applicability of the well known absorption law which states that

$$\begin{aligned} I_{0\lambda} | I_{\lambda} &= \exp(\alpha_{\lambda} \ell_0) \\ &= \exp(\sigma_{\lambda} n_0 \ell_0) \quad , \end{aligned} \quad (5-17)$$

where $I_{0\lambda}$ and I_{λ} represent the incident and transmitted light intensities at wavelength λ , α_{λ} is the absorption coefficient at S.T.P. (0°C and 1 atm), ℓ_0 is the layer thickness of the absorbing species reduced to S.T.P.

$[\ell_0 = \ell (PT_0/P_0T)$, ℓ being the geometrical length of the absorbing column], σ_{λ} is the absorption cross section and n_0 is the number of absorbing molecules per c.c. at S.T.P. which is $2.687 \times 10^{19} \text{ cm}^{-3}$. The expression (5-16) is valid only if there are no non-linear factors contributing to the process of absorption. The absorbing gas should obey gas laws applicable to perfect gases in the experimental conditions. Reflection, convergence, non-homogeneity of radiation or of the sample gas, scattering fluorescence, decomposition, anisotropy, or saturation will give rise to appreciable deviations from ideality. The magnitude of the incident photon flux $I_{0\lambda}$ also plays a dominant role in the applicability of this law, especially when highly intense beams, such as laser, are employed. Although the law is

strictly true for monochromatic radiation, if the absorption cross section does vary with the wavelength, the use of the absorption law over a finite wavelength range defines what is known as the "effective absorption cross section." Increasing the resolution of measurement does not appreciably affect the value of effective cross section if its variation is small over the bandpass. When the absorption cross section varies appreciably over the wavelength range of the incident radiation, the law as stated above, will not hold and its modified form,

$$\frac{I_{o\lambda}}{I_\lambda} = \exp \left(n_o \ell_o \int_{\Delta\lambda} \sigma_\lambda d\lambda \right) \quad (5-18)$$

should be used. It may be pointed out that $\int_{\Delta\lambda} \sigma_\lambda d\lambda$ may be used only when σ_λ varies smoothly with λ over the wavelength range of interest; otherwise $\sum_{\Delta\lambda} \sigma_\lambda$ should be used. Here $\Delta\lambda$, the wavelength bandpass of incident radiation, is very small. Sometimes it is convenient to rewrite expression (5-17) in terms of effective or integrated absorption coefficient at the wavenumber v as

$$\frac{I_{ov}}{I_v} = \exp \left(\ell_o \int_{\Delta v} \alpha_v dv \right) \quad (5-19)$$

and the integrated absorption coefficient $\int_{\Delta\nu} \alpha_v dv$

$$\int_{\Delta\nu} \alpha_v dv = \frac{1}{\ell_0} \left[\ln \left(\frac{I_{0v}}{I_{cv}} \right) \right] \quad (5-20)$$

Theoretically, this parameter can be expressed as

$$\begin{aligned} \int_{\Delta\nu} \alpha_v dv &= \frac{I_v(\text{absorbed})}{I_{cv}(\text{incident})} \\ &= \frac{8\pi^3}{3hc} \cdot N_m v_{mn} |\langle n | M_e | m \rangle|^2 \end{aligned} \quad (5-21)$$

Equation (5-20) allows one to compare the experimental quantity $\int_{\Delta\nu} \alpha_v dv$ with the theoretical quantity $|\langle n | M_e | m \rangle|$. Combining equations (5-15) and (5-20), the expression for oscillator strength becomes

$$\begin{aligned} f_{mn} &= \frac{m_e c^2}{\pi e^2 N_m} \int_{\Delta\nu} \alpha_v dv \\ &= 1.1312 \times 10^{12} (\text{cm}^{-1}) [\sigma_v \Delta\nu \epsilon] \end{aligned} \quad (5-22)$$

where ϵ is the shape factor which for Lorentzian profile is $\frac{\pi}{2} = 1.57708$ and for the Gaussian profile is $1/2 \sqrt{\frac{\pi}{\log 2}} = 1.0644$. Finally, the expression for f_{mn} may be written as

$$f_{mn} = \delta \sigma_0 \Delta\nu \epsilon \quad (5-23)$$

where δ is a constant, σ_0 is the absorption cross section and

$\Delta\nu$ is the wavenumber range of the incident radiation.

After these general comments, let us discuss the oscillator strength for a transition with specific reference to OH molecule. The frequent occurrence of OH radical in a variety of flames, shocktubes, discharges, plasmas and numerous high temperature sources has served as a great impetus for many studies on oscillator strengths of different radiative transitions in OH spectra. Of all the transitions, the electronic bands involving the transition $A\ 2\Sigma^+ - X\ 2\Pi_g$ have been most widely investigated. Different methods were adopted by different investigators for the determination of f-values. The experimental f-values cited in literature often show a widespread and in some cases require considerable correction for rotation-vibration interaction (Learner, 1962; Golden et al, 1963). Broadly speaking, three models have been adopted for the f-value determination in OH spectra. These are: (a) integrated absorption coefficient measurements, (b) Roschdestwensky's "Hook" method, and (c) "Lifetime" measurements. In fact, the (a) technique was the first ever used in f-value determinations. The earliest measurements on integrated absorption coefficients of OH bands were made by Oldenberg and Rieke (1938b). This was followed by more precise measurements using OH in flames, shocktubes, and flow systems [Dwyer and Oldenberg, 1944; Dyne, 1958; Carrington, 1959; Golden et al, 1963; Watson, 1964; Rouse and Engleman, 1973]. These studies yielded oscillator strength for the

(0,0) band in the range 7×10^{-4} to 11×10^{-4} with a most probable value of 8×10^{-4} . It may be pointed out that the f-value determined, using techniques based on absorption coefficient measurements, were subject to corrections for thermochemistry, spectroscopic resolving power, and other parameters determining OH concentration in the system.

The "Hook" technique (b) was first introduced by Roschdestwensky (1912) in connection with the study of anomalous dispersion of sodium vapor. Later this technique was used by Roschdestwensky and Penkin (1941) for determining f-values of atomic transitions. Anketell and Pery-Thorne (1967) first used it for f-value determination of OH bands. They determined oscillator strengths of the (0,0) and (1,0) bands of the $A \ ^2\Sigma^+ - X \ ^2\Pi_g$ system and found $f_{00} = (14.8 \pm 1.3) \times 10^{-4}$ and $f_{10} = (8.9 \pm 1.7) \times 10^{-4}$. These values give $f_{10}/f_{00} = 0.6 \pm 0.1$ which agrees reasonably well with the value 0.53 as reported by Dieke and Crosswhite (1962). Although this technique shares with various other methods involving absorption coefficient measurements the disadvantage that a determination of OH concentration is required for absolute f-values, it has the advantage of being independent of both the line shape and the instrumental width of the spectrograph.

The technique (c) is conceptually different from either of the two described above. Using this technique, no corrections are needed with respect to the thermochemistry of the

system or the instrumental parameters or the factors determining the OH concentration. The method basically concerns the measurements of lifetimes by suddenly removing the radio-frequency excitation from the sample gas, thus leaving the excited molecular system to decay spontaneously, and then recording the time elapsed until the detection of the last photon. Optically any transition can be selected which originates from the level to be measured. Knowing the radiative lifetime, f-value may be calculated according to the relation,

$$f = \frac{m_e c \lambda^2}{8\pi^2 e^2} \cdot \frac{d_n}{d_m} \left(\frac{1}{\tau} \right), \quad (5-24)$$

where d_n and d_m are the degeneracy factors for the n^{th} and m^{th} states. Yet, in spite of the fact that this technique is potentially the most reliable for f-value determinations in general and OH bands in particular, sometimes it so happens that the lifetimes of the states are substantially modified due to mixing of levels of the electronic states (Douglas, 1966). In such cases, the apparent lifetime values will not lead to absolute f-values. Various authors (Bennett and Dalby, 1964; Elmegreen and Smith, 1972; Sutherland and Anderson, 1973) have measured f-values for a number of OH transitions using this technique. Tables 5-9 through 5-11 present the f-value data of different transitions reported by Sutherland and Anderson (1973) based on their lifetime measurements by the delayed coincidence technique. The best data based on absorption coefficient measurements are by Rouse and Engleman (1974) and these are presented in table 5-12.

TABLE * 5-9 OSCILLATOR STRENGTHS OF THE (0,0) BAND

N ^{**}	P ₁	Q ₁	R ₁	O ₁₂	P ₁₂	Q ₁₂	P ₂	Q ₂	R ₂	Q ₂₁	R ₂₁	S ₂₁
1				1.57								
2		6.66					2.20					
3	4.81		2.95		2.45							
4		7.81		0.523		1.20						
5	4.73		3.70		1.36							
6		8.71		0.318		0.630						
7	4.86				0.860							
8			0.210									
9			3.73									
10		7.97			0.286						0.111	
11	4.18		4.43		0.340					0.317		0.095
12		8.93		0.097		0.241		8.47	4.12	0.203		0.261
13	4.84		4.15		0.297		4.30	8.37		0.178		
14		8.52	3.86	0.075		0.161	4.24					
15	4.38	7.91			0.205	0.142					0.047	
16	4.07			0.062	0.175				3.79		0.141	0.056
17				0.052				7.62	3.69	0.094		0.139
18							3.95	7.39		0.084		0.044
19			3.54				3.69	7.08	3.56		0.088	
20		7.16	3.64					7.08	3.40		0.110	
21	3.58	6.87	3.36				3.53	6.76				
22	3.46	6.76					3.37					
23	3.40											

*Sutherland and Anderson (1973)

TABLE* 5-10 OSCILLATOR STRENGTHS OF THE (1,0) BAND

N ^{''}	P ₁	Q ₁	R ₁	O ₁₂	P ₁₂	Q ₁₂	P ₂	Q ₂	R ₂	Q ₂₁	R ₂₁	S ₂₁
1										0.903		0.547
2										0.414		
3								1.87				
4							0.999					
5		2.24	0.903				0.284		2.19	1.02	0.351	
6	1.28				0.301			1.16	2.27	1.09	0.238	0.289
7			1.12	0.079				1.18	2.36	1.13	0.196	0.218
8		2.45	1.12			0.095	1.23				0.139	
9	1.32	2.44			0.170	0.096				1.12		0.126
10	1.29		0.923	0.053	0.119				2.35	1.13	0.089	0.099
11		2.32		0.028		0.069		1.20	2.33		0.063	
12	1.23				0.098		1.12					

^{*} Sutherland and Anderson (1973)

TABLE* 5-11 OSCILLATOR STRENGTHS OF THE (1,1) BAND

N ^{''}	P ₁	Q ₁	R ₁	O ₁₂	P ₁₂	Q ₁₂	P ₂	Q ₂	R ₂	Q ₂₁	R ₂₁	S ₂₁
1										1.81	1.04	1.37
2												0.297
3								4.73				
4							2.54					
5		5.61	2.31				0.634					
6	3.25				0.746			6.01				
7							3.89	5.74	2.85	0.612	0.705	
8		6.15	2.81	0.182				2.97	5.96			
9	3.32	6.13	2.84				0.341	3.07				
10	3.25				0.297	0.269				2.88		0.301
11			2.80	0.109	0.326					2.83	0.202	0.270
12	3.09			0.077		0.183		5.94	5.80			0.171
					0.224		3.03		2.99			

* Sutherland and Anderson (1973).

TABLE 5-12 AVERAGE BAND f-VALUES ($\times 10^4$) FOR OH DETERMINED FROM UNBLENDED ROTATIONAL LINES

OH(0,0)		OH(1,0)		
	T = 1375 K		T = 1424 K	
P ₁ (2)	9.12	8.98	P ₁ (1)	2.25
P ₁ (4)	8.15	8.67	P ₁ (2)	2.41
P ₁ (5)	8.77	8.82	P ₁ (3)	2.37
P ₁ (6)	8.97	8.81	P ₁ (4)	2.37
P ₁ (8)	9.26	9.16	P ₁ (5)	1.99
P ₁ (9)	9.46	9.46	P ₁ (6)	2.30
P ₂ (7)	9.06	9.02	P ₁ (7)	2.28
Q ₁ (4)	8.56	8.08	P ₁ (8)	2.39
Q ₁ (5)	8.49	7.98	P ₁ (9)	2.04
Q ₁ (6)	8.62	8.10	P ₂ (5)	2.08
Q ₁ (8)	9.01	8.76	P ₂ (6)	2.29
Q ₁ (10)	9.49	9.32	P ₂ (7)	2.25
Q ₁ (13)	9.29	9.38	P ₂ (8)	2.50
Q ₁ (14)	9.22	9.30	Q ₁ (3)	2.31
Q ₂ (5)	8.72	8.42	Q ₁ (4)	2.18
Q ₂ (6)	9.19	8.80	Q ₁ (5)	2.27
Q ₂ (8)	8.77	8.81	Q ₁ (7)	2.33
Q ₂ (9)	9.32	9.23	Q ₁ (8)	2.47
Q ₂ (11)	9.32	9.33	Q ₁ (10)	2.29
Q ₂ (12)	9.13	9.51	Q ₁ (11)	2.31
Q ₂ (13)	8.48	9.46	Q ₁ (12)	2.40
R ₁ (4)	8.92	8.91	Q ₁ (13)	2.54
R ₁ (5)	8.97	8.96	Q ₂ (4)	2.52
R ₁ (6)	9.03	8.83	Q ₂ (6)	2.58
R ₁ (15)	--	9.61	Q ₂ (7)	2.38
R ₂ (1)	8.44	9.52	Q ₂ (9)	2.15
R ₂ (2)	9.46	8.93	Q ₂ (10)	2.31
R ₂ (3)	8.88	8.94	Q ₂ (11)	2.28
R ₂ (4)	8.74	8.90	Q ₂ (12)	2.40
R ₂ (7)	8.81	8.89	Q ₂ (13)	2.57
R ₂ (9)	9.17	9.29	R ₁ (3)	1.83
R ₂ (10)	8.72	9.28	R ₁ (7)	2.46
R ₂ (13)	--	9.99	R ₁ (8)	2.14
			R ₁ (9)	2.44
			R ₁ (10)	2.31
			R ₂ (5)	2.17
			R ₂ (8)	2.45
			R ₂ (10)	2.38

*Rouse and Engleman (1974)

IONIZED RADICAL OH⁺ AND ITS BAND SPECTRA

The observed Spectrum of the ionized hydroxyl radical OH⁺ is characterized by an electronic transition of the type $^3\Pi - ^3\Sigma$. Discussed below are the general features of band structure arising out of such a transition.

BAND STRUCTURE OF A $^3\Pi - ^3\Sigma$ TRANSITION: In the case of $^3\Pi - ^3\Sigma$ transitions when $^3\Pi$ state satisfies the conditions of Hund case (a), the application of the $J = 0, \pm 1$ and $+ \leftrightarrow -$ selection rules gives 27 branches. They form three sub-bands, $^3\Pi_{0,1,2} \rightarrow ^3\Sigma$, each comprised of nine branches characterizing the rotational structure of each of the sub-bands. (See tables 6-1, 6-2 and 6-3.) Figure 6-1 depicts the transitions scheme for the different nine branches of a

TABLE 6-1 TERM VALUE DIFFERENCES AND SELECTION RULES FOR
 $^3\Pi_0 - ^3\Sigma^-$ TRANSITION

<u>Nomenclature</u>	<u>Term Value Differences</u> cm^{-1}	<u>Selection Rules</u>		<u>Remarks</u>
		ΔN	ΔJ	
P ₁	$F'_1 (N - 1) - F''_1 (N)$	-1	-1	
Q ₁	$F'_1 (N) - F''_1 (N)$	0	0	Main Branches
R ₁	$F'_1 (N + 1) - F''_1 (N)$	+1	+1	
$Q_{P_{12}}$	$F'_1 (N - 2) - F''_2 (N)$	-2	-1	
P _{Q₁₂}	$F'_1 (N - 1) - F''_2 (N)$	-1	0	
Q _{R₁₂}	$F'_1 (N) - F''_2 (N)$	0	+1	
N _{P₁₃}	$F'_1 (N - 3) - F''_3 (N)$	-3	-1	Satellite Branches
$Q_{Q_{13}}$	$F'_1 (N - 2) - F''_3 (N)$	-2	0	
P _{R₁₃}	$F'_1 (N - 1) - F''_3 (N)$	-1	+1	

TABLE 6-2 TERM VALUE DIFFERENCES AND SELECTION RULES FOR
 $^3\Pi_1 - ^3\Sigma^-$ TRANSITION

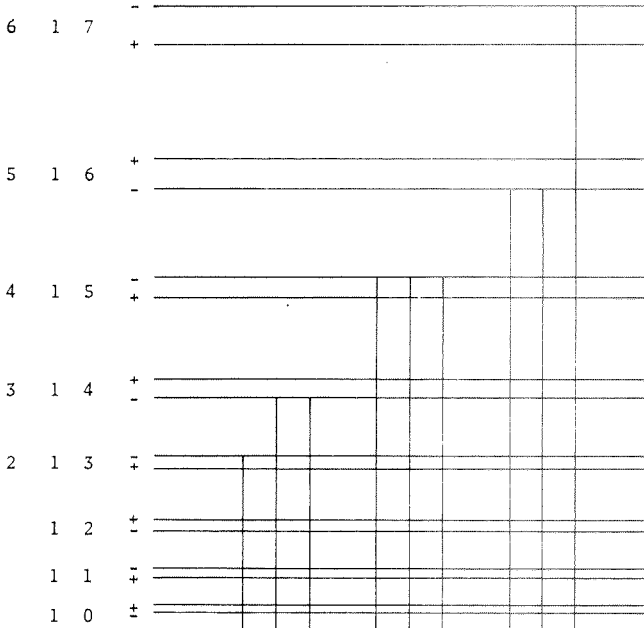
Nomenclature	Term Value Difference cm^{-1}	Selection Rules ΔN	Selection Rules ΔJ	Remarks
P_2	$F'_2 (N - 1) - F''_2 (N)$	-1	-1	
Q_2	$F'_2 (N) - F''_2 (N)$	0	0	Main Branches
R_2	$F'_2 (N + 1) - F''_2 (N)$	+1	+1	
$Q_{P_{21}}$	$F'_2 (N) - F''_1 (N)$	0	-1	
$R_{Q_{21}}$	$F'_2 (N + 1) - F''_1 (N)$	+1	0	
$S_{R_{21}}$	$F'_2 (N + 2) - F''_1 (N)$	+2	+1	Satellite
$O_{P_{23}}$	$F'_2 (N - 2) - F''_3 (N)$	-2	-1	Branches
$P_{Q_{23}}$	$F'_2 (N - 1) - F''_3 (N)$	-1	0	
$Q_{R_{23}}$	$F'_2 (N) - F''_3 (N)$	0	+1	

TABLE 6-3 TERM VALUE DIFFERENCES AND SELECTION RULES FOR
 $^3\Pi_2 - ^3\Sigma^-$ TRANSITION

Nomenclature	Term Value Difference cm^{-1}	Selection Rules ΔN	Selection Rules ΔJ	Remarks
P_3	$F'_3 (N - 1) - F''_3 (N)$	-1	-1	
Q_3	$F'_3 (N) - F''_3 (N)$	0	0	Main Branches
R_3	$F'_3 (N + 1) - F''_3 (N)$	+1	+1	
$Q_{P_{32}}$	$F'_3 (N) - F''_2 (N)$	0	-1	
$R_{Q_{32}}$	$F'_3 (N + 1) - F''_2 (N)$	+1	0	
$S_{R_{32}}$	$F'_3 (N + 2) - F''_2 (N)$	+2	+1	Satellite
$R_{P_{31}}$	$F'_3 (N + 1) - F''_1 (N)$	+1	-1	Branches
$S_{Q_{31}}$	$F'_3 (N + 2) - F''_1 (N)$	+2	0	
$T_{R_{31}}$	$F'_3 (N + 3) - F''_1 (N)$	+3	+1	

$$\left[{}^3\Pi_0(R) \right]$$

N' F' J' P'



$$\left[{}^3\Sigma^- \right]$$

N'' F'' J'' P''

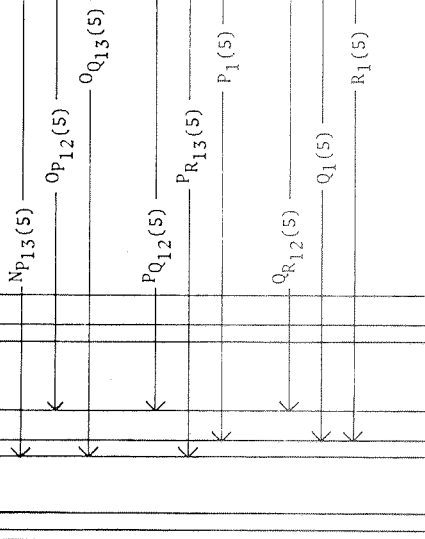
6 2 6 +
5 2 5 -
3 4 6 -
4 2 5 4 +
3 3 5 3 +6 2 6 +
5 2 5 -
3 4 6 -
4 2 5 4 +
3 3 5 3 +6 2 6 +
5 2 5 -
3 4 6 -
4 2 5 4 +
3 3 5 3 +

Figure 6-1 Schematic of the various branches of OH⁺ rotational structure expected in an electronic transition ${}^3\Pi_0 - {}^3\Sigma^-$.

typical $^3\Pi_0^- - ^3\Sigma$ sub-band. The transition schemes applicable to the other two sub-bands can be drawn in a similar manner. All these branches, however, are not to be expected in every $^3\Pi - ^3\Sigma$ band. The observed structure will depend upon the degree of approximation of the $^3\Pi$ state to Hund case (a) or to case (b) or, in other words, upon the value of the coupling constant (A/B_v). If the $^3\Pi$ state is in a case (b), eight of the branches corresponding to the selection rules $\Delta N = \pm 2$ (O and S forms) and $\Delta N = \pm 3$ (N and T forms) are absent. The band thus consists of nine main branches and ten weak satellite branches. These weaker branches are normally grouped around three main triplets $P_{1,2,3}$, $Q_{1,2,3}$, and $R_{1,2,3}$ and do not form three distinct sub-heads. With a $^3\Pi$ state intermediate between case (a) and (b), the latter ten satellites are all stronger than in case (b) and the former eight also appear feebly. As in all $\Pi - \Sigma$ transitions, the Q branch is the strongest of all in each band. In passage from case (a) to case (b) with increasing J and N in a given band, the nine main branches form three P, Q, and R contracting triplets. Yet, if the spin separations in the $^3\Sigma$ state are negligibly small, a band will be reduced by coincidences of neighbors to apparently a 15-branch band structure (five in each sub-band) and in a case (b) 19-branch band to apparently a 9-branch band (the three main triplets). Again, if in the latter case, the $^3\Pi$ state also has negligibly small spin separations, these triplets will appear to form single P, Q, and R branches, like those

of a $^1\Pi$ - $^1\Sigma$ band. Such a situation actually exists in the case of $^3\Pi$ - $^3\Sigma$ band systems of NH, PH, N₂, and H₂ etc. As an example, perhaps the best known $^3\Pi$ - $^3\Sigma$ band system is the First Positive of N₂. All but one of the predicted 27 branches have been identified in an analysis of six bands by Naude (1932). Here the $^3\Pi$ state is regular and intermediate between (a) and (b).

The $^3\Pi_i$ - $^3\Sigma^-$ band structure of OH⁺ conforms to an intermediate case of Hund (a) and (b) when $^3\Pi$ state is inverted. Spin multiplets of the ground state $^3\Sigma^-$ are also not too close and manifest themselves in the structure. All the 27 principal and satellite branches have actually been identified for a number of bands and it has been possible to establish combinatorial relations between the diverse branches.

OBSERVED SPECTRA OF OH⁺

A $^3\Pi_i \rightarrow X ^3\Sigma^-$ (3983 - 3332 \AA): Rodebush and Wahl (1933) were probably the first to identify OH⁺ as a diatomic emitter. While investigating the reactions of the OH radical in the electrodeless discharge in water vapor at low pressure, they discovered two new bands degraded to the red with heads at 3565 and 3332 \AA and attributed to ionized OH radical. In addition to the two bands discovered by Rodebush and Wahl (1933), Loomis and Brandt (1936) identified two new bands at 3983 and 3695 \AA . These bands were observed by using improved conditions of the electrodeless discharge and a 21-foot concave grating with a dispersion of 1.25 $\text{\AA}/\text{mm}$. Loomis and Brandt

were thus able to investigate the rotational structure of all the four bands which were assigned to a electronic transition $A\ ^3\Pi_i \rightarrow X\ ^3\Sigma^-$. The state $^3\Pi_i$ was found to be inverted and approaching Hund case (a) for the lower N values and case (b) for higher N values. A number of satellite branches were also identified. Weniger and Herman (1958) reinvestigated the emission spectrum of the OH^+ molecule. They used a modified configuration of the discharge tube and thereby produced a very strong emission spectrum. As a result, they observed two additional bands with heads at 3958 and 3830\AA . However, they reported the rotational analysis of three bands (3695 , 3830 , and 3958\AA). O'Connor (1962) studied the emission spectrum produced by a condensed discharge in water vapor and carried out a detailed rotational analysis. He assigned a number of bands to OD^+ . The wavelengths of six band heads so far observed are shown in the Deslandres table 6-4. Merer et al (1969) investigated the OH^+ produced by a radiofrequency discharge in

TABLE 6-4 THE DESLANDRES SCHEME OF $A\ ^3\Pi_i - X\ ^3\Sigma^-$
FOR OH^+ R-HEADS OF THE BANDS[†]

v''	0	1	2	3
0	3565	3983		
1	3332	3695		
2			3830	
3				3958

[†]In Rosen's book (1970) the (0,1) and (3,3) bands are misprinted as 3893 and 3953, respectively.

water vapor mixed with helium. Using a 21-foot grating spectrograph and the spectrum in the first and second order, they observed irregularities in the Λ -doubling of the $A\ ^3\Pi$ state. The irregularities, caused by various rotational perturbations, have been found to occur in the rotational levels of all the three components $^3\Pi_0$, $^3\Pi_1$, and $^3\Pi_2$. These perturbations are of two kinds: local perturbations and perturbations affecting all levels. Local rotational perturbations were first observed by Loomis and Brandt (1936) and were quite prominent in the $v' = 1$ level. Kovacs (1958) has shown that such rotational perturbations are to be expected if there is a strong interaction between the state $^3\Pi_i$ and $^1\Sigma^+$. A careful analysis of the observed rotational perturbations suggested that there is in fact an interaction between the $A\ ^3\Pi_i$ and another state $B\ ^1\Sigma^+$ which lies about 1200 ± 50 cm^{-1} above the $A\ ^3\Pi$ state. Merer et al (1969) also detected the perturbations affecting all the levels of $A\ ^3\Pi$ state in OH⁺ similar to those described for other hybrides by Horani et al (1967) and Dixon and Lamberton (1968). A schematic of the molecular states and the electronic transitions is shown in figure 6-2. This figure also shows the values of the relevant spectroscopic constants.

In this band system defined by $A\ ^3\Pi_i \rightarrow X\ ^3\Sigma^-$, there are three sub-band systems, namely, $^3\Pi_0 \rightarrow ^3\Sigma^-$, $^3\Pi_1 \rightarrow ^3\Sigma^-$, and $^3\Pi_2 \rightarrow ^3\Sigma^-$. In each sub-system, there are nine sub-branches, three for each triplet component of the lower state. So there

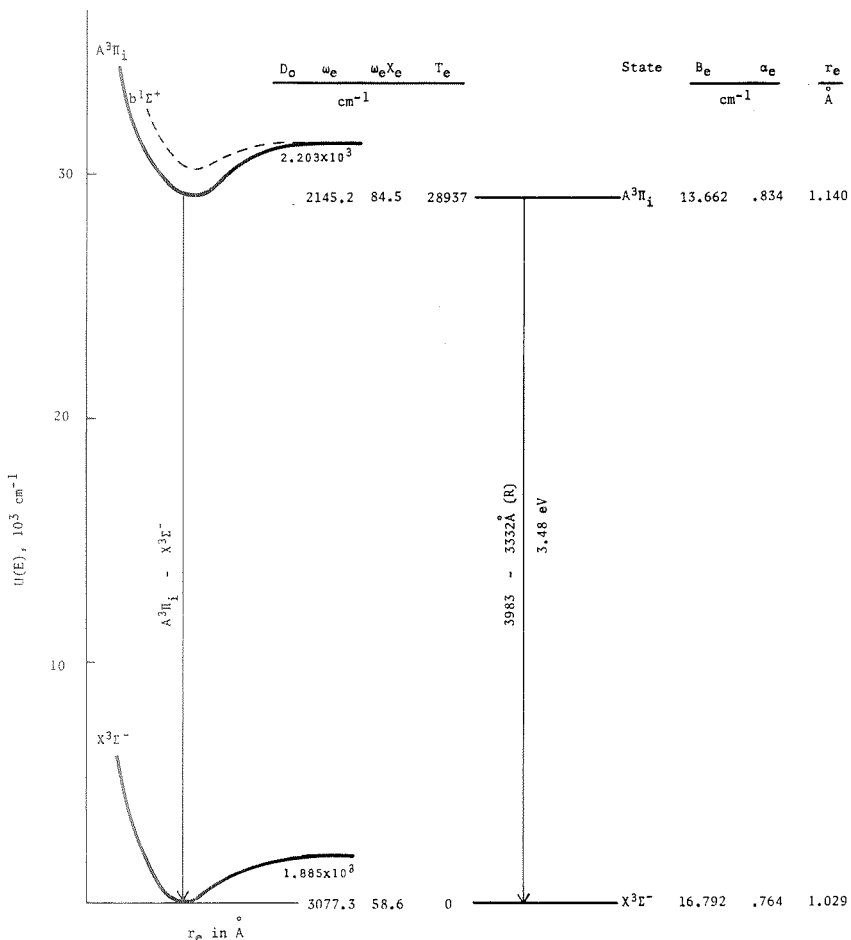


Figure 6-2 Electronic states and the observed electronic transitions in OH^+ . The values of the various spectroscopic constants (Rakotoarijimy, 1970) are also given.

are 27 branches. Rakotoarijimy (1969, 1970) studied these bands under the very high dispersion (0.8 and 0.6 \AA/mm) obtained in the higher orders (10th, 11th, 12th and 13th) of the spectrum using a grating spectrograph (Jaco Elbert). His precise measurements of the (0,0), (0,1), (1,0), (1,1), and (2,2) enabled him to identify the 27 principal and satellite branches for each band except the (2,2). The wavenumbers of the rotational lines identified in these bands are given in table B-1 (Appendix B). He also reported the new values of the rotational and vibrational constants given in table 6-5.

OH⁺ Radical in Interstellar Space: A group of lines observed in the spectrum of comets (3560 - 3600 \AA) corresponds to the first few rotational lines of the (0,0) band due to OH⁺. Similarly, the cometary radiations observed in the region (3907 - 4033 \AA) have been attributed to the (1,0) band of this very molecule.

During the study of the spectrum of the comet, named Cunningham 1941 I, Humaerts (1945) tried to identify some of the observed emission lines of the molecule OH⁺. Recently Rakotoarijimy (1969) presented a detailed identification of some of the OH⁺ lines with reference to the cometary wavelengths given by Swings (1942). These are given in table 6-6.

TABLE* 6-5 ROTATIONAL AND VIBRATIONAL CONSTANTS OF OH⁺

	State 3Σ ⁻	State 3Π _i
B ₀	16.410	13.245
D ₀	-1.885	-2.203
H ₀	-0.995	-0.235
B ₁	15.646	12.411
D ₁	-1.655	-2.176
H ₁	-1.315	-0.440
B _e	16.792	13.662
D _e	-2.00x10 ⁻³	-2.216x10 ⁻³
α _e	0.764	0.834
β _e	0.230x10 ⁻³	0.027x10 ⁻³
I _e	1.666x10 ⁻⁴⁰ gr/cm	2.048x10 ⁴⁰ gr/cm
r _e	1.029x10 ⁻⁸ cm	1.140x10 ⁻⁸ cm
ω _e	3077.3	2145.2
ω _e · ω _e	58.6	84.5
H _e	1.453x10 ⁻⁷	1.447x10 ⁻⁷
λ	0.690	
γ	-0.163	

* Rakotoarijimy (1970)
 Note: All constants are in units of cm⁻¹ unless specified otherwise.

TABLE* 6-6 COMET WAVELENGTHS AND THEIR ASSIGNMENTS IN OH⁺

Comet's Wavelength		Rakotoarijimy	Branches Assigned to 0-0 Band
Å	cm ⁻¹	cm ⁻¹	
3565.0	28042.5	28042.0	R _{P₃₁(2)} + R _{P₃₁(3)} band head
3565.7	28037.6	28037.6	R _{P₃₁(4)}
3572.2	27986.0	27985.3	P ₃₃ (1)
3577.3	27946.1	27946.5	Q _{P₂₁(1)} + Q ₂₂ (1)
3584.3	27891.5		CN Band
3589.4	27851.9	27851.8	Q _{R₁₂(3)}
Branches Assigned to (1,0) Band			
3987.2	25073.2	25073.6	R ₂₂ (5) + R _{Q₂₁(4)} + R ₂₂ (4)
3992.6	25039.3	25040.7	R ₂₂ (1)
3997.5	25008.6	25009.6	R ₁₁ (9) ?
4002.2	24979.2	24978.1	Q _{P₂₁(2)} + Q _{P₃₂(4)} + Q ₃₃ (4)
4007.5	24946.2	24947.6	Q ₃₃ (5) ?
4013.2	24910.7	24910.8	Q _{R₁₂(2)} + Q ₁₁ (2)
4027.6	24821.7	24820.8	P _{R₁₃(3)}

The numbers within brackets are the N values in the Lower State.

* Rakotoarijimy (1969)

APPENDIX A

TABLE A-1 OH IN THE SOLAR SPECTRUM
SUMMARY

Laboratory				Sun				
Electronic Transition	Vibrational Transition	Wavelength Range A	Total Number of Lines	Summary of Counts				Total
				Present	Blend	Masked	Absent	
A $^2\Sigma^+$ - X $^2\Pi$	0,0	3021 - 3362	283	108	63	69	43	283
	1,1	3109 - 3378	231	52	56	81	42	231
	2,2	3184 - 3372	159	15	5	23	15	58
		Total	673	175	124	173	100	572
	3,3	3253 - 3356	73	0				
	1,0	2811 - 3050	219	0				
	0,1	3428 - 3545	119					
	2,1	2854 - 3070	186	0				
	1,2	3483 - 3545	56					
	3,2	2944 - 3060	119	0				

The wavenumbers should be increased by about 0.2 cm^{-1}

TABLE A-2 OH IN THE SOLAR SPECTRUM

 $A^2\Sigma^+ - X^2\Pi (0,0)$

Laboratory							Sun				Remarks		
O ₁	P ₁	P ₂	Q ₁	Q ₂	R ₁	R ₂	S ₁	Intensity	Wavenumber cm ⁻¹	Wavelength Å	Wavelength Å	Solar Identification	
					15,16	2+2+2	33088.89*	3021.285					A
					14,17	3+1	33083.82	3021.749	3021.719				M
					13	4	33073.92	3022.652					A
					18	1	33073.07	3022.730	3022.747				M
					12	5	33059.25	3023.994					A
					11	7	33039.96	3025.760					A
					10	9	33016.31	3027.927	3027.890				M
					9	11	32988.40	3030.490	3030.484				P
					8	14	32956.39	3033.433	3033.434				M
					7	18	32920.61	3036.730	3036.754				M
					6	22+3	32881.22*	3040.368	3040.35				P
					5	26	32838.48	3044.325	3044.333				P
					4	29	32792.81	3048.565	3048.569				P
					3	30	32744.63	3053.051	3053.068				M
					2	28	32694.55	3057.727					A
					1	19	32643.36	3062.523	3062.52				P
					9	402	32632.25	3063.565	3063.555				P
					8,10,9'	415+378+44	32630.55	3063.725	3063.729				P
					8'	55	32628.46	3063.921					P
					10'	31	32627.94	3063.970					M
					7	415	32625.61	3064.189					M
					11	346	32625.11	3064.236	3064.216				B
					7'	68	32623.68	3064.370	3064.377				M
					11'	27	32622.39	3064.491	3064.515				M
					6	397	32617.51	3064.950	3064.955				P

TABLE A-2 (Continued)

 $A^2\Sigma^+ - X^2\Pi (0,0)$

Laboratory							Sun						
O_1	P_1	P_2	Q_1	Q_2	R_1	R_2	S_1	Intensity	Wavenumber cm^{-1}	Wavelength A	Wavelength A	Solar Identification	Remarks
								310+83	32615.97	3065.095	3065.094	OH Cr I	B
								20	32613.02	3065.372			A
								363	32606.60	3065.976	3065.994	OH - Mn I	B
								100	32605.13	3066.114	3066.144	OH - Al I	B
								271	32602.96	3066.318	3066.364	Ti II V I	M
								15	32599.82	3066.613			A
								304	32593.16	3067.240	3067.262	Fe I	M
								114	32591.92	3067.356	3067.386	OH -	B
					10			352	32588.68	3067.661	3067.657	OH	P
						9		373	32587.47	3067.775	3067.781	OH	P
					14	11	230+323	32585.84	3067.920	3067.939	OH - Fe I	B	
					14'	8	11+383	32582.14	3068.277	3068.281	OH	P	
						12	290	32578.63	3068.608	3068.598	OH	P	
					3		234	32577.61	3068.704	3068.725	OH - Fe II	B	
					3'		126	32576.60	3068.799	3068.796	OH	P	
						7	378	32572.59	3069.177	3069.181	OH	P	
						13	255	32567.30	3069.675	3069.681	OH VI	B	
							193	32564.78	3069.913	3069.915	OH	P	
					15'		9	32561.27	3070.244	3070.265	Mn I	M	
					2		152	32560.48	3070.318			M	
					2'		127	32559.53	3070.392	3070.380	OH	P	
						6	359	32558.79	3070.478	3070.492	OH	P	
						14	218	32551.72	3071.145	3071.145	OH - Fe II	B	
					1		69	32542.56	3072.009	3071.965	Co I	M	
					1'		102	32541.99	3072.063	3072.115	Ti II	M	
						5	325	32540.55	3072.199	3072.182	OH	P	
						16	159	32539.38	3072.508	3072.528	OH - Co I	B	
						16'	6	32535.67	3072.660	3072.670	OH?	P	
						15	183	32531.76	3073.028	3072.984	Ti II	M	
						4	273	32517.58	3074.369	3074.385	OH	P	

TABLE A-2 (Continued)

 $A^2\Sigma^+ - X^2\Pi(0,0)$

Laboratory									Sun				
O ₁	P ₁	P ₂	Q ₁	Q ₂	R ₁	R ₂	S ₁	Intensity	Wavenumber cm ⁻¹	Wavelength Å	Wavelength Å	Solar Identification	Remarks
					17	16		131	32509.61	3075.123	3075.135	OH	P
					17'	5		151	32507.38	3075.334	3075.355	OH	P
					3			204	32505.77	3075.486		A	
					17			125	32489.49	3077.028	3077.027	OH	P
									32478.48	3078.071	3078.044	Fe I - OH	B
					18			102	32475.28	3078.373	3078.387	OH	P
		1				239			32474.58	3078.440			
		1'			18'	166			32474.28	3078.468	3078.445	OH Fe I	M
		2				3			32471.28	3078.753	3078.662	Ti II Fe II	M
		2'				437			32458.65	3079.951			
						152			32458.07	3080.006	3079.979	OH - Fe I	B
					2			138	32455.70	3080.231	3080.245	OH	P
		3			18	98			32444.91	3081.255	3081.247	OH Fe I	B
		3'				616			32441.90	3081.541	3081.550	OH	P
						130			32441.07	3081.620			A
1					252			32440.60	3081.665	3081.680	OH	P	
					80			32436.38	3082.065	3082.035	-OH	B	
		4			2			32432.27	3082.456			A	
		4'			766			32423.63	3083.278	3083.282	OH	P	
					111			32422.62	3083.374	3083.382	OH	P	
					1			32415.51	3084.050	3084.055	OH	P	
		5			19	68		32406.64	3084.894	3084.897	OH	P	
		5'				77			32403.47	3085.196	3085.206	OH	P
						884			32402.10	3085.317	3085.331	Cr II	M
		20				93			32392.66	3086.226	3086.229	OH	P
2					335			32390.94	3086.390	3086.400	Co I - OH	B	
		6			2			32388.38	3086.634	3086.636		M	
		6'			974			32380.99	3087.338	3087.345	OH	P	
					77			32379.49	3087.481	3087.453	Fe I - OH	B	
					59			32363.49	3089.008	3089.000	OH	P	

TABLE A-2 (Continued)

A $2\Sigma^+$ - X 2Π (0,0)

Laboratory								Sun					
O ₁	P ₁	P ₂	Q ₁	Q ₂	R ₁	R ₂	S ₁	Intensity	Wavenumber cm ⁻¹	Wavelength A	Wavelength A	Solar Identification	Remarks
3	21	7'	7					995	32355.88	3089.734	3089.745	OH	P
			2,3					62+293+439 + 95+100	32354.55	3089.861	3089.868	OH	P
			2',3'					94	32350.27	3090.270	3090.222	Fe I - Co I	M
			4'					589	32349.29	3090.364	3090.374	OH	P
			4										
		5'	1'					70	32348.40	3090.449	3090.486	OH OH	{B
			1					139	32348.15	3090.473		OH	B
			47						32344.08	3090.862	3090.868		P
			416+83						32340.69	3091.186	3091.213	CH OH	B
			5					712	32338.86	3091.361	3091.371	OH	P
	21	8'	8					1000	32328.06	3092.394	3092.403	OH	P
			8'					50	32326.15	3092.577	3092.598	CH OH	B
			6'					71	32325.38	3092.650	3092.712	Al I	M
			6					808	32323.96	3092.786	3092.851	Al I (OH)	M
								45	32315.37	3093.609	3093.608	OH	P
		7'	1'					143	32314.19	3093.722	3093.723	OH	P
			7					58	32306.49	3094.459	3094.469	OH	P
			9					855	32304.83	3094.618	3094.626	OH	P
			9'					973	32297.38	3095.342	3095.347	OH	P
								40	32295.15	3095.546	3095.554	OH	P
4	22	2,2'						35	32290.40	3096.000			A
								492	32289.12	3096.124	3096.138	OH Cr II	B
								114+154	32286.76	3096.349	3096.324	Fe II - OH	B
								48	32283.62	3096.650	3096.624	- OH	B
								873	32281.74	3096.830	3096.902	Mg I	M
	22	10'	10					912	32263.45	3098.586	3098.588	OH	P
								34	32262.11	3098.715	3098.720	OH	P
								31	32261.16	3098.807	3098.825	OH	P
								38	32256.97	3099.210	3099.235	Zr II OH	B
								860	32254.86	3099.411	3099.418	OH	P

TABLE A-2 (Continued)

 $A^2\Sigma^+ - X^2\Pi (0,0)$

Laboratory									Sun				
Ω_1	P_1	P_2	Q_1	Q_2	R_1	R_2	S_1	Intensity	Wavenumber cm^{-1}	Wavelength A	Wavelength A	Solar Identification	Remarks
2	5	3'						158	32253.54	3099.538	3099.575	OH - OH	{ B
								33+215	32252.97	3099.593			
		11	10'		23			546	32235.96	3101.229	3101.242	OH	P
								26	32231.51	3101.657			A
								842+30	32226.47	3102.142	3102.148	OH	P
	4'	11'	10					24+871	32224.23	3102.358	3102.369	OH	P
								148	32214.79	3103.267	3103.284	OH	P
		4			23			307	32214.01	3103.342	3103.349	OH	P
								25	32203.57	3104.348	3104.349	OH	P
								23	32192.44	3105.421	3105.464	Ni I	M
3	6	12	11		23			763	32189.94	3105.663	3105.677	OH	P
								43+752	32186.27	3106.017	3106.032	OH	P
		12'						18	32183.55	3106.279	3106.241	Ti II	M
								582	32180.83	3106.542	3106.559	Fe II OH-Zr II	B
								131	32171.36	3107.457	3107.459	OH - Ti I	B
	5'				24			384	32170.36	3107.553	3107.565	OH - Cr II	B
								19	32167.27	3107.852	3107.854		M
		12'	12					18	32154.66	3109.069	3109.073	Fe I-Hf II	M
								690	32151.97	3109.330	3109.333	OH CH	B
		13						664	32142.73	3110.223	3110.245	OH-	B
4	7	13'	13		24			14+18	32139.70	3110.517	3110.529	OH	P
								607+111	32123.54	3112.082	3112.077	Ti II - Fe I OH	B
		6"	6					441	32122.52	3112.181	3112.214	OH	P
								44+14	32113.29	3113.075	3113.097	OH	P
								611	32110.35	3113.361	3113.384	OH	P

TABLE A-2 (Continued)

 $A^2\pi^+ - X^2\Pi (0,0)$

Laboratory								Sun					
O ₁	P ₁	P ₂	Q ₁	Q ₂	R ₁	R ₂	S ₁	Intensity	Wavenumber cm ⁻¹	Wavelength Å	Wavelength Å	Solar Identification	Remarks
5	7'	7	14'	14	25	25		14	32097.35	3114.622	3114.628	OH	M
								569	32095.83	3114.769	3114.778		P
								11	32092.65	3115.077	3115.043		M
								94	32072.36	3117.048	3117.037		P
								481	32070.89	3117.191	3117.201		P
	8	15	14'	14	25	25		13	32070.03	3117.275	3117.249	Cr II	M
								10	32068.18	3117.455	3117.432		M
								527	32065.05	3117.759	3117.768		P
								609	32063.74	3117.886	3117.890	OH - Ti I	B
								478	32045.43	3119.668	3119.678		B
9	8'	15'	15	15'	26	26		8	32042.10	3119.992	3120.012	OH - Fe II	B
								41	32036.08	3120.578	3120.602		P
								10+11	32021.98*	3121.953	3121.969		M
								8+63	32019.34*	3122.210	3122.219		M
								76	32017.43	3122.397	OH CH	A	
	9'	16	16	16	26	26		447	32016.08	3122.528	3122.570	OH OH - Cr II	B
								493	32015.69	3122.566	B		
								531+48	32001.156*	3123.945	3123.959		P
								10	31994.69	3124.616	3124.638		P
								399	31991.48	3124.929	3124.918		P

TABLE A-2 (Continued)

A $^2\Sigma^+$ - X $^2\Pi$ (0,0)

Laboratory										Sun														
O ₁	P ₁	P ₂	Q ₁	Q ₂	R ₁	R ₂	S ₁	Intensity	Wavenumber cm ⁻¹	Wavelength Å	Wavelength Å	Solar Identification	Remarks											
6	10	17	27	27	27	27	27	36+48	31954.81*	3128.515	3128.521	OH	P											
								7	31940.34	3129.933	3129.947	Y II?	M											
		17'						548	31936.84	3130.276	3130.267	V II - OH	B											
								324	31933.87	3130.567	3130.567	OH Fe II	B											
								4	31390.19	3130.928			A											
	10'	17'	27					7	31913.37	3132.578			A											
								4	31910.47	3132.863			A											
		17						305	31906.78	3133.225	3133.216	OH	P											
								49	31897.55	3134.132	3134.116	Fe I Ni I	M											
								475	31895.44	3134.339	3134.337	OH Cr II	B											
7	11	18	28	28	28	28	28	265	31872.57	3136.588	3136.590	OH	P											
								31+505	31869.52	3136.888	3136.890	OH	P											
		18'						3	31868.61	3136.978			A											
								5	31852.68	3138.547	3138.518	Fe I	M											
								3	31850.29	3138.783	3138.786	M	P											
	11'	18	28	28	28	28	28	250	31846.40	3139.166	3139.164	OH	P											
								38	31832.84	3140.503	3140.511	OH	P											
		11						445+9	31830.53*	3140.731	3140.757	OH - Ca I	B											
								5+22	31825.88*	3141.190	3141.181	Ca I	M											
								205	31807.44	3143.011	3143.016	OH	P											
8	12	19'	29	29	29	29	29	2	31803.39	3143.412			A											
								459	31799.49	3143.797	3143.764	. Ti II CH - OH	B											
		19						2	31786.16	3145.115	3145.091	Fe I - Cr II	M											
								194	31782.09	3145.518	3145.526	OH	P											
	12'							26	31781.47	3145.579			M											
								30+15	31765.06*	3147.195	3147.235	Cr II	M											
	20							407	31762.53	3147.456	3147.447	OH - OH	B											
								3	31758.54	3147.851			A											
								159	31738.44	3149.844	3149.852	OH	P											
13	13	29	29	29	29	29	29	3	31731.99	3150.485	3150.512		M											
								405	31726.79	3151.001	3151.005	OH	P											

TABLE A-2 (Continued)

 $A^2\Sigma^+ - X^2\Pi (0,0)$

Laboratory									Sun									
O_1	P_1	P_2	Q_1	Q_2	R_1	R_2	S_1	Intensity	Wavenumber cm^{-1}	Wavelength \AA	Wavelength \AA	Solar Identification	Remarks					
9	13	20						151	31713.78	3152.293	3152.262	Ti II-OH	P					
								23	31694.26	3154.235	3154.200	Fe II Ti II	M					
		21						363	31691.53	3154.507	3154.493	OH Fe I	B					
								21+143	31690.39*	3154.621	3154.643	OH	P					
								122	31665.38	3157.112	3157.143	OH - Fe I _p	B					
	14	30						2	31657.83	3157.865	3157.882	Fe I-V II	M					
								350	31651.40	3158.507	3158.521	OH	P					
		21						115	31641.40	3159.505	3159.531	Ni I OH-Cr I	B					
								2	31631.34	3160.510	3161.598	A	A					
								17	31620.45									
10	14	30						318	31617.51	3161.892	3161.901	OH	P					
								17	31595.81	3164.064	3164.068	CH	M					
		21						92	31588.27	3164.819	3164.833	V II OH	B					
								297	31573.14	3166.336	3166.335	OH	P					
								88	31564.85	3167.168	3167.177	OH	P					
	15	22						1	31550.49	3168.609			A					
								13	31543.65	3169.296			A					
		22						272+7	31540.50*	3169.613	3169.616	OH	P					
								1	31523.80	3171.292			A					
								68	31506.92	3172.991	3172.997	OH	P					
11	16	31						14	31498.73	3173.816	3173.840	OH	P					
								248	31492.12	3174.482	3174.480	OH	P					
		23						65+2	31484.02*	3175.299	3175.314	OH Fe I	B					
								10	31465.81	3177.339	3177.302	Co I - CH	M					
								228	31460.48	3177.675	3177.680	OH	P					
	17	32						50	31421.22	3181.645	3181.641	OH	P					
								186	31408.19	3182.965	3182.990	Fe I-Ni I	M					
		24						1+1	31406.08	3183.180			A					
								11+48	31398.78	3183.919	3183.964	V I	M					
								7	31380.97	3185.727			A					

TABLE A-2 (Continued)

 $A^1\Sigma^+ - X^1\Pi (0,0)$

Laboratory										Sun			
O ₁	P ₁	P ₂	Q ₁	Q ₂	R ₁	R ₂	S ₁	Intensity	Wavenumber cm ⁻¹	Wavelength Å	Wavelength Å	Solar Identification	Remarks
18	18	17'	25	25				188+3+3	31377.45*	3186.084	3186.104	OH	P
								37	31331.06	3190.802	3190.849	Fe I	M
								164	31321.42	3191.784	3191.799	OH	P
								35	31308.97	3193.053	3193.054	OH	P
13	19	18'	26	26				8	31296.74	3194.301	3194.849	OH Ce II?	A
								5	31295.11	3194.467			A
								158	31291.38	3194.848			B
								26	31236.22	3200.489	3200.469	Ni I - Fe I	M
								133	31231.62	3200.961	3200.962	OH	P
14	20	19'	26	26				25	31214.52	3202.715	3202.695	CH OH	B
								4	31206.13	3203.576	3203.980	OH	A
								124+2	31202.23*	3203.977			P
								6	31191.94	3205.034			A
								102	31138.83	3210.500	3210.480	OH	P
15	21	20'	27	27				19	31136.65	3210.725	3210.724	CH OH	B
								18	31115.28	3212.934	3212.892	Mn	M
								3	31113.99	3213.063	3213.474	OH	A
								95+4	31109.97*	3213.479			P
								5	31084.69	3216.092			A
16	22	21'	28	28				78	31042.95	3220.420	3220.433	OH	P
								13	31032.05	3221.548	3221.545	OH	P
								2	31018.77	3222.927	3222.944	Fe II?	M
								74	31014.52	3223.369	3223.364	OH	P
								13	31011.01	3223.734	3223.744	OH?	P
17	22	22'	29	29				4	30975.13	3227.468	3230.727	OH Mn I	A
								60	30943.87	3230.729			B
								9	30922.38	3232.974	3232.938	Ni I	M
								1	30920.28	3233.193	3233.167	Ni I	M
								56	30915.87	3233.654	3233.669	OH	P

TABLE A-2 (Continued)

 $A^2\Sigma^+ - X^2\Pi (0,0)$

Laboratory								Sun									
0 ₁	P ₁	P ₂	Q ₁	Q ₂	R ₁	R ₂	S ₁	Intensity	Wavenumber cm ⁻¹	Wavelength Å	Wavelength Å	Solar Identification	Remarks				
17	23	23	29	45	30813.99*	3241.489	3235.149	9	30901.59	3235.149	3239.170	Fe I	A				
								3+1	30863.24*	3239.170			A				
								45	30841.55	3241.447			M				
		23	30					42+35	30813.99*	3244.346	3244.354	OH	P				
								6	30807.15	3245.067	A						
18	24	24	30	33	30735.83	3252.609	3247.220	6	30786.72	3247.220	3251.218	OH	A				
								2	30748.87	3251.218			A				
								33	30735.83	3252.597			P				
		24	31					32	30708.50	3255.491	3255.497	OH- Cr I	B				
								4	30686.32	3257.812			M				
19	25	25	31	32	30666.26	3259.989	3259.989	4	30666.26	3259.976	3263.597	Fe I Cr I	M				
								1	30632.23	3263.597			A				
								24	30626.72	3264.185			P				
		25	32					23	30599.58	3267.080	3267.062	Fe II-OH	B				
								3	30539.85	3273.740			M				
26	26	26	32	33	30514.00	3276.262	3276.262	17	30514.00	3276.243	3279.154	OH	P				
								17	30487.11	3279.133			P				
								12	30397.55	3288.795	3288.813	Zr II	M				
		27	32					12	30370.91	3291.679			M				
								9	30277.20	3301.862			B				
27	28	28	32	34	30250.81	3304.754	3304.754	8	30250.81	3304.749	3318.367	OH?- Ti I-Co I	B				
								6	30153.06	3315.462			A				
								6	30126.65	3318.369			M				
		28	32					4	30024.67	3329.641	3329.632	Fe I	M				
								4	29998.38	3332.558			M				
31	31	31	32	35	29891.82	3344.439	3344.439	3	29891.82	3344.439	3347.375	OH? Fe I	A				
								3	29865.33	3347.371			M				
		32	32					2	29754.34	3359.892			A				
								2	29728.27	3362.839			A				

TABLE A-3 OH IN THE SOLAR SPECTRUM

 $A^2\Sigma^+ - X^2\Pi (1,1)$

Laboratory								Sun					
O ₂	P ₁	P ₂	Q ₁	Q ₂	R ₁	R ₂	S ₁	Intensity	Wavenumber cm ⁻¹	Wavelength Å	Wavelength Å	Solar Identification	Remarks
							3	5	32147.10	3109.801	3109.803	OH?	P
							2	4	32101.06	3114.262			A
							1	3	32053.54	3118.879			A
			8				67		32025.16	3121.643	3121.604	Ti II Co I	M
			7				68		32023.93	3121.762	3121.783	OH Fe I	B
			9,8'				65+9		32022.86	3121.867	3121.859	Cr II - OH	B
			7'				11+10		32021.98*	3121.953	3121.969	Cr II	M
			9'				7		32020.56	3122.091	3122.079	Ti II	M
			6				63+8		32019.34*	3122.210	3122.219	OH CH	B
			6'				13		32017.81	3122.360			A
			10				62		32016.73	3122.465			A
			10'				6		32014.36	3122.696	3122.664	Fe I	M
			5				57		32011.67	3122.958	3122.949	OH	P
			5'				16		32010.25	3123.096	3123.092	Ti I	M
			11				57		32006.79	3123.434	3123.443	OH	P
			11'				4		32004.20	3123.687	3123.698	Fe II?	M
			4				48+531		32001.56*	3123.945	3123.959	OH	M
			4'				18		32000.03	3124.094	3124.097	Fe I	M
			12				51		31992.79	3124.801	3124.803	OH - Ge I	B
			12'				3		31990.07	3125.067	3125.053	Cr II - CH	M
			3				37		31988.34	3125.236	3125.288	V II	{M
			3'				20		31987.38	3125.329			M}
				9			60		31977.16	3126.329	3126.332	OH	P
				8			61		31975.78	3126.464	3126.472	OH	P
			13				45		31974.59	3126.580			{B
				10			57		31974.20	3126.618	3126.617	CH OH OH	B}
			2				24		31973.63	3126.674			A
			2'				20		31972.91	3126.745	3126.767	Fe I	M
			13'				3		31971.62	3126.871	3126.847	Fe I _p	M
				7			62		31969.91	3127.038	3127.047	OH	P
				11			53+6		31966.74*	3127.347	3127.362	OH	P

TABLE A-3 (Continued)

$$A \ ^2\Sigma^+ - X \ ^2\Pi \ (1,1)$$

Laboratory								Sun					
O ₂	P ₁	P ₂	Q ₁	Q ₂	R ₁	R ₂	S ₁	Intensity	Wavenumber cm ⁻¹	Wavelength Å	Wavelength Å	Solar Identification	Remarks
								6	31959.51	3128.055	3128.036	OH - OH	B
				1				57	31957.78	3128.224		Sc II OH	A
				1'				11	31957.20*	3128.281	3128.289	OH	M
								16+492	31954.81*	3128.515	3128.521	OH	P
								48+36	31952.12	3128.779	3128.776	OH Y II?	B
								14					
								14'	31948.91	3129.093	3129.107	Fe I	M
								5	31944.43	3129.532	3129.532	OH	P
								13	31938.40	3130.123	3130.137	OH - Ti I	B
								15	31925.20	3131.418	3131.446	OH	P
								4	31924.40	3131.496	3131.526	OH - Cr II	B
								15'	31921.78	3131.753			A
								14	31917.40	3132.182	3132.189	OH	P
								3	31899.00	3133.989	3133.966	Fe I p - OH	B
								16	31893.67	3134.514	3134.541	OH - OH	{ B
								37	31893.01	3134.578			{ B
								1					
				1'				26	31892.80	3134.599	3134.626	OH	P
								15	31891.72	3134.705	3134.716	OH Hf II	B
								31	31890.01	3134.873			A
								1					{ B
				2				68	31876.78	3136.174	3136.195	OH Fe I	{ M
				2'				24	31876.24	3136.227			
								2	31867.82	3137.056	3137.025	Co I? - OH	B
								16	31861.28	3137.705	3137.710	OH	P
								39	31860.78	3137.749	3137.765	Co I - OH	B
				3				96	31859.31	3137.894	3137.896	OH	P
				3'				20	31858.55	3137.969			A
								17	31857.39	3138.083	3138.076	V II - OH	B
								17'	31855.65	3138.452			A
								120	31840.07	3139.791	3139.761	V II Sc II - OH	B
								17	31839.10	3139.886			A
				4				1	31830.53*	3140.731	3140.757	OH - Ca I	M
				4'				9+445					

TABLE A-3 (Continued)

A 2¹⁺ - X 2¹ (1_{1,1})

O ₂	P ₁	P ₂	Q ₁	Q ₂	R ₁	R ₂	S ₁	Laboratory			Wavelength Å	Wavelength Å	Solar Identification	Remarks
								Intensity	Wavenumber cm ⁻¹	Sun				
2	6 ¹	5 ¹	5 ¹	5 ¹	17	17	22 ⁺	31825.88*	31411.190	31411.181	Ca I	N	-OH	B
								1.59	31411.909	31411.908				
			18	18	15	15	31818.60	31412.025	3142.021	OH	P	OH	B	
								31817.44	3142.042	3142.156				
								18	31816.17	3142.142				
	5 ¹	2 ¹	2 ¹	2 ¹	52	52	31812.39	3142.522	3142.511	OH	P	OH	B	
								152	31794.56	3144.284				
			18	18	12	12	31793.15	3144.424	3144.326	CH OH?	B	OH	B	
								17	31785.59	3145.472				
								15	31772.15	3146.504				
5	19	19	2 ¹	2 ¹	43+16	43+16	68	31771.57	3146.560	3146.598	OH	N	N	B
								68	31770.85	3146.631				
			19	19	15	15	31770.03	3146.712	3146.934	OH	A	P	B	
								158	31767.67	3146.916				
								10 ⁺ 22 ⁺ 11	31766.00	3147.112				
	7 ¹	7 ¹	1,1 ¹	1,1 ¹	15+30	15+30	31765.06*	3147.195	3147.235	Cr II	A	N	A	
								93	31764.36	3147.274				
			4 ¹	4 ¹	65	65	31762.99	3147.447	3147.267	Fe I - OH	B	B	B	
								15	31753.91	3148.509				
								112	31752.72	3148.427				
5	19	19	14	14	14	14	31740.03	3149.687	3148.440	Fe I OH Cr I	A	A	P	
								163 ⁺ 11	31737.73	3149.915				
			19	19	22	22	31736.31	3150.056	3149.898	OH - Cr II	B	B	B	
								12	31735.71	3150.314				
								9	31718.69	3151.806				
	7 ¹	7 ¹	6 ¹	6 ¹	136	136	31715.47	3152.125	3152.117	OH	A	A	P	
								76	31712.16	3152.454				
			7 ¹	7 ¹	24	24	31707.21	3152.947	3152.457	OH	P	P	B	
								18	31707.01	3152.957				
								156	31704.62	3153.191				
4	2 ¹	2 ¹	1 ¹	1 ¹	7 ¹	7 ¹	8+12 ⁷	31704.62	3153.191	Fe I OH	B	B	B	
								9	31717.10	3151.964				

TABLE A-3 (Continued)

A $^2\Sigma^+$ - X $^2\Pi$ (1,1)

Laboratory									Sun				
O ₂	P ₁	P ₂	Q ₁	Q ₂	R ₁	R ₂	S ₁	Intensity	Wavenumber cm ⁻¹	Wavelength Å	Wavelength Å	Solar Identification	Remarks
3	3	3	20	8 ¹	8	21	9 ¹	6	31702.60	3153.405	3154.420	Fe I Ni I - OH	A
								8	31692.20	3154.445			M
								143+21	31690.39*	3154.621			B
								11	31689.32	3154.727			A
								25	31674.69	3156.184	3156.190	OH	P
	4	4	21	10 ¹	10 ¹	21	9 ¹	33	31674.12	3156.241	3156.272	Fe I OH	M
								148	31668.20	3156.831	3156.845		P
								5	31665.98	3157.052	3157.031	Fe I	M
								6	31663.32	3157.317	3157.294	-OH CH OH?	M
								9	31661.95	3157.454	A		
5	5	4	21	9	9	21	138	31661.26	3157.523	3157.501	-OH CH OH?	B	
								85	31659.36	3157.712	3157.751	B	
								23	31636.55	3159.989	OH Cr II Fe I	A	
								48	31635.77	3160.067		3160.082	B
								8	31633.08	3160.336		3160.347	M
	6	6	22	11 ¹	10 ¹	22	10 ¹	5	31630.38	3160.605	3160.612	Cr I CH V II - OH	M
								137+133	31628.22	3160.821	3160.801		B
								4	31625.95	3161.048	3161.053	Mn I	M
								7	31610.35	3162.609	3162.570	Ti II	M
								92	31604.30	3163.214	3163.223	OH	P
7	5	5	22	11 ¹	11 ¹	22	11 ¹	7	31599.67	3163.678	3163.683	Fe I Zr II OH	M
								20+4	31593.48	3164.297	3164.295		B
								60	31592.51	3164.394	3164.418	OH	P
								124	31590.97	3164.548	3164.548	OH	P
								124	31584.96	3165.151	3165.157	OH Fe Ip	B
	12 ¹	12 ¹	22	12 ¹	12 ¹	22	12 ¹	3	31582.40	3165.407	3165.420	Zr II	M
								6	31571.17	3166.534	-OH	A	
								3	31552.55	3168.402		A	
								114	31549.90	3168.668	3168.672	P	
								95	31540.77	3168.982	3168.955	B	

TABLE A-3 (Continued)

A $2\Sigma^+$ - X 2Π (1,1)

Laboratory							Sun						
O ₂	P ₁	P ₂	Q ₁	Q ₂	R ₁	R ₂	S ₁	Intensity	Wavenumber cm ⁻¹	Wavelength Å	Wavelength Å	Solar Identification	Remarks
4	6	6						18	31546.02	3169.058	3169.075	OH-Fe Ip	B
		6						69	31544.86	3169.174	3169.192	[Oii-Cr II]	B
								7+272	31540.50*	3169.613	3169.616	OH	M
								100	31537.98	3169.866	3169.861	OH	P
								2	31535.18	3170.148	3170.128		M
	7	13						5	31531.66	3170.502	3170.481		M
		13'						2	31508.67	3172.815			A
			13'					101	31504.86	3173.198	3173.210	OH	P
			13					5	31503.56	3173.329			A
					23			15	31494.57	3174.235	3174.221	Fe Ip	M
5	8	7						75	31493.16	3174.377	3174.380	OH	P
		7						96	31487.30	3174.968	3174.953	OH	P
		14						95	31486.60	3175.039	3175.045	[Sn I OH]	B
		14'						2+65	31484.02*	3175.299	3175.314	OH Fe I	M
								6	31464.92	3177.227			A
	8		14'					2	31458.98	3177.826	3177.822		M
			14					4	31457.66	3177.960			A
					24			89	31455.88	3178.140	3178.161	OH	P
								12	31439.22	3179.824			A
		8	8					78	31437.64	3179.984	3179.966	OH	P
6	9	15						82	31432.83	3180.470	3180.491	OH	P
		15'						1+4	31429.95	3180.762	3180.746	Fe I	M
								95	31423.71	3181.393	3181.420	OH Cr II	B
								1+1	31406.08*	3183.180			A
								76	31402.83	3183.509	3183.520	OH	P
								6	31385.40	3185.277			A
		9						10	31380.30	3185.795	3185.804	OH	P
6	9							81	31378.50	3185.977	3185.979	OH	M
								3+188+3	31377.45*	3186.084	3186.104	OH	P
			16		25			69	31374.47	3186.387	3186.383	OH	P

TABLE A-3 (Continued)

A $^2\Sigma^+$ - X $^2\Pi$ (1,1)

Laboratory									Sun				
O ₂	P ₁	P ₂	Q ₁	Q ₂	R ₁	R ₂	S ₁	Intensity	Wavenumber cm ⁻¹	Wavelength Å	Wavelength Å	Solar Identification	Remarks
10	10'	16'	25	16'	16	10'	10	1+9	31370.78*	3186.762	3186.752	Fe II	M
								88	31358.00	3188.010	3188.034	OH Cr I	B
								1+3	31350.14	3188.860			A
								64	31345.70	3189.512	3189.317	OH	P
								8+8	31317.74*	3192.158			A
	7	17'	26	17'	17	11'	11	76	31315.80	3192.356	3192.396	Fe I	M
								57+7	31312.12*	3192.732	3192.724	OH	P
								1	31308.07	3193.145			A
								5	31302.07	3193.757	3193.734	Fe Ip Fe IIp	M
								82	31289.40	3195.051	3195.085	OH OH	B
11	11'	17'	26	17	17	11'	11	1	31288.59	3195.133	3195.140	Ru II CH	M
								54	31284.47	3195.554	3195.593	Ni I - Y II	M
								2,3	31264.35*	3195.610	3197.596	V II?- CH	M
								6	31251.95	3198.879	3198.902	Fe I?-Ir I?	M
								72+3	31249.76*	3199.103	3199.137	OH-	B
	12	18	26	18	18	12'	12	46+3	31245.66*	3199.523	3199.527	Fe I	M
								43	31219.00	3202.255	3202.257	OH	P
								75	31217.83	3202.376	3202.382	V I OH	B
								4	31215.09	3202.657	3202.667	Fe Ip	M
								5	31182.67	3205.986	3206.007	Ti II	M
12	12'	19	26	19	19	13'	13	67	31180.23	3206.237	3206.238	OH	P
								37	31175.02	3206.773	3206.763	-OH	B
								35+14	31149.18*	3209.433	3209.434	OH	P
								67	31143.17	3210.043	3210.046	OH	P
	13	20	26	20	20	14	14	3+3	31124.70*	3211.958			A
								4+95	31109.97*	3213.479	3213.474	OH	M
								60	31107.44	3213.740	3213.744	OH - Fe I	B
								29	31100.10	3214.499	3214.494	OH	P
								27	31075.04	3217.091	3217.097	V I V II	M
								58+5+4	31065.67*	3218.061	3218.075	OH	P

TABLE A-3 (Continued)

 $A^2\Gamma^+ - X^2\Pi (1,1)$

Laboratory									Sun				
O ₂	P ₁	P ₂	Q ₁	Q ₂	R ₁	R ₂	S ₁	Intensity	Wavenumber cm ⁻¹	Wavelength Å	Wavelength Å	Solar Identification	Remarks
10		14'						3	31034.10	3221.335			
		14						3+53	31031.29	3221.627	3221.659	Ni I	M
			21					22	31020.73	3222.750	3222.729	Ti I	M
				21				21	30996.33	3225.260	3225.267	OH	P
								50+9+3	30984.97*	3226.443	3226.446	OH	P
11	15							2	30954.87	3228.579			
		15'						46	30951.88	3228.892	3228.900	Fe I OH	A
		15						17+10+1	30936.75*	3231.473	3231.472	OH	B
			22					2	30934.68	3231.689	3231.707	Fe II Zr II	P
				22				16	30913.01	3233.954	3233.976	Fe I Mn I	M
12	16							42	30901.10	3235.200	3235.187	Fe I - OH	M
		16'						2	30872.32	3238.216	3238.213	Ti I	B
		16						39	30869.17	3238.547	3238.553	OH	P
			23					13	30848.20	3240.748		A	A
				23				2	30835.17	3242.118	3242.108		M
13								13	30824.92	3243.196	3243.214	OH	P
								35+42	30813.99*	3244.346	3244.354	OH	P
								32	30782.97	3247.615	3247.569	Cu I	M
								9+12	30754.71*	3250.600	3250.637	Fe I	M
								9	30731.86	3253.017	3253.038	OH	P
14	17							29+2+2	30723.76*	3253.875	3253.844	Fe I	M
		17						27	30693.41	3257.092	3257.103	OH - Fe I	B
			24					7	30656.06	3261.061	3261.065	Cd I	M
				24				7+1+1	30633.70*	3263.441	3263.466	Fe Ip	M
								23	30630.09	3263.826	3263.838	OH-	B
15	18							22	30600.42	3266.990	3266.950	Fe II	M
		18						5	30552.13	3272.154		A	A
			25					18	30532.97	3274.208	3274.226	OH - Fe Ip	B
				25				5	30530.13	3274.513		A	A
								17+7	30503.90*	3277.328	3277.358	Fe II	M

TABLE A-3 (Continued)

A $^2\pi^+$ - X $^2\Pi$ (1,1)

O ₂	P ₁	P ₂	Q ₁	Q ₂	Laboratory					Sun					Remarks					
					R ₁	R ₂	S ₁	Intensity	Wavenumber cm ⁻¹	Wavelength A	Wavelength A	Solar Identification								
21	21	27	27	27	27	27	27	3	30442.80	3283.906	3283.933	V II OH	M	B	M					
								14	30432.37	3285.032	3285.022									
		21						3+1	30421.17*	3286.242	3286.258									
								14	30403.78	3288.121	3288.155									
	22	22	28	28	28	28	28	11	30328.14	3296.322		Ti II-	M	A	A					
								2+5	30327.68*	3296.372	3296.377									
								2	30306.32	3298.695	3298.691									
		23	23	23	23	23	23	10	30299.95	3299.389		NH	M	A	A					
								8+4	30220.11*	3308.106	3308.111									
								8	30192.40	3311.142	3311.110									
24	24	24	24	24	24	24	24	6	30108.36	3320.385	3320.379	Fe I	M	M	M					
								6	30081.91	3323.415	3323.395									
	25	25	25	25	25	25	25	5	29992.50	3333.212	3333.222									
								5	29965.35	3336.232	3336.260									
								4	29872.41	3346.611	3346.602									
26	26	26	26	26	26	26	26	4	29845.53	3349.627	3349.652	Cr II?	M	M	M					
								3	29748.07	3360.601	3360.607									
	27	27	27	27	27	27	27	3	29721.36	3363.621	3363.616	NH	M	M	M					
								2	29619.12	3375.232	3375.215									
								2	29592.56	3378.261										

TABLE A-4 OH IN THE SOLAR SPECTRUM

TABLE A-4 (Continued)

 $A^2\Sigma^+ - X^2\Pi (2,2)$

Laboratory									Sun							
O ₂	P ₁	P ₂	Q ₁	Q ₂	R ₁	R ₂	S ₁	Intensity	Wavenumber cm ⁻¹	Wavelength A	Wavelength A	Solar Identification	Remarks			
1	2	2'	13	15	2	3+72	7	31275.35	3196.485	3197.541	Ti II Fe I	M				
								31264.87	3197.557							
								3+2	31264.35*							
								6	31250.96							
								5	31250.13							
	3	3'	14	2	14	3+72	10	31249.76*	3199.103	3201.512	OH	A				
								6	31248.38							
								14	31246.60							
								3+46	31245.66*							
		4						18	31226.19							
2	4	4'	16	1,15	1,15	3+72	31225.30	3201.609	3203.832	Ti I	M					
								2+5	31216.12							
								5	31211.52							
								8	31203.85							
		5						21	31203.34							
	5'	5'	16	16	16	2+124	31202.23*	3203.977	3206.533	OH	P					
								4	31178.77							
								22	31177.50							
		6'						2	31176.21							
								4	31167.76							
3	7	2,2'	17	17	17	14+35	31158.54	3208.469	3209.433	OH	A					
								2	31157.54							
								10	31156.80							
		3						10+3+2	31155.34							
								2	31150.10							
	7'	4	17	17	17	14+35	31149.18*	3209.433	3209.434	OH	M					
								24	31148.53							
								2	31147.03							
		5'						2	31137.29							
								17+4	31136.04							

TABLE A-4 (Continued)

 $A^2\Sigma^+ - X^2\Sigma(2,2)$

Laboratory										Sun								
O_2	P_1	P_2	Q_1	Q_2	R_1	R_2	S_1	Intensity	Wavenumber cm^{-1}	Wavelength \AA	Wavelength \AA	Solar Identification	Remarks					
4	1'	6'	18	18	18	18	18	3+3	31124.70	3211.958	3211.958	3212.517	A					
								2	31119.28	3212.517								
		6						3	31118.57	3212.590								
								19	31117.96	3212.653								
								24	31116.24	3212.831								
	2,2'	8'	18	18	18	18	18	1	31114.57	3213.003	3213.003	3213.993	A					
								11	31104.99	3213.993								
		7'						3+4	31097.55	3214.764								
								1	31096.72	3214.848								
								20	31095.16	3215.009	3215.029	OH	P					
5	3,3'	9	18	18	18	18	18	3	31087.49	3215.803	3215.803	3216.532	Cr II					
								24	31080.44	3216.532								
		9'						1	31078.50	3216.752								
								1	31069.52	3217.662								
								21	31067.82	3217.839	3217.841	Ni I	M					
	10	10'	19	19	19	19	19	5+4+58	31065.67*	3218.061	3218.061	3219.429	OH?					
								3	31063.77	3218.258								
								13	31052.42	3219.435								
								22	31041.05	3220.613	3220.607	Co I	P					
								1	31038.92	3220.834								
4'	4	9'	19	19	19	19	19	1	31037.97	3220.933	3220.933	3221.135	OH - Ti I					
								21	31036.09	3221.130								
		9						2	31035.49	3221.398								
								3	31028.02	3221.966								
								7	31027.31	3222.040								
		10'						2	31103.28	3224.537								
								1	31002.17	3224.653								
6	11	10	20	20	20	20	20	20	30999.98	3224.881	3224.925	Fe I	M					
								21	30997.79	3225.093	3225.122	OH	P					
								14	30997.24	3225.166	A							

TABLE A-4 (Continued)

 $A^2\Sigma^+ - X^2\Pi (2,2)$

Laboratory									Sun								
O_2	P_1	P_2	Q_1	Q_2	R_1	R_2	S_1	Intensity	Wavenumber cm^{-1}	Wavelength \AA	Solar Identification	Remarks					
4	7	5,5'	11'	20	11	12	12	1	30995.51	3225.346	OH	M					
								9+3+50	30984.97*	3226.443							
		6	6'					2	30973.74	3227.613		M					
								19	30959.61	3228.086	3228.103						
								19	30950.83	3230.002	3229.990						
	8	7	7'	13	12	13	13	14	30939.35	3231.201	3231.222	OH? - Ce II	B				
								3	30937.73	3231.370							
		8	8'					1+10+17	30936.75*	3231.473	3231.472		P				
								18	30914.94	3233.752	3233.762		M				
								17	30899.79	3235.338	3235.327						
5	9	7	7'	14	13	14	14	2	30885.95	3236.787	OH	P					
								11	30884.62	3236.926	3236.923						
		8	8'					14	30878.47	3237.571	3237.583		P				
								16	30865.95	3238.885	3238.897		B				
								1+5	30863.24*	3239.170							
	6	8	8'	15	15	15	15	15	30844.71	3241.115	3241.138	OH? - Sm II	B				
								2	30830.03	3242.658							
		9	9'					12	30828.51	3242.819	3242.834		P				
								14	30814.55	3244.287							
								14	30812.58	3244.495	3244.498						
7	10	10	10'	16	16	16	16	1+13	30785.44	3247.355	Fe I Fe IIp Sc II?	A					
								2	30770.13	3248.971							
		11	11'					12	30768.41	3249.153		A					
								12+9	30754.71*	3250.600	3250.637						
								13	30747.49	3251.364	3251.353						
								11	30721.82	3254.080	3254.060						
								1	30706.41	3255.713							

TABLE A-4 (Continued)

A $^2\Sigma^+$ - X $^2\Pi$ (2,2)

O ₂	Laboratory							Sun				
	P ₁	P ₂	Q ₁	Q ₂	R ₁	R ₂	S ₁	Intensity	Wavenumber cm ⁻¹	Wavelength Å	Solar Identification	Remarks
11								13	30677.20	3258.814	Fe II	M
		17						9+2+2	30653.79*	3261.302		A
	11	11						1+2	30638.59*	3262.920		
			17					11	30636.79	3263.112	OH	P
								9	30625.62	3264.302		
12								12+1	30603.61*	3266.650	Cr I -	M
		18						8	30581.21	3269.043		
	12	12						1+1	30567.65*	3270.493	OH	P
			18					10	30565.36	3270.738		
								8	30553.98	3271.956		
13								10+1	30526.69*	3274.881	Ni II	M
		19						7+17	30503.90*	3277.328		
			13					9	30490.25	3278.795		
				19				7	30477.58	3280.158		
	14							9	30446.32	3283.526		
14								6	30421.81	3286.172		
		20						8	30411.45	3287.291		
	14		20					6	30396.26	3288.934		
				21				8	30362.54	3292.587		
								5	30334.62	3295.617		
15								7	30328.91	3296.238		
		15						5	30309.73	3298.325		
			21					7	30275.12	3302.095		
	16	16	22					6+4	30242.63	3305.643	Fe II	M
				22				4	30217.95	3308.342		
17								6	30184.11	3312.051		
		17						5	30152.65	3315.507		
			23					3	30144.34	3316.421		
				23				3+3	30120.44*	3319.053		
	18							5	30089.32	3322.485		

TABLE A-4 (Continued)

A $^2\Sigma^+$ - X $^2\Pi$ (2,2)

Laboratory									Sun				
O ₂	P ₁	P ₂	Q ₁	Q ₂	R ₁	R ₂	S ₁	Intensity	Wave number cm ⁻¹	Wavelength Å	Wavelength Å	Solar Identification	Remarks
		18						4+3	30058.68*	3325.873			
19								4	29990.76	3333.405			
	19							4	29960.78	3336.741			
20								3	29888.18	3344.846			
	20							3	29858.81	3348.136			
21								3	29781.53	3356.825			
	21							2	29752.48	3360.072			
22								2	29670.76	3369.367			
	22							2	29642.30	3372.592			

Notes - The symbols in Appendix (Tables 1-4) have the following meaning

- A OH absent from the solar spectrum.
- B OH present in the solar spectrum, blended.
- M OH masked in the solar spectrum.
- P OH present in the solar spectrum, unblended.
- || denotes a predominant contributor
- | contributor stronger than others
- In the case of blends, to distinguish the laboratory lines shorter than the solar wavelength from those that are longer.
- (OH) OH in parenthesis indicates that it is masked in the solar spectrum.
- * Blend

TABLE* B-1 WAVENUMBERS OF ROTATIONAL LINES OF OH⁺
BAND (0,0), TRANSITION $^3\Pi_0^+$ - $^3\Sigma^-$

N	P ₃	Q ₃	Q _{P₃₂}	R ₃	R _{P₃₁}	R _{Q₃₂}	S _{R₃₂}	S _{Q₃₁}	T _{R₃₁}
0									
1	27 933.83	28 008.25	28 009.08	28 040.15	28 039.47	28 040.15	28 116.53	28 131.79	28 222.48
2	27 988.71	27 983.71	044.63	042.03	044.64	149.72	147.38	266.70	
3	876.11	952.85	952.85	043.96	042.03	043.96	176.86	174.78	321.74
4	814.73	919.90	919.90	039.47	037.60	039.47	198.63	196.86	371.45
5	747.49	882.18	882.18	029.98	028.42	028.42	214.37	214.37	416.48
6	680.72	839.87	839.87	015.12	013.87	014.60	225.33	222.48	451.90
7	606.46	792.23	792.10	27 994.53	27 993.23	27 994.53	229.98	228.98	481.86
8	528.42	739.62	738.64	967.86	966.40	964.90	225.33	225.33	502.78
9	444.87	680.72	680.72	933.83	932.84	932.84	216.79	214.37	516.15
10	356.43	616.12	614.43	893.56	891.74	891.74	198.63	195.19	520.20
11	261.83	544.76	543.25	846.31	843.65	846.31	174.78	172.87	520.20
12	161.12	467.45	466.02	792.40	789.49	789.49	139.83	141.05	510.44
13	27 054.66	383.57	383.57	730.84	728.40	730.84	101.63	28 099.29	490.18
14	26 942.84	293.17	291.60	662.12	660.79	660.07	28 051.52	051.52	462.22
15	824.06	195.03	195.03	585.45	583.10	583.10	27 993.23	27 993.23	423.09
16	699.40	27 090.56	27 088.91	501.02	499.66	499.66	926.45	927.49	374.64
17	568.46	26 978.92	26 875.84	408.62	407.05	406.52	851.79	851.79	318.27
18	431.01	859.49	857.27	308.61	307.09	306.22	767.90	768.88	251.65
19	287.38	732.58	731.83	198.92	198.52	198.52	673.96	673.96	172.87
20	26 136.15	598.51	595.17	27 081.36	27 079.64	27 078.84	570.06	571.02	28 084.07
21	25 978.89	455.91	453.51	26 954.95	26 953.21	26 951.37	455.80	457.35	27 983.71
22	814.50	306.20	303.32	818.66	817.34	814.86	332.31	334.41	872.21
23	642.77	26 146.83	26 143.61	673.48	672.56	669.57	198.53	200.73	749.49
24	463.50	25 980.70	25 977.79	518.49	517.32	513.69	27 052.77	27 056.14	614.22
25	276.49	805.11	801.39	353.89	352.32	350.75	26 898.54	26 898.54	464.83
26	25 081.98	620.47	616.45	26 178.37	26 176.05	26 174.61	--	--	304.18
27	24 877.76	426.20	422.64	25 993.05	25 991.14	25 989.14	--	--	--
28	--	222.90	220.01	796.31	794.99	793.08	--	--	--
29	--	25 009.60	25 005.51	--	--	--	--	--	--
30	--	24 785.92	24 782.52	--	--	--	--	--	--

* Rakotoanijimy (1970)

TABLE B-1 (Continued)

BAND (0,0), TRANSITION $^3\Pi_1 - ^3\Sigma^+$									
N	$S_{P_{22}}$	P_2	$P_{Q_{23}}$	Q_2	$Q_{P_{21}}$	$Q_{R_{23}}$	R_2	$R_{Q_{21}}$	κ_{21}
0									
1									
2			27 926.45	27 945.36	27 946.56	27 944.15	27 998.17	27 998.99	28 091.20
3	27 779.41	27 884.73	883.74	930.82	932.84	930.82	28 009.08	28 011.16	112.70
4	700.96	834.75	833.63	908.89	910.16	908.89	015.12	016.10	143.39
5	614.43	779.34	779.34	880.94	882.50	880.94	014.59	016.10	168.72
6	522.30	720.47	720.47	848.05	849.45	848.05	28 008.25	28 009.08	188.15
7	424.87	655.84	655.84	808.99	910.71	809.28	27 995.98	27 997.23	201.85
8	322.12	509.52	509.52	714.13	715.11	715.11	951.81	953.94	206.10
9	216.63	427.78	427.78	428.72	657.29	658.98	658.26	919.90	922.03
10	27 104.06	341.28	341.28	594.27	596.68	594.26	880.94	883.18	182.92
11	26 985.81	247.03	248.14	524.26	526.99	524.26	834.75	837.29	158.66
12	862.07	149.00	149.00	448.08	450.81	449.74	781.74	784.37	128.44
13	732.59	27 043.68	27 043.68	365.63	368.66	366.62	721.57	724.25	088.54
14	600.20	26 932.76	26 932.76	276.10	278.84	277.15	653.49	655.73	28 040.15
15	460.41	814.86	817.34	178.96	181.99	181.25	577.96	580.50	27 983.71
16	315.12	691.05	692.73	27 075.13	27 078.39	27 076.56	493.95	497.75	919.90
17	164.18	560.92	562.58	26 964.47	26 966.99	26 966.15	402.21	405.01	843.65
18	26 006.31	424.26	426.72	845.61	849.74	848.69	302.72	307.50	762.95
19	25 844.42	281.01	283.31	719.46	723.15	721.79	193.72	198.52	667.95
20	676.46	26 130.60	26 133.53	585.90	590.86	588.33	27 076.56	27 081.36	566.43
21	25 501.96	25 973.97	25 976.58	444.09	449.42	447.07	26 950.63	26 954.95	451.99
22	321.23	810.00	812.35	294.73	299.58	298.23	814.86	818.66	328.99
23	25 135.07	638.75	641.33	26 136.15	26 140.28	26 140.28	669.57	673.48	195.08
24	24 942.63	460.00	463.56	25 970.10	25 974.67	25 973.17	515.61	520.31	27 052.77
25	740.81	273.43	276.49	794.99	798.17	789.17	350.75	355.41	26 897.02
26	536.78	25 078.70	25 081.98	610.80	616.45	614.15	26 174.61	26 180.49	728.46
27	323.05	24 875.00	24 879.37	417.02	422.64	421.70	25 991.14	25 996.57	26 545.34
28	--	--	--	213.77	220.01	217.67	794.99	800.12	351.27
29	--	--	--	25 000.89	25 006.21	25 004.33	--	--	--
30	--	--	--	24 777.74	24 783.90	782.52	--	--	--

TABLE B-1 (Continued)

BAND (0,0), Transition $^3\Pi_2 - ^3\Sigma^-$

N	$N_{P_{13}}$	$O_{P_{12}}$	$O_{Q_{13}}$	P_1	$P_{Q_{12}}$	$P_{R_{13}}$	Q_1	$Q_{R_{12}}$	R_1
0									
1									
2									
3									
4	27 570.06	27 707.12	27 689.17	27 797.78	27 797.93	27 799.18	27 864.26	27 863.38	27 953.94
5	473.15	636.34	636.34	724.25	722.79	725.53	836.80	835.58	975.81
6	366.62	558.65	562.45	674.62	673.96	675.77	811.80	810.71	975.81
7	252.86	477.31	478.50	617.45	615.73	617.45	779.37	776.20	967.86
8	133.51	388.23	390.45	552.85	550.56	558.04	739.61	737.91	952.84
9	27 004.86	290.08	294.45	481.71	478.50	484.09	692.55	690.07	930.82
10	26 872.94	27 079.64	27 083.65	320.43	317.05	322.12	577.96	574.40	864.26
11	734.95	26 963.52	26 969.29	229.56	226.65	231.66	510.41	507.56	819.97
12	590.86	842.80	848.69	132.65	129.68	134.59	436.65	432.85	768.88
13	440.32	715.83	721.52	27 029.34	27 025.30	27 030.23	354.99	351.65	709.86
14	284.72	583.75	588.33	26 918.99	26 917.53	26 921.56	266.61	263.34	643.16
15	25 125.46	444.93	450.73	803.62	801.25	805.49	170.67	167.93	568.43
16	25 958.89	300.42	306.20	681.07	678.63	682.59	27 067.64	27 064.66	485.75
17	788.66	26 151.86	26 155.61	552.01	548.06	554.47	26 957.97	26 954.94	395.05
18	612.43	25 995.26	26 000.29	416.41	411.65	417.93	840.04	836.35	296.31
19	433.22	833.81	25 838.07	274.03	270.00	275.54	714.53	709.81	188.11
20	245.50	664.11	668.80	26 124.50	26 120.12	26 125.46	581.60	577.66	27 071.58
21	25 055.36	490.06	496.90	25 968.49	25 964.01	25 970.10	440.32	436.08	25 946.37
22	24 858.23	310.98	315.64	805.11	801.39	807.07	291.45	287.38	811.28
23	658.07	25 123.51	25 130.23	634.73	629.75	635.97	26 133.53	26 128.68	667.40
24	--	24 932.89	24 939.35	456.63	451.48	458.51	25 967.74	25 963.07	512.94
25	239.32	732.28	737.27	270.48	265.75	272.71	793.08	788.03	349.28
26	24 021.95	526.49	532.67	25 076.79	25 071.76	25 078.70	609.27	604.34	26 176.05
27	23 797.41	312.12	319.87	24 875.00	24 870.12	24 877.13	415.90	410.42	25 990.34
28	--	24 093.43	--	666.60	659.94	668.57	213.77	208.77	794.99
29	--	--	--	450.45	--	450.45	--	--	--
30	--	--	--	24 227.81	--	24 229.19	--	--	--
31	--	--	--	23 995.68	--	23 997.82	--	--	--

TABLE B-1 (Continued)

BAND (0,1), TRANSITION $^3\text{H}_0 - ^3\text{E}^-$

N	P_3	Q_3	$Q_{P_{32}}$	R_3	$R_{P_{31}}$	$R_{Q_{32}}$	$S_{R_{32}}$	$S_{Q_{31}}$	$T_{R_{31}}$
0									
1	25 050.87	25 076.79	25 081.98	25 081.98	25 083.20	25 175.99	25 158.9	25 249.84	
2	24 976.03	026.06	027.03	090.51	089.31	091.61	195.86	194.51	314.89
3	926.65	25 004.33	25 004.33	095.65	094.50	095.65	25 229.02	226.80	374.72
4	873.41	24 978.08	24 978.08	097.79	096.69	097.79	256.96	255.52	429.85
5	815.33	947.63	947.63	095.65	094.50	094.50	280.22	279.89	480.04
6	754.58	914.08	914.08	089.31	088.05	088.05	299.92	299.92	525.60
7	691.75	877.13	877.13	079.19	076.79	078.70	312.94	312.94	566.58
8	623.77	835.72	835.72	063.12	061.37	062.25	--	321.23	597.70
9	553.87	789.79	788.46	042.83	041.67	041.69	325.39	325.39	624.20
10	479.15	739.40	739.40	25 016.54	25 013.80	25 016.54	321.23	321.23	642.77
11	400.39	684.27	684.27	24 985.40	24 983.14	24 985.40	312.94	311.82	658.18
12	316.99	623.77	623.77	948.38	946.23	947.63	296.81	296.81	666.12
13	229.19	558.03	557.10	905.42	903.83	903.83	274.21	274.21	664.11
14	136.80	486.93	484.69	856.63	854.51	854.51	245.50	245.50	655.59
15	24 039.69	410.82	409.42	801.21	798.76	798.76	208.77	208.77	638.75
16	23 937.54	328.47	326.14	739.40	737.27	737.27	164.35	164.35	615.30
17	830.38	240.35	237.78	671.07	670.03	668.57	113.61	114.82	580.81
18	718.26	146.39	144.31	595.08	592.00	592.00	25 055.36	25 055.36	537.65
19	600.57	24 046.18	24 043.22	512.71	510.73	509.81	24 986.36	24 987.55	486.93
20	477.70	23 939.54	23 936.44	422.36	420.25	420.25	910.79	912.48	424.14
21	348.77	825.98	823.10	324.30	323.05	--	--	--	352.82
22	214.07	706.13	702.77	218.04	217.25	215.52	732.28	--	272.71
23	23 073.77	578.59	574.54	24 104.48	101.96	24 100.89	628.14	630.74	--
24	22 927.09	444.36	442.40	23 982.08	23 981.03	23 978.84	518.05	--	--
25	773.02	301.96	298.39	850.41	849.38	847.87	--	--	--
26	--	23 152.07	148.91	--	--				

TABLE B-1 (Continued)

BAND (0,1), TRANSITION $^3\Pi_1 - ^3\Sigma^-$

N	$Q_{P_{23}}$	P_2	$P_{Q_{23}}$	Q_2	$Q_{P_{21}}$	$Q_{R_{23}}$	R_2	$R_{Q_{21}}$	$S_{R_{21}}$
0									
1									
2		24 930.85	24 987.55	24 967.54	24 987.54	24 985.40	25 040.76	25 045.13	25 119.88
3	24 830.14	886.58	930.85	977.33	978.08	977.33	055.36	056.44	160.24
4	761.39	837.57	886.58	961.29	963.23	961.29	067.00	068.86	194.51
5	679.16	837.57	939.35	941.87	939.35	913.49	072.63	073.62	226.80
6	596.01	729.99	785.92	913.49	915.19	069.90	073.62	074.99	253.84
7	509.81	670.03	670.55	849.20	850.69	849.20	061.37	064.43	293.80
8	418.55	605.48	606.52	810.13	811.72	810.12	047.59	050.87	314.15
9	324.30	536.78	537.80	765.96	768.98	766.58	028.45	031.30	306.60
10	226.33	463.79	464.66	717.53	721.06	718.46	25 004.01	25 006.21	305.32
11	124.59	386.41	--	663.74	666.59	664.41	24 974.10	24 977.33	299.48
12	24 019.09	304.67	305.76	604.23	606.52	605.48	937.95	941.87	283.67
13	23 908.34	218.04	219.22	539.81	543.25	541.09	895.92	898.57	263.42
14	794.07	126.81	128.51	469.84	472.59	471.27	847.98	850.69	235.14
15	675.70	24 030.54	24 032.97	394.57	397.98	397.98	793.35	796.75	198.36
16	552.47	23 929.10	23 931.29	313.17	316.99	315.60	732.28	737.27	158.29
17	427.69	823.10	825.98	225.84	229.19	227.81	664.41	668.57	107.00
18	293.52	711.37	713.94	132.58	136.80	134.32	589.23	592.00	25 048.47
19	157.01	594.26	597.01	24 032.97	24 035.50	24 035.50	506.87	510.73	24 980.66
20	--	471.41	474.07	23 926.68	23 931.29	23 929.10	417.54	422.36	906.33
21	--	343.72	346.94	813.95	817.29	816.27	319.87	324.30	820.85
22	--	209.51	--	694.05	698.48	--	214.48	219.22	729.99
23	--	23 070.07	--	567.60	572.10	--	24 100.89	104.48	628.14
24	--	22 923.23	--	432.55	--	435.22	23 978.84	--	513.68
25	--	770.56	--	291.69	296.56	295.61	847.87	23 851.92	--
26	--	609.65	--	141.75	146.52	146.52	--	--	--

TABLE B-1 (Continued)

(BAND (0,1), TRANSITION $^3\pi_2 - ^3\Sigma^-$

N	$N_{P_{13}}$	$O_{P_{12}}$	$O_{Q_{13}}$	P_1	$P_{Q_{12}}$	$P_{R_{13}}$	Q_1	$Q_{R_{12}}$	R_1
0									
1									
2									
3									
4	24 630.74	24 752.55	25 755.99	24 844.42	24 843.79	24 847.98	24 909.30	24 908.40	24 974.10
5	540.22	624.71	628.14	782.52	779.65	783.90	911.63	910.79	25,000.89
6	440.52	551.46	555.67	740.22	739.40	740.81	895.81	893.05	020.52
7	337.08	472.59	475.03	691.75	689.57	693.31	877.76	876.15	033.76
8	227.81	--	--	637.49	--	638.74	853.77	852.28	040.76
9	24 113.97	297.01	--	577.63	575.48	580.25	823.93	821.98	041.69
10	23 995.68	201.30	206.88	443.08	440.52	444.33	788.46	785.92	036.87
11	871.00	24 104.48	106.99	368.28	365.66	369.19	747.56	744.24	25 009.60
12	744.78	23 999.44	24 004.45	288.37	285.29	289.96	701.52	698.61	24 987.55
13	612.67	892.36	23 895.37	203.42	201.30	204.90	592.00	589.23	959.25
14	478.15	778.04	781.62	113.97	110.49	115.48	528.93	526.48	924.82
15	340.06	661.44	664.67	24 019.09	24 015.37	24 020.62	460.33	457.77	884.40
16	196.33	--	543.46	23 919.06	23 916.15	23 920.01	385.89	--	837.57
17	--	--	419.15	813.95	810.23	816.27	305.76	301.98	783.90
18	--	281.43	284.82	702.77	--	702.77	219.22	215.52	723.97
19	--	146.52	151.64	587.24	583.54	589.13	126.81	123.47	657.09
20	--	--	--	465.42	460.94	465.99	24 027.91	24 022.81	582.25
21	--	--	--	338.24	--	337.11	922.36	918.41	501.12
22	--	--	--	204.86	--	206.09	810.23	805.59	412.48
23	--	--	--	23 065.96	--	--	690.60	687.06	315.60
24	--	--	--	22 919.35	--	--	564.76	559.94	210.53
25	--	--	--	767.00	--	--	430.47	426.98	24 097.79
26	--	--	--	607.65	--	--	289.60	284.82	134.41
27	--	--	--	--	--	--	140.13	134.41	708.15
							--	--	561.93

TABLE B-1 (Continued)

Band (1,0), Transition ${}^3\Pi_0 - {}^3\Sigma^-$

N	P ₃	Q ₃	Q _{P₃2}	R ₃	R _{P₃1}	R _{P₃2}	S _{R₃2}	S _{Q₃1}	T _{R₃1}
0									
1	29 902.19	29 955.40	29 955.40	30 006.77	30 005.34	30 004.55	30 082.01	30 082.01	30 167.32
2				009.12	006.77	009.12	108.48	107.17	220.37
3	842.72	920.10	920.10	30 004.55	30 002.73	30 004.55	126.66	122.04	265.29
4	779.11	879.13	879.13	29 993.14	29 991.47	29 993.14	139.48	137.75	--
5	710.60	832.83	832.83	973.30	971.63	973.30	144.65	142.13	332.08
6	633.77	780.63	780.63	946.38	944.83	946.38	140.54	139.48	354.25
7	549.45	721.21	721.21	911.66	910.06	911.66	--	128.62	367.39
8	459.77	654.75	654.51	869.21	868.05	869.21	109.78	108.48	369.56
9	362.35	581.77	579.76	818.64	818.64	818.64	082.01	081.09	362.70
10	257.91	498.91	498.91	759.92	758.59	758.59	30 042.64	041.19	348.44
11	146.18	409.40	409.40	692.45	691.57	691.57	29 995.33	29 995.40	321.12
12	29 027.27	311.52	310.19	616.19	616.19	--	--	--	286.01
13	28 900.55	205.74	204.24	531.54	530.19	530.19	875.07	875.07	242.78
14	766.49	29 091.56	29 091.56	438.54	437.44	437.44	798.69	798.69	185.62
15	624.79	28 969.24	28 969.24	335.77	335.77	--	712.43	714.01	122.04
16	476.09	837.99	836.44	224.52	224.52	224.52	618.58	620.22	30 027.11
17	318.27	697.54	695.97	29 107.01	29 107.01	29 107.01	510.68	514.60	29 944.83
18	28 154.51	550.45	548.50	28 957.85	28 956.33	28 953.99	395.20	395.20	842.72
19	27 985.91	392.04	390.83	822.31	821.27	819.54	265.43	265.91	728.43
20	786.13	225.23	222.48	673.06	671.38	670.54	29 128.41	29 129.72	604.97
21	602.66	28 048.81	28 044.64	510.44	508.33	506.94	28 976.07	28 978.15	464.55
22	406.52	27 863.38	27 861.14	338.59	337.15	335.06	813.74	816.27	314.81
23	27 198.52	667.92	664.30	28 153.98	28 152.28	28 149.42	640.41	611.76	
24	26 982.73	462.34	459.19	27 959.29	27 958.30	27 955.18	451.90	456.44	
25	756.99	247.03	243.89				253.80		
26	522.55	27 020.37	27 016.23						
27		26 783.06	26 778.87						
28			534.34	530.56					
29			274.23	270.00					

TABLE B-1 (Continued)

Band (1,0), Transition $^3\Pi_1 - ^3\Sigma^-$

N	$^0P_{23}$	P_2	$P_{Q_{23}}$	Q_2	$Q_{P_{21}}$	$Q_{R_{23}}$	R_2	$R_{Q_{21}}$	$S_{R_{21}}$
0									
1									
2		29 860.84	29 848.65	29 926.47	29 926.47	29 925.19	29 968.28	29 969.57	30 041.19
3	29 761.37	805.47	805.47	904.38	904.38	904.38	974.46	976.65	072.75
4	74.30	745.66	745.66	841.07	877.07	875.07	973.30	975.62	096.48
5	581.77	679.59	679.59	799.83	843.73	841.07	964.41	967.12	112.13
6	481.48	605.72	604.97	751.11	752.50	751.11	947.92	949.47	119.69
7	376.73	524.67	524.67	694.72	695.86	694.72	891.88	895.36	109.79
8	265.43	437.44	438.54	630.31	633.77	630.31	850.66	854.27	30 093.87
9	146.18	342.48	343.39	558.16	560.37	559.02	802.04	805.47	067.27
10	29 019.33	239.92	239.92	479.03	481.48	480.26	744.71	747.69	031.80
11	28 886.56	129.72	130.74	391.48	395.20	392.76	678.59	680.35	29 985.67
12	747.24	29 012.26	29 014.21	295.75	298.76	297.02	603.20	605.72	--
13	600.99	28 886.56	28 886.56	192.85	195.18	195.18	519.52	520.38	854.27
14	447.46	753.68	754.94	29 088.91	29 091.56	29 091.56	426.96	431.10	785.07
15	286.68	613.09	614.93	28 944.88	28 949.32	28 946.40	324.68	329.07	703.67
16	28 129.24	464.72	466.83	819.54	822.30	821.27	213.08	217.66	609.00
17	27 929.26	307.74	309.46	681.41	686.22	683.93	29 091.56	29 095.27	502.75
18	751.90	28 143.39	28 146.21	535.02	539.68	537.96	28 960.77	28 964.74	388.31
19	562.45	27 970.92	27 973.00	378.11	382.02	380.15	819.54	822.30	259.77
20	366.62	789.24	792.10	212.33	216.79	214.37	667.86	673.06	29 122.81
21	27 161.12	600.07	602.78	28 036.61	28 040.15	28 039.47	506.94	512.27	28 974.08
22	26 946.93	402.21	405.01	27 851.79	27 856.21	27 854.60	333.96	338.59	810.86
23	728.46	27 195.03	27 198.52	657.29	661.99	660.79	28 151.21	28 158.66	640.41
24	498.00	26 979.54	26 982.73	451.99	455.80	455.09	27 956.79	27 963.24	455.34
25	263.08	754.46	757.93	237.31	243.25	240.74	751.90	757.72	
26	018.87	520.31	522.55	27 013.31	27 019.03	016.23	533.71	537.76	
27		276.58							

TABLE B-1 (Continued)

Band (1,0), Transition $^3\Pi_2$ - $^3\Sigma^-$

N	$N_{P_{13}}$	$Q_{P_{12}}$	$Q_{Q_{13}}$	P_1	$P_{Q_{12}}$	$P_{R_{13}}$	Q_1	$Q_{R_{12}}$	R_1
0									
1									
2									
3									
4	29 541.11	29 679.59		29 773.92	29 773.92	29 772.14	29 341.07	29 842.08	29 899.23
5	438.54	607.20	29 604.97	688.92	691.57	687.91	834.86	836.76	917.91
6	527.37	524.67	632.07	633.77	630.31	795.14	821.81	926.47	925.18
7	329.07	437.44	435.18	566.02	569.21	761.37	761.37	914.81	
8	205.74	337.42	335.77	492.16	495.10	718.42	719.69	895.36	
9	29 077.26	232.28	229.69	409.40	412.94	666.61	669.38	866.89	
10	28 939.74	29 119.95	29 116.01	319.16	319.32	409.40	605.72	609.00	829.66
11	797.76	28 998.49	28 994.13	219.22	221.15	217.66	536.82	539.39	785.07
12	645.12	866.67	863.22	29 112.85	29 116.01	29 111.48	373.93	376.73	662.32
13	485.64	730.64	725.80	28 992.25	28 994.90	28 990.67	279.26	281.55	588.90
14	319.59	584.81	580.19	870.90	873.57	869.08	176.10	179.08	507.13
15	28 141.05	432.17	428.70	739.65	742.87	738.10	29 064.42	29 067.95	416.11
16	27 963.24	274.22	268.20	600.99	604.91	598.97	28 944.06	28 946.40	314.81
17	775.53	28 105.46	28 099.29	455.95	456.45	451.90	814.71	817.70	204.24
18	582.19	27 930.82	27 924.48	298.07	301.29	295.06	676.31	679.62	29 083.97
19	--	746.57	743.33	28 134.40	28 138.13	28 132.59	529.97	533.08	28 953.99
20	27 173.42	558.65	552.85	27 963.24	27 967.86	27 961.37	373.54	378.11	813.74
21	26 961.44	361.79	358.00	782.90	786.13	781.74	208.47	212.33	663.71
22	741.84	27 158.32	27 151.86	594.27	597.89	592.46	28 033.43	28 037.60	503.45
23	515.61	26 944.47	26 939.60	396.39	400.52	395.05	27 849.45	27 854.60	333.96
24	231.02	726.08	728.46	27 191.89	27 196.48	198.52	655.84	660.07	28 158.66
25	26 039.06	499.71	492.13	26 978.92	26 984.02		451.99	457.35	27 966.40
26	25 801.39	263.08	265.25	755.62	760.47		237.31	242.26	
27	26 020.98	25 766.75							

TABLE B-1 (Continued)

Band (1,1), Transition $^3\Pi_0$ - $^3\Sigma^-$

N	P ₃	Q ₃	Q _{P₃₂}	R ₃	R _{P₃₁}	R _{Q₃₂}	S _{R₃₂}	S _{Q₃₁}	T _{R₃₁}
0									
1									
2	26 946.93	27 024.91	27 025.30	27 046.59	27 046.08	27 047.82	27 125.84	27 123.84	27 211.79
3	893.83	26 972.20	26 972.65	001.22	002.33	054.66	052.76	054.66	154.16
4	836.35	937.69	937.69	038.63	057.06	056.14	057.06	155.75	266.61
5	775.79	898.54	898.54	038.63	049.50	051.18	036.84	178.96	317.98
6	708.62	855.25	855.25	27 020.37	27 019.03	27 020.37	209.75	195.03	361.79
7	634.26	805.49	805.49	26 996.01	26 994.27	26 996.01	213.08	208.47	397.26
8	555.32	750.44	749.17	965.03	963.52	964.47	213.08	213.08	427.78
9	470.46	689.31	688.28	926.94	925.93	925.93	212.73	205.68	450.81
10	380.47	621.98	621.18	883.02	881.73	882.24	189.94	189.94	464.83
11	284.72	548.06	547.53	830.89	828.19	830.89	166.16	166.67	471.49
12	182.97	468.05	467.01	772.59	770.33	770.33	136.25	135.74	471.49
13	26 075.15	381.20	380.47	706.23	704.71	704.71	097.37	095.99	460.44
14	25 961.54	287.38	236.13	634.26	632.54	632.54	27 048.72	27 048.72	439.87
15	840.56	184.41	182.97	551.32	550.19	550.20	26 994.27	--	378.27
16	716.72	26 076.06	26 076.06	462.61	460.41	460.41	930.07	930.07	337.79
17	580.81	25 959.99	25 957.99	368.96	368.02	--	856.08	856.08	262.99
18	440.34	836.80	834.16	244.60	244.60	244.60	778.87	778.87	200.73
19	294.25	705.94	704.26	130.60	128.64	128.08	663.39	665.56	125.84
20	25 144.87	566.58	563.73	26 010.38	26 008.92	26 007.42	575.03	577.67	27 040.26
21	24 972.49	419.74	417.13	25 877.67	25 876.40	25 875.72	345.94	345.94	826.65
22	805.35	265.75	263.42	732.56	731.39	730.03	208.78	210.53	704.71
23	628.14	25 097.79	25 094.50	580.15	578.72	576.83	26 066.68	068.70	
24	24 922.24	24 920.52	416.01	414.24	412.28				
25		737.27							

TABLE B-1 (Continued)

Band (1,1), Transition $^3\Pi_1 - ^3\Sigma^-$

N	$O_{P_{23}}$	P_2	$P_{Q_{23}}$	Q_2	$Q_{P_{21}}$	$Q_{P_{23}}$	R_2	$R_{Q_{21}}$	$S_{R_{21}}$
0									
1									
2	26 879.21	26 907.67	26 907.67	26 959.65	26 959.65	26 957.97	27 011.13	27 011.80	27 083.65
3	803.62	858.22	858.22	946.37	946.93	946.37	021.21	022.17	117.32
4	728.46	803.62	803.62	926.94	--	926.94	025.11	027.32	149.00
5	645.82	744.05	744.05	865.09	867.67	865.09	27 013.31	27 015.23	183.94
6	556.60	679.39	679.39	825.11	826.65	825.11	26 997.74	26 998.92	193.72
7	460.41	609.17	609.17	778.87	--	778.87	875.84	978.92	195.03
8	360.05	533.22	533.22	726.08	728.46	726.08	946.93	948.73	188.11
9	253.22	451.31	452.46	667.02	669.57	667.40	910.92	913.16	174.56
10	141.29	363.10	363.83	602.06	604.54	603.14	867.67	870.42	154.16
11	26 024.69	268.76	270.00	530.17	532.48	530.56	817.34	819.68	127.05
12	25 903.12	168.62	169.55	452.46	453.51	452.46	759.53	762.34	097.37
13	775.06	26 061.46	26 062.46	368.02	371.36	368.96	694.03	697.77	27 029.34
14	641.33	25 948.36	25 949.70	283.31	287.38	284.72	621.18	625.75	26 979.93
15	503.27	828.78	330.15	159.84	163.04	161.39	540.22	543.47	917.64
16	366.71	702.68	704.26	26 057.74	26 061.50	26 059.40	450.73	453.51	845.61
17	191.92	570.28	572.94	25 943.98	25 948.36	25 946.37	353.89	357.97	766.42
18	25 036.87	429.85	--	821.83	825.11	823.30	247.91	251.93	675.48
19	24 872.14	284.95	287.95	691.77	695.22	694.07	133.53	137.23	576.27
20	723.97	25 130.23	25 133.31	553.77	558.14	555.77	26 008.62	26 012.04	461.98
21	534.57	24 969.15	24 971.62	406.32	412.28	410.42	25 875.72	25 882.25	343.84
22	350.73	801.21	805.35	251.39	255.51	253.84	733.14	737.90	211.36
23	24 160.59	624.71	628.14	25 089.31	25 096.69	25 094.50	580.81	585.08	
24	23 963.87	440.52	444.33	24 915.14	24 922.24	24 920.52	418.10	422.64	
25	761.41	249.48	251.21	732.28	737.27	735.66			

TABLE B-1 (Continued)

Band (1,1), Transition $^3\Pi_2$ - $^3\Sigma^-$										
N	$N_{P_{13}}$	$O_{P_{12}}$	$O_{Q_{13}}$	P_1	$P_{Q_{12}}$	$P_{R_{13}}$	Q_1	$Q_{R_{12}}$	R_1	
0										
1	26 785.38	26 796.62	26 801.25	26 848.69	26 847.20	26 849.79	26 886.88	26 886.88	26 942.85	
2	697.77	733.85	736.22	821.41	819.68	822.85	882.24	881.73	964.47	
3	604.54	663.39	665.56	747.63	745.37	749.17	871.70	870.52	978.92	
4	508.03	589.03	591.77	697.77	695.93	699.40	826.65	825.11	983.40	
5	406.42	507.02	511.02	640.40	638.46	642.46	792.43	790.45	969.62	
6	294.73	420.81	423.06	576.27	575.03	577.67	750.38	749.17	951.36	
7	178.17	325.55	329.41	504.94	502.70	507.02	701.84	699.40	925.93	
8	26 052.01	224.99	226.13	426.72	424.26	427.97	645.82	643.15	893.83	
9	25 922.51	115.08	119.31	342.38	338.72	343.84	582.67	579.23	847.20	
10	785.31	26 001.19	26 003.30	251.93	247.91	253.22	512.62	509.31	801.25	
11	642.77	25 882.25	25 884.08	146.83	144.36	148.38	433.31	432.15	744.05	
12	497.55	753.25	758.11	26 045.59	26 042.87	26 047.29	351.27	348.03	682.59	
13	337.82	620.47	626.21	25 934.64	25 931.75	25 936.33	258.75	255.65	610.24	
14	181.41	482.48	486.93	816.75	814.50	818.29	159.02	155.61	530.56	
15	25 018.96	337.82	340.71	691.77	686.89	693.11	26 052.72	26 049.50	441.63	
16	24 847.98	185.36	190.25	560.51	555.77	561.74	25 938.56	25 935.13	346.77	
17	671.07	25 028.45	25 031.30	421.70	418.10	422.64	816.75	812.35	240.58	
18	486.93	24 866.35	--	276.49	272.70	277.77	686.89	682.96	127.17	
19	323.05	694.24	24 718.46	25 123.51	25 118.12	25 125.60	548.32	543.91	26 003.15	
20	24 117.17	518.05	527.71	24 963.23	24 958.82	24 965.81	402.59	397.93	25 871.81	
21	23 920.01	335.53	346.41	796.75	791.86	798.76	247.83	242.71	733.14	
22	714.95	24 146.39	24 154.09	623.77	620.34	624.71	25 088.05	--	579.72	
23	509.28	23 949.46	23 960.00	443.08	439.72	441.37	24 916.11	24 911.63	421.70	
24	291.69		756.21				732.28	726.67		

TABLE B-1 (Continued)

Band (2,2)

N	R ₃	R ₂	R ₁	P ₃	P ₂	P ₁	Q ₂	Q ₂	Q ₁
0									
1	26 010.1	25 974.7	25 904.2				25 988.6	25 925.2	25 850.8
2	017.8	985.7	930.5	25 912.3	25 872.8	25 791.7	964.8	911.3	846.1
3	017.8	988.6	942.3	858.3	823.3	752.9	936.3	891.6	835.5
4	012.9	986.6	948.3	800.1	767.4	712.5	902.1	862.5	816.7
5	26 001.9	977.8	945.2	740.2		662.3	860.6	830.1	789.8
6	25 933.5	962.1	934.6	670.6		605.7	819.7	791.7	758.1
7	959.8	939.9	913.0	597.7	572.9	540.8	769.1	743.5	714.1
8	929.3	911.3	890.6	519.0	497.6	470.1	714.1	691.7	666.7
9	891.6	875.7	858.0	436.1	416.0	389.3	654.2	631.4	610.8
10	847.4	832.9	816.7	345.6	327.3	306.6	587.6	566.6	548.3
11	795.0	781.7	765.8	249.8	233.5	216.0	512.6	494.7	479.9
12	737.9	724.4	712.5	147.6	133.3	116.5	--	414.2	399.8
13	672.0	658.2	648.5	25 038.3	25 026.1	25 009.6	345.6	328.8	315.6
14	597.7	585.1	576.1	24 925.5	24 912.5	24 899.6	251.4	235.1	223.1
15	512.6	504.5	496.9	805.5	791.9	782.5	148.4	134.2	122.7
16	421.7	416.0	407.9	679.6	666.6	657.1	25 040.8	25 027.6	25 016.5
17	324.7	318.3	311.8	541.9	534.6	526.5	24 925.5	24 913.5	24 902.6
18	217.7	--	206.4	400.4	394.6	--	802.9	791.9	779.7
19	25 101.5	25 097.8	25 091.6	225.4	249.0	242.6	670.5	659.9	649.6
20	24 977.3	24 972.4	24 967.5	24 099.1	24 094.1	24 088.8	530.5	520.9	510.7
21	844.4	840.2	835.7	23 937.5	23 933.2	23 927.8			
22	698.6	697.5	694.2	770.2	765.8	760.1			
23	545.3	545.3	543.2	593.0	589.1	583.9			

REFERENCES

Anketell, J.; and Pery-Thorne, A.: 1967, Oscillator Strengths in the $^2\Sigma^+$ - $^2\Pi$ Band System of OH by the Hook Method. Proc. Roy. Soc. (London) A301, 343-353.

Ball, J. A.; Dickinson, D. F.; Gottlieb, C. A.; and Radford, H. E.: 1970, The 3.8 cm Spectrum of OH. Laboratory Measurement and Low Noise Search in W_3 (OH). Astron. J. 75, 762-763.

Ball, J. A.; Gottlieb, C. A.; Meeks, M. L.; and Radford, H. E.: 1971, Search for the $^2\Pi_{1/2}$, $J = 5/2$ Excited State of OH in W_3 . Astrophys. J. 163, L33-34.

Barrett, A. H.: 1967, Radio Observations of Interstellar Hydroxyl Radicals. Science 157, 881-889.

Barrow, R. F.: 1956, The B $^2\Sigma^+$ - A $^2\Sigma^+$ Band-System of OH and OD. Ark Fysik. 11, 281-290.

Barrow, R. F.; and Downie, A.: 1956, The Identification of a Band System, B ($^2\Sigma^+$) - A $^2\Sigma^+$, in OH and OD. Proc. Phys. Soc. (London). A69, 178-180.

Bass, A. M.; and Broida, H. P.: 1953, A Spectrophotometric Atlas of the $^2\Sigma^+$ - $^2\Pi$ Transition of OH. Natl. Bur. Std., circular #541, (USA). 1-22.

Bass, A. M.; and Garvin, D.: 1962, Analysis of the Hydroxyl Radical Vibration Rotation Spectrum Between 3900Å and 11500Å. J. Mol. Spectrosc. 9, 114-123.

Bauman, R. P.: 1966, Absorption Spectroscopy. John Wiley and Sons, Inc., New York. p. 280.

Benedict, W. S.; Plyler, E. K.; and Humphreys, C. J.: 1953, The Emission Spectrum of OH from 1.4 to 1.7μ. J. Chem. Phys. 21, 398-402.

Bennett, R. G.; and Dalby, F. W.: 1964, Experimental Determination of the Oscillator Strength of the Violet System of OH. J. Chem. Phys. 40, 1414-1416.

Benoist, S.: 1955, Contribution a L'étude du spectre de la Molecule OH. Ann. Phys. (France) 10, 363-376.

Bolton, J. G.; Van Damme, K. J.; Gardner, F. F.; and Robinson, B. J.: 1964, Observations of OH Absorption Lines in the Radio Spectrum of the Galactic Center. Nature 201, 279.

Bunn, F. E.; and Gush, H. P.: 1972, Spectrum of the Airglow Between 3 and 4 Microns. *Can. J. Phys.* 50, 213-215.

Callear, A. B.; and Van Den Bergh, H. E.: 1971, An Hydroxyl Radical Infrared Laser. *Chem. Phys. Lett.* (Netherlands). 8, 17-18.

Carlone, C.; and Dalby, F. W.: 1969a, Spectrum of Hydroxyl Radical. *Can. J. Phys.* 47, 1945-1957.

Carlone, C.; and Dalby, F. W.: 1969b, The Spectrum of the Hydroxyl Radical. Depository of Unpublished Data, National Research Council Library, National Research Council of Canada.

Carrington, T.: 1959, Line Shape and f Value in the OH $^2\Sigma^+ - ^2\Pi$ Transition. *J. Chem. Phys.* 31, 1243-1252.

Carrington, A.; and Lucas, N. J. D.: 1970, Electron Resonance of Gaseous Diatomic Hydrides I. 170 O Hyperfine Quadrupole Interactions in OH and OD. *Proc. Roy. Soc. (London) A* 314, 567-583.

Chamberlain, K.; and Cuther, H. B.: 1933, New Lines in the Electronic Band Spectrum of Neutral OH. *Phys. Rev.* 44, 927-930.

Chamberlain, J. W.; and Roesler, F. L.: 1955, The OH Bands in the Infrared Airglow. *Astrophys. J.* 121, 541-547.

Chamberlain, J. W.: 1961, Physics of the Aurora and Airglow. Academic Press. New York and London.

Churg, A.; and Levy, D. H.: 1970, The Magnetic Resonance Spectrum of vibrationally Excited OH and a Prediction of the Radio-Astronomy Spectrum. *Astrophys. J.* 162, L161-L165.

Cook, A. H.: 1966, Suggested Mechanism for the Anamalous Excitation of OH Microwave Emissions from H-II Regions. *Nature* 210, 611-612.

Cook, A. H.: 1969, The Hydroxyl Molecule in Interstellar Space. *Physica.* 41, 1-23.

Czarny, J.; and Felenbok, P.: 1968, Etude a Très Haute Résolution de la Transition B $^2\Sigma^+ - A ^2\Sigma^+$ de OH et OD a L'aide D'une Source Haute Fréquence Mise au Point a cet Effect. *Ann. Astrophys. (France)* 31, 141-152.

Czarny, J.; Felenbok, P.; and Lefebvre-Brion, H.: 1971, High Vibrational Level Predissociation in the $A^2\Sigma^+$ State of OD. *J. Phys. B: Atom. Molec. Phys.* 4, 124-132.

Dawson, D. H.; and Johnston, H. L.: 1933, Further Studies in the Spectrum of the OH Molecule: A New (2,2) Band's Satellite Series in $\lambda 3122$; Λ -Type Doubling and Electronic Spin Doubling. *Phys. Rev.* 43, 980-981.

Dejardin, G.; Janin, J.; and Peyron, M.: 1953, Analysis of the (4,0), (5,1) and (6,2) Bands of the Rotation-Vibration Spectrum of the Molecule OH. *Cahiers. Phys.* 46, 3-16.

Destombes, J.; Marliere, C.; Rohart, F.; and Burie, J.: 1974, Spectroscopic Hertzienne-Nouvelle Analyse du Spectre Hertzien du Radical Hydroxyl. *C. R. Acad. Sc. (Paris)*. 278, 275-278.

Dieke, G. H.: 1925, On the Structure of the Ultraviolet Bands of Water Vapor. *Akademie von Wetenschappen, Amsterdam. Adfiling Natuurkunde, Proc. Roy. Acad. Amsterdam* 28, 174-181.

Dieke, G. H.; and Crosswhite, H. M.: 1948, The Ultraviolet Bands of OH. Fundamental Data. *Bumblebee Series Report No. 87*, The Johns Hopkins University, Baltimore, Md. U.S.A.

Dieke, G. H.; and Crosswhite, H. M.: 1962, The Ultraviolet Bands of OH. Fundamental Data. *J. Quant. Spectrosc. Radiat. Transfer* 2, 97-199.

Diekinson, D. F.; and Turner, B. E.: 1972, Classification of New OH Sources. *Astrophys. Lett.* 11, 1-5.

Dieter, N. H.; and Ewen, H. I.: 1964, Radio Observations of the Interstellar OH Line at 1667 Mc/s. *Nature* 201, 279-281.

Dixon, R. N.; and Lamberton, H. M.: 1968, The $A^3\Pi_1 - X^3\Sigma^-$ Band Systems of AsH and AsD. *J. Mol. Spectry.* 25, 12-33.

Douglas, A. E.: 1966, Anomalously Long Radiative Lifetimes of Molecular Excited States. *J. Chem. Phys.* 45, 1007-1015.

Douglas, A. E.: 1974, Absorption of OH in the 1200\AA Region. *Can. J. Phys.* 52, 318-323.

Dousmanis, G. C.; Sanders, T. M.; and Townes, C. H.: 1955, Microwave Spectra of the Free Radicals OH and OD. *Phys. Rev.* 100, 1735-1754.

Drake, J.; and Nicholls, R. W.: 1969, The \bar{r} -centroid Approximation and Molecular Spectra. *Chem. Phys. Lett. (Netherlands)* 3, 457-459.

Ducas, T. W.; Geoffrion, L. D.; Osgood, R. M.; and Javan, A.: 1973, Observations of Laser Oscillations in Pure Rotational Transitions of OH and OD Free Radicals. *Appl. Phys. Lett.* 21, 42-44.

Dwyer, R. J.; and Oldenberg, O.: 1944, The Dissociation of H_2O into H + OH. *J. Chem. Phys.* 12, 351-361.

Dyne, P. J.: 1958, Uncertainties in the Measurement of the Oscillator Strength of the Ultraviolet Bands of OH. *J. Chem. Phys.* 28, 999-1000.

Easson, I.; and Pryce, M. H. L.: 1973, Calculated Potential Energy Curves of OH. *Can. J. Phys.* 51, 518-529.

Elmergreen, B. G.; and Smith, W. H.: 1972, Direct Measurement of the Lifetimes and Predissociation Probabilities for the Rotational Levels of the OH and OD A $^2\Sigma^+$ State. *Astrophys. J.* 178, 557-564.

Elvey, C. T.: 1950, Note on the Spectrum of the Airglow in the Red Region. *Astrophys. J.* 111, 432-433.

Felenbok, P.: 1963, Contribution a L'etude du Spectre Moleculaire des Radicaux OH et OD. *Ann. Astrophys. (France)* 26, 393-428.

Felenbok, P.; and Czarny, J.: 1964, Identification du Systeme C $^2\Sigma^+$ - X $^2\Pi_1$ de OH et OD dans L'ultra-violet du vide. *Ann. Astrophys. (France)* 27, 244-246.

Foner, S. N.; and Hudson, R. L.: 1956, Ionization Potential of the OH Free Radical by Mass Spectrometry. *J. Chem. Phys.* 25, 602-603.

Fraser, P. A.: 1954a, A Method of Determining the Electronic Transition Moment for Diatomic Molecules, *Can. J. Phys.* 32, 515-521.

Fraser, P. A.: 1954b, Vibrational Transition Probabilities of Diatomic Molecules III. *Proc. Phys. Soc. (London)* A67, 939-941.

Frost, A. A.; and Oldenberg, O.: 1936a, Kinetics of OH Radicals as Determined by Their Absorption Spectrum I. The Electric Discharge through Water Vapor. *J. Chem. Phys.* 4, 642-648.

Frost, A. A.; and Oldenberg, O.: 1936b, Kinetics of OH Radicals as Determined by Their Absorption Spectrum II. The Electric Discharge through H_2O_2 . *J. Chem. Phys.* 4, 781-784.

Gardner, F. F.; Robinson, B. J.; Bolton, J. G.; and Van Damme, K. J.: 1964, Detection of the Interstellar OH Lines at 1612 and 1720 Mc/Sec. *Phys. Rev. Lett.* 13, 3-5.

Gaydon, A. G.; and Wollfran, A. G.: 1951, Predissociation in the Spectrum of OH; the Vibrational and Rotational Intensity Distribution in Flames. *Proc. Roy. Soc. (London) A.* 208, 63-75.

Gaydon, A. G.: 1968, Dissociation Energies and Spectra of Diatomic Molecules. Chapman and Hall, Ltd, London.

Gaydon, A. G.; and Kopp, I.: 1971, Predissociation in the Spectrum of OH; A Reinterpretation. *J. Phys. B: Atom. Molec. Phys.* 4, 752-758.

Golden, D. M.; Del Greco, F. P.; and Kaufman, F.: 1963, Experimental Oscillator Strength of OH, $^2\Sigma \rightarrow ^2\Pi$, by a Chemical Method. *J. Chem. Phys.* 39, 3034-3041.

Goldstein, S. J.; Gundersmann, E. J.; Penzias, A. A.; and Lilly, A. E.: 1964, OH Absorption Spectra in Sagittarius. *Nature* 203, 65-66.

Grebe, L.; and Holtz, O.: 1912, Ursprung und Struktur der Ultravioletten Wasserdampfbanden $\lambda = 3064$. *Ann. Phys. (Germany)* 39, 1243-1250.

Gundersmann, E. J.: 1965, Observations of the Interstellar Hydroxyl Radical. Ph.D. Thesis, Harvard University, Cambridge, Mass.

Herman, R. C.; and Hornbeck, G. A.: 1953, Vibration-Rotation Bands of OH. *Astrophys. J.* 118, 214-227.

Herman, L.; Felenbok, P.; and Herman, R.: 1961, Spectre D'Emission des Radicaux OH et OD. *J. Phys. Radium. (France)* 22, 83-92.

Heurlinger, T.: 1917, Untersuchungen Über die Struktur der Bandenspektra. Dissertation, University of Lund (Sweden).

Herzberg, G.: 1950, Molecular Spectra and Molecular Structure I. Spectra of Diatomic Molecules. Van Nostrand Reinhold Company.

Hill, E.; Van Vleck, J. H.: 1928, On the Quantum Mechanics of the Rotational Distortion of Multiplets in Molecular Spectra. *Phys. Rev.* 32, 250-272.

Horani, M.; Rostas, J.; and Lefebvre-Brion, H.: 1967, Fine Structure of $^3\Sigma^-$ and $^3\Pi$ States of NH, OH $^+$, PH, and SH $^+$. *Can. J. Phys.* 45, 3319-3331.

Hunaerts, J.: 1945, Sur la Presence de la Molecule OH $^+$ dans les Cometes. Brussels Observatoire Royal de Belgique *Bulletin Astronomique* 3, 320-326.

Jack, D.: 1927, The Band Spectrum of Water Vapour. *Proc. Roy. Soc. (London)* A 115, 373-390.

Jack, D.: 1928a, The Band Spectrum of Water Vapour - II *Proc. Roy. Soc. (London)* A 118, 647-654.

Jack, D.: 1928b, The Band Spectrum of Water Vapour - III. *Proc. Roy. Soc. (London)* A 120, 222-234.

Johnston, H. L.; Dawson, D. H.; and Walker, M. K.: 1933, A New Band in the Spectrum of the OH Molecule. *Phys. Rev.* 43, 473-480.

Kovacs, I.: 1958, On the Spin-Orbit Interaction in Diatomic Molecules I. *Can. J. Phys.* 36, 309-328.

Kovacs, I.: 1969, Rotational Structure in the Spectra of Diatomic Molecules. American Elsevier Publishing Company, Inc., New York.

Kvifte, G.: 1959a, Auroral and Nightglow Observations at As Norway. *J. Atmos. Terr. Phys.* 16, 252-258.

Kvifte, G.: 1959b, Nightglow Observations at Ås during the I.G.Y. Geofys. Publ. 20, 1-15.

Learner, R. C. M.: 1962, The Influence of Vibration-Rotation Interaction on Intensities in the Electronic Spectra of Diatomic Molecules I. The Hydroxyl Radical. *Proc. Roy. Soc. (London)* A 269, 311-326.

Lefebvre-Brion, H.: 1971, Intensity Anomaly in the Photoelectron Spectrum of NO. *J. Phys. (France)* 32, C52-C-107.

Litvak, M. M.; McWhorter, A. L.; Meeks, M. L.; and Zeiger, H. J.: 1966, Maser Model for Interstellar OH Microwave Emission. *Phys. Rev. Lett.* 17, 821-826.

Litvak, M. M.: 1969, Infrared Pumping of Interstellar OH. *Astrophys. J.* 156, 471-492.

Litvak, M. M.: 1972, 'Non-Equilibrium Processes in Interstellar Molecules' in *Atoms and Molecules in Astrophysics*, Edited by T. R. Carson and M. J. Roberts, Academic Press, New York, p. 201-276.

Loomis, F. W.; and Brandt, W. H.: 1936, The Band Spectrum of OH⁺. *Phys. Rev.* 49, 55-67.

Lowe, R. P.; and Lytle, E. A.: 1973, Balloon-Borne Spectroscopic Observation of the Infrared Hydroxyl Airglow. *Appl. Opt.* 12, 579-583.

MacDonald, R.; Buijs, H. L.; and Gush, H. P.: 1968, Spectrum of the Night Airglow Between 3 and 4 Microns. *Can. J. Phys.* 46, 2575-2578.

Madden, R. P.; and Benedict, W. S.: 1955, Pure Rotational Lines of OH. *J. Chem. Phys.* 23, 408-409.

McGee, R. X.; Robinson, B. J.; Gardner, F. F.; and Bolton, J. G.: 1965, Anomalous Intensity Ratios of the Interstellar Lines of OH in Absorption and Emission. *Nature* 208, 1093-1095.

McKinley, J. D.; Garvin, D.; and Boudart, M. J.: 1955, Production of Excited Hydroxyl Radicals in the Hydrogen Atom-Ozone Reaction. *J. Chem. Phys.* 23, 784-786.

Meinel, A. B.: 1950a, OH Emission Bands in the Spectrum of the Night Sky I. *Astrophys. J.* 111, 555-564.

Meinel, A. B.: 1950b, OH Emission Bands in the Spectrum of the Night Sky II. *Astrophys. J.* 112, 120-130.

Merer, A. J.; Achter, E. K.; Harani, M.; and Rostas, J.: 1969, Reanalysis of the A $^3\Pi_u$ - X $^3\Sigma^-$ System of OH⁺ and OD⁺. *Can. J. Phys.* 47, 1723-1724.

Michel, A.: 1957, Das C $^2\Sigma^+$ \rightarrow A $^2\Sigma^+$ Bandensystem von OH. Z. Naturforsch. 12A, 887-896.

Michels, H. H.; and Harris, F. E.: 1969, Predissociation Effects in the A $^2\Sigma^+$ State of the OH Radical. Chem. Phys. Lett. (Netherlands) 3, 441-442.

Mizushima, M.: 1972, Molecular Parameters of OH Free Radical. Phys. Rev. A 5, 143-157.

Moore, C. E.; and Broida, H. P.: 1959, OH in the Solar Spectrum. J. Res. Natl. Bur. Std. A (USA), 63A, 279-295.

Moreels, G.; Evans, W. F.; Blamont, J. E.; and Jones, A. V.: 1970, A Balloon-Borne Observation of the Intensity Variation of the OH Emission in the Evening Twilight. Planet. Space. Sci. 18, 637-640.

Mulliken, R. S.: 1931, The Interpretation of Band Spectra. Part IIc. Empirical Band Types. Rev. Mod. Phys. 3, 89-155.

Mulliken, R. S.; Christy, A.: 1931, A-Type Doubling and Electron Configurations in Diatomic Molecules. Phys. Rev. 38, 87-119.

Naudé, S. M.: 1932, Quantum Analysis of the Rotational Structure of the First Positive Bands of Nitrogen (N₂). Proc. Roy. Soc. (London) A 136, 114-144.

O'Connor, S.: 1962, The Rotational Analysis of the (2,1), (0,0) and (0,1) Bands of the $^3\Pi$ - $^3\Sigma^-$ System of OD⁺. Proc. R. Irish Acad. 62, 73-92.

Oldenberg, O.: 1935, The Lifetime of Free Hydroxyl. J. Chem. Phys. 3, 266-275.

Oldenberg, O.; and Rieke, F. F.: 1938a, The Absorption Spectrum of Free Hydroxyl Calibrated for a Chemical Test. J. Chem. Phys. 6, 1969.

Oldenberg, O.; and Rieke, F. F.: 1938b, Kinetics of OH Radicals as Determined by their Absorption Spectrum III. A Quantitative Test for Free OH Possibilities of Transition. J. Chem. Phys. 6, 439-447.

Oldenberg, O.; and Rieke, F. F.: 1938c, Kinetics of OH Radicals Determined by Their Absorption Spectrum IV. Pressure Broadening and the Line Spectrum as Background. J. Chem. Phys. 6, 779-782.

Pears, R. W. B.; and Gaydon, A. G.: 1965, The Identification of Molecular Spectra, Chapman and Hall Ltd., London.

Perkins, F.; Gold, T.; and Saltpeter, E. E.: 1966, Maser Action in Interstellar OH. *Astrophys. J.* 145, 361-365.

Pick, D. R.; Llewellyn, E. J.; and Jones, A. V.: 1971, Twilight Airglow Measurements of the OH and O₂ Bands by Means of Balloon-Borne Instruments. *Can. J. Phys.* 49, 897-905.

Plyler, E. K.; and Humphrey, C. J.: 1948, Infrared Emission Spectra of Flames. *J. Res. Natl. Bur. Std.* 40, 449-456.

Poynter, R. L.; and Beaudet, R. A.: 1968, Predictions of Several OH Λ -Doubling Transitions Suitable for Radio Astronomy. *Phys. Rev. Lett.* 21, 305-308.

Radford, H. E.: 1961, Microwave Zeeman Effect of Free Hydroxyl Radicals. *Phys. Rev.* 122, 114-130.

Radford, H. E.: 1962, Microwave Zeeman Effect of Free Hydroxyl Radicals: $^2\Pi_{1/2}$ Levels. *Phys. Rev.* 126, 1035-1045.

Radford, H. E.: 1964, 18 cm Spectrum of OH. *Phys. Rev. Lett.* 13, 534-535.

Radford, H. E.: 1968, Scanning Microwave Echo Box Spectrometer. *Rev. Sci. Instr.* 39, 1687-1691.

Rakotoarijimy, D.: 1969, Quelques Resultants Recents Concernant la Structure Fine du Spectre de la Molecule OH⁺. *Physica* 41, 29-34.

Rakotoarijimy, D.: 1970, Contribution a L'etude du Radical OH⁺ (Systeme de Bandes $^3\Pi_g \rightarrow ^3\Sigma^-$). *Physica* 49, 360-382.

Robinson, B. J.; and McGee, R. X.: 1967, 'OH Molecules in the Interstellar Medium' in Annual Review of Astronomy and Astrophysics, edited by L. Goldberg, Annual Reviews Inc., California (U.S.A.), Vol. 5, p. 183-212.

Rodebush, W. H.; and Wahl, M. H.: 1933, The Reactions of the Hydroxyl Radical in the Electrodeless Discharge in Water Vapor. *J. Chem. Phys.* 1, 696-702.

Rogers, A. E. E.: 1967, Emission and Absorption of Microwave Radiation by Interstellar OH. Ph.D. Thesis, M.I.T., Cambridge, Massachusetts.

Roschdestwensky, D. S.: 1912, Anomale Dispersion in Natriumdampf. Ann. Phys. (Germany) 39, 307-345.

Roschdestwensky, D. S.; and Penkin, N. P.: 1941, Determination of the Vibrator Strength in the Atomic Spectra. J. Phys. (USSR) 5, 319-337.

Rosen, B.: 1970, International Tables of Selected Constants No. 17 - Spectroscopic Data Relative to Diatomic Molecules. Pergamon Press.

Rosen, B.: 1973, Diatomic Molecules - A Critical Bibliography of Spectroscopic Data, National Center of Scientific Research, Paris, France.

Rouse, P. E.; and Engleman, R.: 1973, Oscillator Strengths from Line Absorptions in a High-Temperature Furnace - I. The (0,0) and (1,0) Bands of the $A^2\Sigma^+ - X^2\Pi_i$ Transition in OH and OD. J. Quant. Spectrosc. Radiat. Transfer. 13, 1503-1521.

Schuler, H.; and Woeldike, A.: 1943, Über den Anregungsmechanismus im H_2O - Molekül auf Grund der Befunde an seinem Emissionsspektrum im Sichtbaren. Physikalisch., Z. 44, 335-340.

Schuler, H.; Reinebeck, L.; and Michel, A.: 1954, Is There a Spectrum of the OH^- Ion? Z. Naturforsch. 9A, 279-285.

Schuler, H.; and Michel, A.: 1956, On a New Band System of the OH Radical or Ion. Z. Naturforsch. 11A, 403-406.

Shklovskii, I. S.: 1966, Astronomical Tsirkular No. 372.

Silverman, S.; Herman, R. C.: 1949, The Infrared Emission Spectra of the Oxy-hydrogen and Oxy-deuterium Flames. J. Opt. Soc. Am. 39, 216-218.

Stoebner, A.; and Delbourgo, R.: 1967, Contribution a L'étude Spectrographique de la Séquence 0-2 de la Transition $A^2\Sigma^+ - X^2\Pi$ du Radical OH. J. Chem. Phys. (France) 64, 1115-1123.

Sutherland, R. A.; and Anderson, R. A.: 1973, Radiative and Predissociative Lifetimes of the $A^2\Sigma^+$ State of OH. J. Chem. Phys. 58, 1226-1234.

Swings, P.: 1942, The Line Spectrum of the Solar Corona. *Astron. Soc. Pacific* 54, 117-137.

Swing, P. and Meinel, A. B.: 1951, 'Spectra of Night Sky and Aurora' in the Atmospheres of the Earth and Planets, Edited by Gerard P. Kuiper, The University of Chicago Press, Chicago, Illinois.

Tanaka, T.; and Koana, Z.: 1933, Classification of Unrecorded Band-Systems of Neutral OH. Determination of the Constants. *Proc. Phys. Maths. Soc. (Japan)* 15, 272-290.

Tanaka, T.; and Siraishi, M.: 1933, The $\lambda 2875$ Band of Neutral OH. *Proc. Phys. Maths. Soc. (Japan)* 15, 195-209.

Tanaka, T.; and Koana, Z.: 1934, On the Band-System of Neutral OH. III. Identification of the $(2', 2')$, $(3', 0')$, $(3', 3')$, $(4', 1')$, $(4', 2')$, $(4', 3')$ and $(4', 4')$ Bands. Formulation of the Wave-Numbers of the Null Lines. *Proc. Phys. Maths. Soc. (Japan)* 16, 365-400.

Ter Meulen, J. J.; and Dymanus, A.: 1972, Beam Maser Measurements of the Ground State Transition Frequencies of OH. *Astrophys. J.* 172, L21-L23.

Turner, B. E.; Palmer, P.; and Zuckerman, B.: 1970, Detection of the $^2\Pi_{3/2}$, $J = 7/2$ State of Interstellar OH at a Wavelength of 2.2 cm. *Astrophys. J.* 160, L125-L129.

Turner, B. E.: 1972, On the Distribution of OH in the Galaxy I. Correlation with Continuum Sources and with Formaldehyde. *Astrophys. J.* 171, 503-518.

Wallace, L.; and Jones, A.: 1955, Infrared Spectrum of the Nightsky Near 10,000A. *Nature*. 175, 950-951.

Wallace, L.: 1960, The Constants of the $^2\Pi - ^2\Pi$ OH Bands. *Astrophys. J.* 132, 894-897.

Wallace, L.: 1962a, Band-Head Wavelengths of C₂, CH, CN, CO, NH, NO, O₂, OH, and Their Ions. *Astrophys. J. (Suppl.)* 68, 165-290.

Wallace, L.: 1926b, The OH Nightglow Emission. *J. Atmos. Sci.* 19, 1-16.

Watson, W. W.: 1924, The Emission Spectrum of Water Vapor. *Astrophys. J.* 60, 145-158.

Watson, R.: 1964, Shock Tube Measurements of the Oscillator Strengths for the $A^2\Sigma - X^2\Pi$ OH Electronic Bands. *J. Quant. Spectrosc. Radiat. Transfer.* 4, 1-7.

Weast, R. E.: 1970, *Handbook of Chemistry and Physics*, 50th edition. The Chemical Rubber Company, U.S.A. p. E-82.

Weaver, H. F.; and Williams, D. R. W.: 1964, OH Absorption Profile in the Direction of Sagittarius A. *Nature* 201, 380.

Weaver, H.; Williams, D. R. W.; Dieter, N. H.; and Lum, W. T.: 1965, Observations of a Strong Unidentified Microwave Line and of Emission from the OH. *Nature* 208, 29-31.

Weniger, S.; and Herman, R.: 1958, Extension du Systeme $A^3\Pi_i - X^3\Sigma^-$ de OH⁺. *J. Phys. Rad.* 19, 582-589.

Weinreb, S.; Barrett, A. H.; Meeks, M. L., and Henry, J. C.: 1963, Radio Observations of OH in Interstellar Medium. *Nature* 200, 829-831.

NATIONAL AERONAUTICS AND SPACE ADMINISTRATION
WASHINGTON, D.C. 20546

OFFICIAL BUSINESS
PENALTY FOR PRIVATE USE \$300

SPECIAL FOURTH-CLASS RATE
BOOK

POSTAGE AND FEES PAID
NATIONAL AERONAUTICS AND
SPACE ADMINISTRATION
45¢



POSTMASTER:

If Undeliverable (Section 158
Postal Manual) Do Not Return

"The aeronautical and space activities of the United States shall be conducted so as to contribute . . . to the expansion of human knowledge of phenomena in the atmosphere and space. The Administration shall provide for the widest practicable and appropriate dissemination of information concerning its activities and the results thereof."

—NATIONAL AERONAUTICS AND SPACE ACT OF 1958

NASA SCIENTIFIC AND TECHNICAL PUBLICATIONS

TECHNICAL REPORTS: Scientific and technical information considered important, complete, and a lasting contribution to existing knowledge.

TECHNICAL NOTES: Information less broad in scope but nevertheless of importance as a contribution to existing knowledge.

TECHNICAL MEMORANDUMS: Information receiving limited distribution because of preliminary data, security classification, or other reasons. Also includes conference proceedings with either limited or unlimited distribution.

CONTRACTOR REPORTS: Scientific and technical information generated under a NASA contract or grant and considered an important contribution to existing knowledge.

TECHNICAL TRANSLATIONS: Information published in a foreign language considered to merit NASA distribution in English.

SPECIAL PUBLICATIONS: Information derived from or of value to NASA activities. Publications include final reports of major projects, monographs, data compilations, handbooks, sourcebooks, and special bibliographies.

TECHNOLOGY UTILIZATION PUBLICATIONS: Information on technology used by NASA that may be of particular interest in commercial and other non-aerospace applications. Publications include Tech Briefs, Technology Utilization Reports and Technology Surveys.

Details on the availability of these publications may be obtained from:

SCIENTIFIC AND TECHNICAL INFORMATION OFFICE

NATIONAL AERONAUTICS AND SPACE ADMINISTRATION

Washington, D.C. 20546